
# EVALUATION OF ENHANCEMENT METHODS FOR THE PRODUCTION OF BIOGAS FOR ANAEROBIC CO-DIGESTION OF SEWAGE SLUDGE WITH INDUSTRIAL WASTEWATER

Submitted in fulfilment of the requirements for the degree of:

**Master of Engineering in the Department of Chemical Engineering,**

**Faculty of Engineering and the Built Environment**

**at Durban University of Technology**

**By**

**Denzil Erwin Estrice (21549710)**

**Date: 2024**

**Supervisor: Prof M. Chetty**

**Signature**

**Co-supervisor: Prof T.H. De Koker**

**Signature**

# Declaration

I, **Denzil Erwin Estrice**, clearly state the following:

i. The research reported in this thesis, except where otherwise indicated, is my original work.

ii. No one has submitted this thesis for any degree or examination at another institution.

iii. This thesis does not contain data, pictures, graphs, or additional information from another author unless expressly acknowledged as being sourced from other persons.

iv. It does not contain other authors' writing unless expressly acknowledged as being sourced from other authors. Where other written sources have been quoted, then:

   a. their words have been re-written, but the general information attributed to them has been referenced.

   b. Where their exact words have been used, their writing has been placed inside quotation marks and referenced.

v. Where I have reproduced a publication of which I am an author, co-author or editor, I have indicated in detail which part of the paper was actually written by myself alone and have fully referenced such publications.

vi. This thesis does not contain text, graphics or tables copied and pasted from the Internet, unless expressly acknowledged, and the source being detailed in the thesis and the references section.

Signature: Date: 11 June 2024

Supervisor (Prof. M. Chetty)

Signature: Date: 12 June 2024

Co-supervisor (Prof. T.H de Koker)

Signature: Date: 12 June 2024

# Acknowledgements

To the Great I AM, I would like to express my gratitude to my Lord and Saviour for granting me the strength to accomplish such an achievement (Mathew 6 v 33).

I would like to express my sincere gratitude to Prof. Maggie Chetty, without whom this would not be possible; thank you for your dedication. I will forever be grateful for your commitment to helping me achieve this goal.

To my parents, Mr and Mrs Estrice, thank you for your unwavering support and encouragement; you have set a stellar example for us, your children.

Lastly, to my dear wife, thank you for standing by my side and helping me realise this goal. Your support, encouragement and love will forever be appreciated.

# Dedication

This dissertation is dedicated to my dear wife, loving parents, and siblings.

# Abstract

The worldwide move towards a sustainable, equitable future faces two major obstacles: unsustainable waste management and access to clean energy (Kwietniewska and Tys, 2014). Alternative renewable energy sources are needed to curb global warming and the consumption of non-renewable fuels (Akinbami et al., 2021). Industrial and municipal wastewater with high organic matter content has increased due to rapid industrialisation in many emerging nations. If appropriately treated, wastewater may produce biogas through anaerobic digestion to generate green energy (Chrispim et al., 2021). While anaerobic digestion is a mature technology, challenges around process efficiency remain. Thus, much research has examined ways of enhancing anaerobic digestion (AD) efficacy.

This research evaluated the suitability and investigated the effects of intermediate municipal landfill leachate and sugar industry wastewater as co-substrates in the AD of sewage sludge. The effects of biochar addition synthesised from sugarcane bagasse at three pyrolysis temperatures ($350^0$C, $450^0$C and $550^0$C) together with ultrasonic pretreatment as a potential enhancement method were evaluated with respect to four key performance indicators: (I) biogas yield, (II) biogas quality, (III) COD and (IV) Volatile Solid (VS) removal.

Response surface methodology (RSM) was employed to evaluate the following specific objectives: Five objectives were evaluated: (**i**) Characterization of primary sewage sludge, inoculum, and industrial wastewater. The total solids (TS) and volatile solids (VS) for PS were 39.02 (gTS/l) and 29.72 (gVS/L), respectively, falling within the expected range. The results also suggest that the sludge exhibits excellent biodegradability, evidenced by a VS/TS ratio of> 50%. Sugar industry wastewater (SIWW) exhibited a VS/TS ratio of 0.68, indicating a greater presence of organic substances than insoluble ones. The inoculum displayed the lowest VS/TS value, measuring 0.48, indicating a high concentration of microorganisms vs organic materials, confirming its potential use as an inoculum rather than as a substrate. (**ii**) Production and characterisation of biochar (BC) derived from sugarcane bagasse using energy dispersive x-ray, scanning electron microscopy (EDX/SEM), and Fourier transform infrared spectroscopy (FTIR). The BC synthesised at $550^0$C was the most alkaline at a pH of 9.1, followed by 9.0 (BC $450^0$C) and 7.0 (BC $350^0$C). While all the synthesised BC displayed carbon contents > 50 %, BC $550^0$C exhibited the highest at 78.33%. SEM analysis found BC $450^0$C exhibited greater formation of surface micropores. FTIR analysis of the BCs confirmed the presence of carboxyl, carbonyl, carboxyl, hydroxyl, C=N bond, and ether group. (**iii**) Investigate the effect of

Municipal Intermediate Landfill Leachate (ILL) and Sugar Industry Wastewater (SIWW) as co-substrates and optimisation of process parameters with RSM. This was executed in two stages; the first was employed to identify the best-performing IWW. ILL produced the highest biogas yield at (54,35 mL/$gVS_{added}$) vs (12.55ml/$gVS_{added}$) for SIWW; ILL achieved the highest COD removal (46.84%). ILL was found to increase the COD removal by 5.36% compared to the CNTRL. Hence, ILL was selected as the best-performing co-substrate for process optimisation. Optimisation facilitated by (RSM) employing Box–Behnken design with co-substrate loading between (1:20 – 1:5), ISR (1:2– 1.5:1) and temperature (25 – $55^0$C), the optimum co-substrate loading of (1:20), ISR of (1.5:1), and a temperature of $37^0$C, achieved desirability of 90.10%. The RSM-BBD models exhibited a significant correlation ($0.9 < R^2 < 1$) with projected outcomes that aligned well with the experimental data. (**iv**) Investigate the effect of Biochar as an additive on the AD process. This was executed in two stages; the first was employed to identify the best-performing BC. BC 450 produced the highest biogas yield at (50.38mL/$gVS_{added}$) vs (46.88 and 26.57mL/$gVS_{added}$) for BC $350^0$C and BC $550^0$C, respectively; BC $450^0$C also achieved the greatest COD and VS removal of 50.86% and 35.11%, respectively. Hence, BC 450 was selected as the best-performing BC for process optimisation. Optimisation with co-substrate loading between (1:20 – 1:5), BC loading (2.5 – 10 g/L) and temperature (25 – $55^0$C), the optimum co-substrate loading of (1:20), BC loading of (6.7 g/L), and a temperature of $54.99^0$C, achieved desirability of 94.10%. The RSM-BBD models exhibited a significant correlation with projected outcomes that aligned well with the experimental data. (**v**) Investigate the effect of ultrasonic pre-treatment of industrial wastewater on the anaerobic digestion process. ILL was subjected to ultrasonic pretreatment and co-digested employing the optimum process parameters from (**iv**) Process efficiency was assessed with respect to biogas yield, COD and VS removal and biomethane content and achieved a COD and VS removal of 46.18% and 49.21, respectively. The biomethane content peaked at 78.23% $CH_4$. Representing a marginal decrease in COD and VS removal compared to the untreated sample.

# Author's Publications

- Kukwa, D., Chetty, M., Tshemese, Z., **Estrice, D.**, Duma, N. 2021. Resource Reclamation for Biogas and Other Energy Resources from Household and Agricultural Wastes. In: Abomohra, A. and Salama, E. eds. Biogas - Basics, Integrated Approaches, and Case Studies. Rijeka: IntechOpen. Available DOI: 10.5772/intechopen.101747
- Armah, E., Chetty, M., Tshemese, Z., **Estrice, D.**, Adedeji, J., Mutsvene, B., Singh, N. 2022. Biochar: Production, Application, and the Future. In: Bartoli, M. and Giorcelli, M., Tagliaferro, A. eds. Biochar - Productive Technologies, Properties and Applications. Rijeka: IntechOpen. Available 10.5772/intechopen.105070
- **Estrice, D.**, Chetty, M. 2024. Optimising Anaerobic Co-digestion of Sewage Sludge and Municipal Landfill Leachate with Sugarcane Bagasse Derived Biochar Using Response Surface Methodology. Chemical Engineering Transactions, 114. (Accepted, Paper ID: ICLCA24.0228)

**Conference Proceedings**

- Chetty, M., **Estrice, D.** 2024. Optimising Anaerobic Co-digestion of Sewage Sludge and Municipal Landfill Leachate with Sugarcane Bagasse Derived Biochar Using Response Surface Methodology. 10$^{th}$ International Conference on Low Carbon Asia (ICLCA 2024) 21-24 September 2024, Dalian, China (Accepted, Paper ID: ICLCA24.0228)

# Contents

# List of Figures

# List of tables

# List of equations

# Nomenclature

| | |
|---|---|
| AD | Anaerobic Digestion |
| AC | Activated Carbon |
| ACD | Anaerobic Co-digestion |
| APHA | American Public Health Association |
| BBD | Box-Behnken Design |
| BC | Biochar |
| BET | Brunauer-Emmett-Teller |
| BMP | Biochemical Methane Potential |
| BOD | Biological Oxygen Demand |
| CCD | Central Composite Design |
| CCMs | Carbon Conductive Materials |
| CEC | Cation Exchange Capacity |
| COD | Chemical Oxygen Demand |
| DIET | Direct Interspecies Electron Transfer |
| DoE | Design of Experiment |
| DW | Domestic Wastewater |
| DWA | Department of Water Affairs |
| EC | Electrical Conductivity |
| EDX | Energy-Dispersive X-ray Spectroscopy |
| FTIR | Fourier-Transform Infrared Spectroscopy |
| GAC | Granular Activated Carbon |
| GHGe | Green House Gas Emissions |
| ILL | Intermediate Landfill Leachate |
| IWW | Industrial Wastewater |
| HRT | Hydraulic Retention Time |
| LCFA | Long Chain Fatty Aids |
| LOF | Lack of Fit |
| MWW | Municipal Wastewater |
| MSW | Municipal Solid Waste |

| | |
|---|---|
| PS | Primary Sludge |
| RSM | Response Surface Methodology |
| SANS | Southern African National Standards |
| SEM | Scanning Electron Microscopy |
| SS | Sewage Sludge |
| EDX | Energy-Dispersive X-ray Spectroscopy |
| SIWW | Sugar Industry Wastewater |
| TS | Total Solids |
| TN | Total Nitrogen |
| UP | Ultrasonic Pretreatment |
| VFAs | Volatile Fatty Acids |
| VS | Volatile Solids |
| WAS | Waste Activated Sludge. |
| WWT | Wastewater Treatment |
| WWTPs | Wastewater Treatment Plant |

# Chapter 1: Introduction

## 1. Background

### 1.1 Energy crisis: A South African perspective.

Unsustainable waste management and access to and supply of clean energy are two of the most critical barriers to overcome in the global push toward a sustainable and equitable future (Kwietniewska and Tys, 2014). These barriers correspond to the "United Nations' Sustainable Development Goals" (SDGs), ratified in 2015. Oil, coal, and natural gas are the traditional energy sources that have kept the modern industrial world running. On the other hand, these fuels are becoming increasingly limited and are directly tied to climate change and its impact on the environment. Shifting to alternative renewable energy sources is needed to mitigate climate change and extensive fossil fuel usage (Cornelissen et al., 2012). The total world energy consumption is predicted to climb from $5.32 \times 10^{20}$ J in 2008 to $8.12 \times 10^{20}$ J in 2035, according to Cornelissen et al. (2012), which is comparable to a 53 per cent increase in 27 years.

According to the BP Statistical Review of Energy 2013, coal accounts for 72% of South Africa's total primary energy consumption, followed by oil, natural gas, nuclear, and renewables. The most recent energy information administration report (EIA) estimates that South Africa's reliance on coal has resulted in the nation being Africa's top carbon dioxide emitter and the world's 14th largest (Akinbami et al., 2021). This is exacerbated by South Africa's restricted electrical grid, with the gap between peak demand and supply being dangerously thin since the early 2000s. The current situation has heightened the importance of finding sustainable solutions, focusing on renewable resources for bioenergy production. Selected resources and processes must be economically viable to ensure long-term sustainability. In this context, biomass conversion into biofuel has become a key area of interest in recent years.

### 1.2 Municipal and industrial wastewater as a source of renewable energy.

The accelerated industrialisation of many developing nations has resulted in increased industrial and municipal wastewater generation, characterised by their high organic matter content. If suitably treated, wastewater can serve as a viable source of sustainable green energy through biogas production via anaerobic digestion (Chrispim et al., 2021).

Wastewater is water polluted by human activity (Templeton et al., 2011). It emanates from several sources, including domestic activities, Industrial activities, sewage input, and stormwater run-off. Domestic wastewater is usually 99 percent water and 1% solids. Treatment of high-strength wastewater is a challenge for many industries. According to Chan et al. (2016), a COD $\geq$ 10,000 mg/L and a biochemical BOD $\geq$ 5000 mg/L is common in certain wastewaters. These high-strength wastewater streams often require sequenced treatment steps to bring them within specified discharge limits. The Division of Water Technology has long acknowledged the viability of using anaerobic digestion to treat municipal and industrial wastewater and has conducted extensive research into the fundamentals (Montwedi et al., 2021).

Sewage sludge from wastewater treatment works (WWTW) is a well-known feedstock for biogas generation due to its elevated biochemical methane potential compared to biogas produced from other feedstocks. It is said to contain ten times the energy required for its treatment (Bachman, 2015). Sewage sludge is the principal AD feedstock in WWTW and is comprised of secondary and primary sludge. The primary settlers generate primary sludge (raw sludge) via gravitational sedimentation. According to Davidsonn (2007), when digested at optimum conditions, primary sludge can produce 300 – 400 ($Nm^3$/t organic dry matter) of biomethane. The aeration process generates secondary sludge presenting a lower organic matter content and hence has lower biomethane potential when compared to primary sludge. Furthermore, recent research and analysis of SS have shown SS has an approximate energy content of 19 MJ (5.2 kWh/kg) dry weight basis, equivalent to low-grade coal's energy content (Musvoto et al.,2018).

### 1.2.1 Factors influencing the production of energy from wastewater sludge.

In South Africa, the management and disposal of wastewater sludge are governed by three important laws: the “National Water Act (Act 36 of 1998)”, the “National Environmental Management: Waste Act (Act 59 of 2008)”, and the Waste Amendment Act (Act 26 of 2014). The Department of Water and Sanitation (DWS) manages wastewater services under Section 155(7) of the Constitution, “Section 62 of the Water Services Act (No. 108 of 1997)”, and Section 21 of the National Water Act. Sludge is 'waste' under Section 21 of the National Water Act and related provisions. The Department of Water and Sanitation (DWS) authorises wastewater utilities to treat and dispose of wastewater under the National Water Act.

Management activities must follow Chapter 5 of the National Environmental Management: Waste Act, 2008 (Act 59 of 2008) and the Guidelines for the Utilisation and Disposal of

Wastewater Sludge: Volumes 1-5 (WRC, 2006; 2009) under the Water Use Authorisation (WUA). South African utilities must manage sludge according to greenhouse gas emission regulations. The National Environmental Management: Air Quality Act (Act no. 39 of 2004) requires GHG emission limitations.

The primary greenhouse gases emitted by wastewater and sludge treatment procedures are $CH_4$ and $CO_2$, which significantly contribute to the phenomenon of global warming. The global warming potential (GWP) of methane is projected to fall between 28 and 36 $CO_2$-equivalents over a period of 100 years, according to the US EPA in 2021. The data on global greenhouse gas (GHG) emissions during 2000-2010 indicates that $CO_2$ and $CH_4$ accounted for 76% and 16% of the total $CO_2$-equivalent emissions, respectively (Edenhofer et al., 2014). Data provided by the South African Department of Environmental Affairs, showed that between 2000 and 2010, $CO_2$ contributed to 83.2% of total carbon dioxide equivalent emissions, while $CH_4$ accounted for 11.4%. This energy recovery potential has propelled sewage sludge (SS) into the domain of viable, sustainable alternate energy sources.

### 1.3 Enhancing Biogas Production

While AD is a mature technology, several challenges remain regarding the process efficiencies linked to biodegradation rates, often attributed to long acclimation, slow anaerobic microorganism (anaerobe) growth, and the inefficient degradation of intermediate products i.e. butyrate and propionate (Azizi et al., 2019). A large body of research investigating potential augmentation strategies to boost the AD process's efficacy exists. These studies include the effect of chemical pretreatments such as ammonia and alkaline pretreatments; mechanical pretreatments such as hydrothermal, ultrasonic, and microwave pretreatment; Anaerobic co-digestion and, the use of organic and inorganic additives such as Biochars and Nickel (Ni), Cobalt (Co) Iron (Fe), and Iron (Fe), respectively (Abdallah et al., 2019; Yu et al., 2017; Fang et al., 2020; Duet al., 2019)

Anaerobic co-digestion (ACD) is considered a practical approach for treating wastewater streams due to its ability to address nutrient deficiencies, boost biogas generation, and improve economic viability. ACD is a method of introducing energy-dense organic waste materials and effluent streams to wastewater digesters, where bacteria degrade the organic waste generating biogas, among other by-products (Rowan et al., 2022). Studies have shown sewage sludge to be an ideal primary substrate in ACD because of its low inhibitor concentration (Mata-Alvarez et al., 2014). The introduction of energy-dense organic materials and effluent streams increases

the organic loading of the system and substantially increases the biogas production potential (Mata-Alvarez et al., 2014).

ACD has been prominent as a technology that offers a sustainable alternative energy source in biogas, while also contributing to sustainable waste management. Despite the significant rise in biogas installations globally, several issues with ACD processes remain. Numerous potential solutions to these issues have been investigated, including the optimisation of operating parameters and bioreactor configuration, nutrient control, the use of pre-treatments for degradability improvement of various feedstocks, and the use of biological and inorganic additives to aid biomass immobilisation and process stability, mitigate inhibitors and supplement nutrients (Arif et al., 2018; Ye et al., 2018; Mata-Alvarez et al., 2014; Taherzadeh et al., 2008; Carrere et al., 2016).

Conductive carbonaceous compounds, including Biochar (BC), have piqued attention among AD additives due to their capacity to boost methane generation (González et al. 2018). Biochars are porous carbonaceous materials made by thermochemically converting biomass at low oxygen (Pan et al., 2019).

Nanda et al. (2016) identified several benefits BC has over other additives, including the manufacture BC with a broad scope of physicochemical characteristics by feedstock selection, pyrolysis conditions, and the activation process. Studies have validated the feasibility of enhancing methane production with BC addition, citing various probable mechanisms, which include improving buffering capacity, inhibitory mitigation, biomass immobilisation, aiding syntrophic metabolisms, improving digestate quality and biogas upgrading (Pecchi and Baratieri, 2019; Salman et al., 2017).

Using ultrasonic pre-treatment (UP) to enhance the AD process is well-researched and has garnered much focus in recent years. Ultrasonic pre-treatment aims to augment the biodegradability of a substrate by reducing particle size and accelerating microbial molecule solubilisation. UP has been shown to induce cell wall rupture and extracellular polymer degradation, releasing the organics available. In addition, ultrasonic processing (UP) has been demonstrated to enhance the disintegration of intermolecular bonds within the cellular material, resulting in a reduction in the size of biomolecules. This reduction in size enhances their solubility and renders them more prone to digestion (Volschan Junior et al., 2020). The process of cell rupture and hydrolysis is typically broken down into four steps: (I) particle dispersion, (II) inner extracellular polymeric substances (EPS) matrix layer disruption and microbial cells

exposure, (III) cell rupture, and (IV) extracellular and intracellular polymeric compound enzymatic depolymerisation producing glycerol, amino acids, monosaccharides, oligosaccharides, and (LCFA) long-chain fatty acids (Palatsi et al., 2010).

### 1.4 Problem statement

Between 1990 and 2018, global energy consumption (i.e., electricity, gas, coal, biomass, and heat) increased from the approximate equivalent of 8 800 million tonnes of oils to 14 400 million tonnes in 2018, which represents a 63 per cent increase in 30 years (Chiappero et al., 2020). Renewable energy sources supplied roughly 14 per cent of primary energy in 2016, whereas fossil fuels produced 81 per cent of the GHGe (Chiappero et al., 2020). The desire to reduce fossil fuel reliance and GHG emissions while providing sustainable energy alternatives has increased investment and research into green energy-producing technologies. The production of biogas through AD of wastewater and biodegradable waste is a well-established and commercial technology and has been identified as a viable replacement for fossil fuels for heat and electricity generation.

Concentrated organic industrial wastewater, such as landfill leachates, sugar industry effluents, and wastes from various industrial processes, poses severe treatment and discharge problems for the industries, local authorities, and the environment. The controlling authority reluctantly receives these wastewater streams into communal sewers because of the challenges of treating them to the specific discharge limits. As per the “National Guideline for the Discharge of Effluent from Land-based Sources into the Coastal Environment”, if industrial effluent is discharged into a WWTW that disposes of it into the coastal environment, it will undergo necessary pre-treatment as defined by the local authorities. To comply, it is necessary to furnish a thorough account of the waste stream, specifying its volume and quality. This entails listing all compounds contained within, along with their concentrations and loads. The advent of such stringent legislation has left many industries ill-equipped to treat the wastewater produced appropriately.

Anaerobic co-digestion is acknowledged as a suitable treatment method for municipal and industrial wastewater, and like mono-substrate digestion, co-digestion has the potential for energy production. Thus, implementing anaerobic co-digestion as a treatment method is beneficial in two ways: (I) it provides a sustainable treatment method for concentrated organic industrial wastewater, and (II) it serves as a viable mechanism for sustainable energy production i.e. green biogas.

Although the advantages of co-digestion are often praised, its adoption by wastewater treatment plants (WWTW) remains restricted. Limiting factors include the lack of appropriate co-substrates and the ambiguity regarding their effects on biogas quality, and biosolids output. Biogas yield and quality can be enhanced through process optimisation techniques, including the implementation of substrate pretreatment procedures, and the utilisation of additional materials (Ward et al., 2008).

Hence, there exists a need for further research on (I) investigating and identifying suitable co-substrates and (II) evaluating suitable methods/mechanisms to enhance the biogas production of co-digestion systems.

Therefore, this study evaluates the effects of several industrial wastewater streams as co-substrates in the AD of Municipal primary sewage sludge. The ACD systems performance was evaluated to maximise biogas yield and identify the suitability of each industrial wastewater for ACD with MSS. The effects of Biochar addition and Ultrasonic pretreatment as potential enhancement methods were evaluated with respect to biogas yield, COD and (VS) reduction. To further enhance the efficiency of the ACD process, specific process parameters (such as process temperature, co-substrate loading rate, biochar loading, and Inoculum substrate ratio (ISR)) were optimised. The optimisation process was conducted using design of experiment (DOE) techniques, using response surface methodology (RSM). RSM was employed as a method for optimisation and determining and measuring the correlation between various factors and the responses.

**Aims and Objectives**

This research aimed to evaluate the suitability and investigate the effects of Intermediate Municipal Landfill Leachate and Sugar Industry wastewater as co-substrates in the AD of Municipal sewage sludge. The effects of Biochar addition and Ultrasonic pretreatment as potential enhancement methods were evaluated with respect to four key performance indicators: (I) biogas yield, (II) biogas quality, (III) COD and (IV) Volatile Solid (VS) removal. The following specified objectives were assessed:

i. Characterization of primary sewage sludge, inoculum, and industrial wastewater.
ii. Synthesis and characterisation of Biochar derived from sugarcane bagasse.
iii. Investigate the effect of municipal landfill leachate and sugar industry wastewater as co-substrates for AD.

iv. Investigate the effect of the addition of biochar to the anaerobic digestion process with respect to biogas yield.

v. Investigate the effect of ultrasonic pre-treatment of industrial wastewater on the anaerobic digestion process with respect to biogas yield and quality.

## 1.6 Research Outline

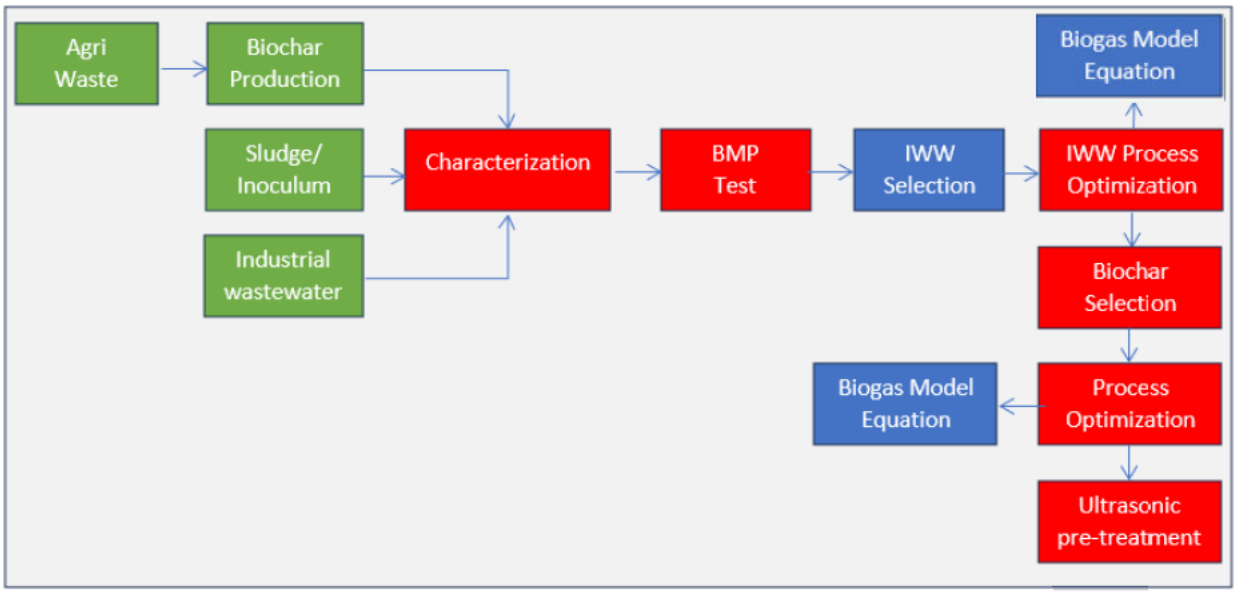


Figure 1-1: Research Outline

**Characterisation.**

The feedstocks were characterised to determine their suitability for anaerobic digestion—the biochar produced with respect to surface morphology and function group analysis, pH and EC.

- **BMP tests.**

BMP tests were conducted to evaluate the effects of each IWW on the AD process and to identify the best-performing IWW at predetermined operating parameters.

- **IWW process optimisation.**

The best forming IWW system was optimised using the BBD matrix derived from the RSM to plan the experiment. An empirical model was created by statistically analysing the findings. This model establishes the relationship between the input variables and the performance indicators of the AD system. The system was optimised using the co-substrate loading rate, initial substrate ratio (ISR), and temperature as parameters. The performance of the AD system

was evaluated with respect to COD and VS removal, as well as biogas yield and quality using established methodologies.

- **Biochar Selection.**

Batch tests were conducted to evaluate the effects of Biochar addition on the AD process. Biochars produced at varied pyrolysis temperatures were evaluated. The optimum operating parameters identified during IWW process optimisation were employed for this batch trial.

- **Biochar system optimisation**

Optimisation of the best-forming Biochar was conducted using the BBD matrix derived from the response surface methodology (RSM) to plan the experiment. An empirical model was created by statistically analysing the findings. This model establishes the relationship between the input variables and the performance indicators of the AD system. The system was optimized based on the co-substrate loading rate, Biochar loading, and temperature. The performance of the AD system was evaluated with respect to COD and VS removal, as well as biogas yield and quality using established methodologies.

- **Ultrasonic pretreatment.**

The effects of ultrasonic pretreatment of the industrial wastewater were investigated. The optimum operating (i.e., co-substrate loading, biochar loading, and temperature) conditions established by the Biochar System Optimization experimental were employed.

### 1.7 Thesis outline

This thesis consists of five chapters, which are outlined below.

**Chapter 1:** Presents a brief background on the issues pertaining to the supply of energy in South Africa and globally and contextualises the potential generation of biogas from the treatment of municipal and industrial wastewater. The shortcomings of biogas production through anaerobic digestion and potential enhancement mechanisms are highlighted. The research aims, objectives, and the research outline are also presented.

**Chapter 2:** Presents a literature review on the generation, treatment, and characterisation of municipal and industrial wastewater in South Africa, together with research conducted on biogas production via anaerobic co-digestion of municipal and industrial wastewater. The factors affecting the anaerobic digestion process are presented. The effect and application of biochar and ultrasonic pretreatment as potential enhancement mechanisms for the anaerobic

process are also discussed. Furthermore, an overview of Design of Experiments (DOE) and Response Surface Methodology (RSM), as well as its application as a statistical tool for optimising processes.

**Chapter 3:** Outlines the research methodology, materials, methods, instruments, and procedures employed in this study. The methodology utilised for process optimisation and data analysis is also addressed.

**Chapter 4:** Presents the discussion of the results obtained for each experimental run. The results are presented with respect to the stated objectives.

**Chapter 5:** Present the conclusion and recommendations; all the significant findings of this research are discussed. Recommendations for further research are also proposed.

# Chapter 2: Literature Review

## 2.1 Introduction

An extensive catalogue of literature focusing on various potential enhancement mechanisms for biogas production through anaerobic digestion exists. Among these mechanisms are pre-treatment methods, including microwave and thermal pre-treatments and ultrasonic and lysis pre-treatments, which are predicated on the facilitation of the hydrolysis of organic matter.
Anaerobic co-digestion is another well-established mechanism for enhancing the AD systems and involves the adding a co-substrate. If carefully selected, using a co-substrate could facilitate increased biogas production. However, the system must be optimised with respect to the co-substrate loading rate and operating conditions (i.e., process temperature) to avoid the excessive presence of inhibitors including volatile fatty acids, ammonia, and other intermediate products.

In this context, carbon conductive materials including Biochar and granular activated carbon as additives to the AD process has garnered much attention from researchers. This is because Biochar displays the ability to act as an adsorber of toxic inhibiting compounds; this property has been widely investigated and shown to successfully mitigate the accumulation of inhibitors coupled with several additional benefits to the AD process. In this light, Biochar as an additive in anaerobic co-digestion systems holds excellent potential for stabilising the ACD system and, by extension, the enhanced combability for biogas generation.
This chapter represents an in-depth overview of the AD process and the literature on the potential enhancement mechanisms for the production of biogas via the anaerobic/co-digestion of municipal and industrial wastewater, with a particular focus on ultrasonic pre-treatment and applicability of Biochar as a biochemical additive to the AD process.

## 2.2 Wastewater generation and wastewater treatment in South Africa

South Africa has approximately 821 registered wastewater treatment plant facilities (WWTP), 50% of which have a designed capacity of less than 0.5 Megalitres per day (ML/d) (Verlicchi and Grillini, 2020). These WWTPs have a total combined designed capacity of 6614 (ML/d) and receive approximately 5258 (ML/d), equating to 80 per cent of the total designed capacity.

Municipal wastewater (MWW) is generated from various domestic activities (i.e., bathing, laundry, ablution, and micturition). It is divided into three categories: (I) yellow-containing urine, (II) brown-containing flushed water and faeces, and (III) black-which is the amalgamation of yellow and brown, including active bacteria (Koul et al., 2022).

Due to its composition, MWW is hazardous and must be treated to avoid contamination of water resources and adverse effects on public and environmental health and safety. The aim of treating MMW is to improve its physical, microbiological, and chemical quality by reducing suspended and biodegradable organics content, nutrients (i.e., nitrates and phosphates), and pathogenic bacteria. MMW generally contains 99.9% water, with the remainder being solids; the general composition of MMW is represented in Figure (2-2) below.

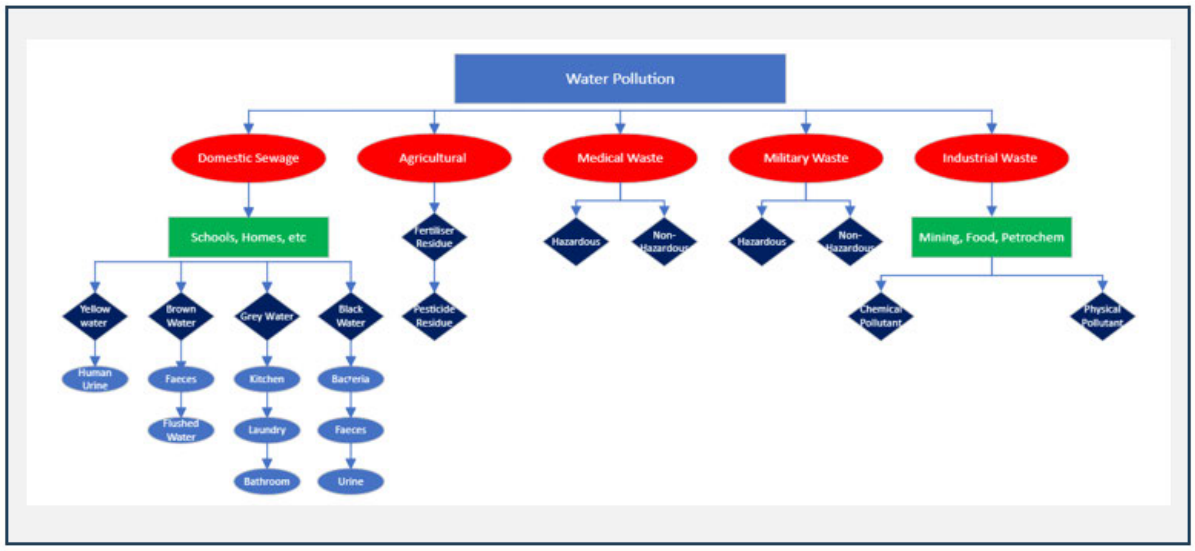


Figure 2-1: Water Pollution schematic (Koul et al., 2022).

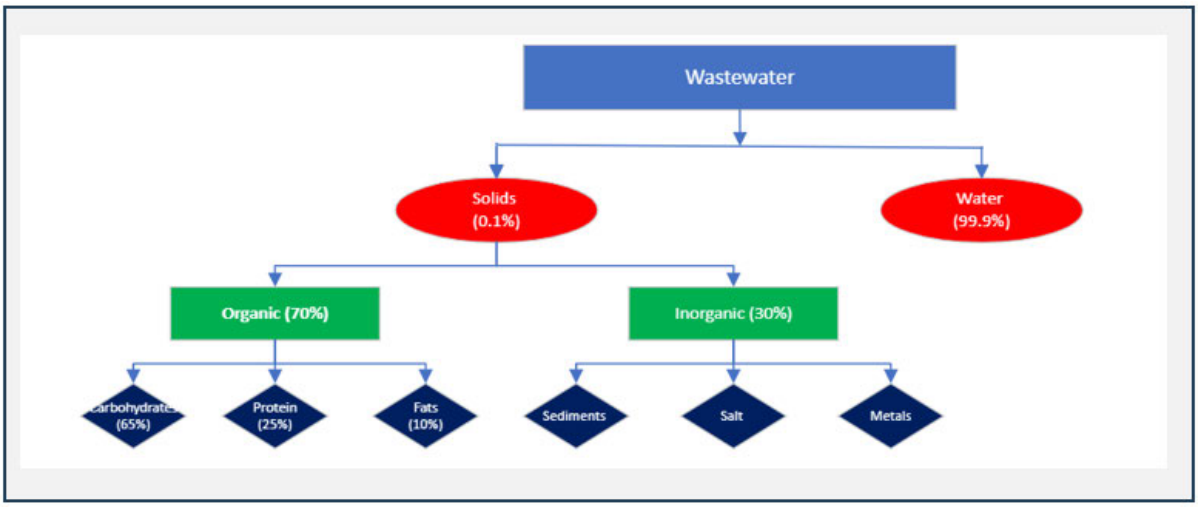


Figure 2-2: Physiochemical content of domestic wastewater (Koul et al., 2022).

The organic and inorganic constituents are used to measure the chemical quality of MWW: BOD, COD, VS and TS, total phosphorus and nitrogen, pH, and alkalinity are commonly considered parameters when measuring MW characteristics (Karim et al., 2007; Bachmann et al., 2015; Von Sperling, 2007). Table (2-1) below presents the characteristics of MWW.

Table 2-1: Chemical characteristics of domestic sewage (Qasim, 2017)

| Parameter | Concentration | | Description |
|---|---|---|---|
| | Range | Standard | |
| **COD (mg/l)** | 200 - 780 | 400 | The oxygen is required to stabilise the carbonaceous organic matter. |
| **BOD (mg/l)** | 110 – 400 | 210 | oxygen required to stabilise (through biological processes) the carbonaceous organic matter. |
| **TS (mg/l)** | 1800 – 370 | 730 | The total dissolved and suspended organic and inorganic solids. |
| **TN (mg/l)** | 85 - 20 | 40 | The total nitrogen including ammonia, organic nitrogen, nitrates and nitrites. |
| **Alkalinity ($CaCO_3$) (mg/l)** | 200 -50 | 100 | Indication of the buffering capacity (resistance to pH change) of the medium. Resulting from the presence of hydroxyl and carbonate ions. |
| **pH** | 7.5 – 6.7 | 7.0 | Indication of the basicity or acidity of the sample. |
| **TOC (mg/l)** | 290 -80 | 150 | Quantify the carbonaceous organic materials by converting organic carbon into carbon dioxide. |

The conventional treatment of MWW is divided into four phases which are preliminary, primary, secondary, and tertiary/advanced treatment.

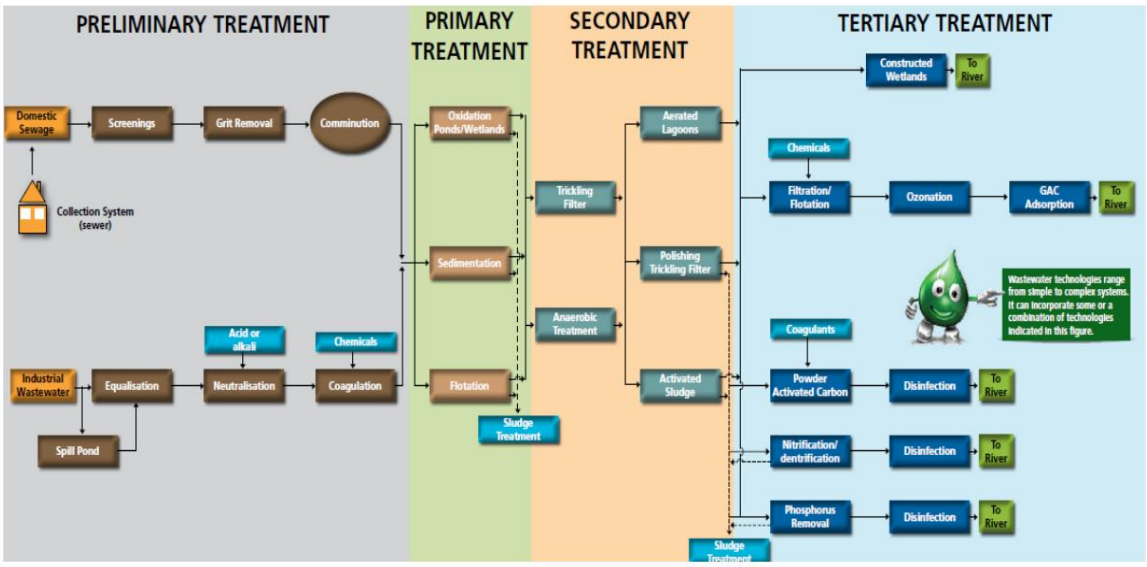


Figure 2-3: WWT process outline (Koul et al., 2022)

### 2.2.1 Preliminary Treatment.

Preliminary treatment involves removing suspended coarse particles and debris from the incoming wastewater stream. This is a critical treatment step as large, suspended debris and other foreign objects hinder subsequent operations and could cause damage to equipment such as pumps. Preliminary treatment removes nearly all non-organic solids (i.e., sand and grit) and up to 25 per cent of the organic load. The waste generated from this process is commonly landfilled. The incoming wastewater is screened before passing through the grit chambers. Grit chambers are used to reduce the formation and accumulation of excess sludge; this is achieved by reducing the incoming velocity of the wastewater, allowing for the settling of heavy suspended solids (Chynoweth and Pullammanappallil, 2020).

### 2.2.2 Primary Treatment.

This process removes fine suspended organic and inorganic particles via conventional sedimentation. Approximately 60 per cent of oil and grease and 70 per cent of the remaining suspended solids are oxidised and settled out during this treatment step. The effluent generated during this step is called primary effluent.

### 2.2.3 Secondary Treatment.

During this process, organic matter and other contaminants, such as ammonia, are further removed. Secondary treatment uses activated sludge. Organic matter and ammonia are broken down via biological processes brought on by mixing microorganisms into the wastewater.

Organic matter is digested by the microorganisms, producing water ($H_2O$) and carbon dioxide ($CO_2$). Ammonia ($NH_3$) is broken down into nitrates ($NH_4NO_3$) and nitrogen ($N_2$) as a result of oxygen uptake.

The primary treatment process pumps effluent into an aeration basin with anoxic and oxic zones. The anoxic zone is filled with microorganisms that are suited to anaerobic conditions and are aimed at nitrogen removal, while the oxic zone relies on excess oxygen ($O_2$) to stimulate beneficial oxygen-consuming bacteria, which are breakdown of organic matter.

### 2.2.4 Tertiary Treatment.

This step involves the disinfection of the effluent in preparation for reuse or discharge into natural water resources and facilitates the removal of turbidity, phosphorus, bacteria, and viruses. Disinfection is achieved through chemical and physical methods such as chlorination ozone and ultra-violet treatment.

## 2.3 The generation and treatment of Sugar industry wastewater.

The sugar industry is the most common of the agro-based industries and is especially prominent in developing countries in South America, Africa, Asia, and Asia. The industry serves as a source of job creation and contributes to the economic development of these developing nations (Fito et al., 2019).

Apart from sugar, the sugar industry generates many by-products, which are categorised into solids and liquids. The solid by-products include press mud (filter cake from juice clarification), while the liquids include molasses (from the sugar crystallisation process) and general wastewater from various other processes. The sugar manufacturing process consists of five key processes: juice extraction, clarification, crystallisation, and centrifugal separation. The manufacturing process is water intensive as many of the processing units require fresh water for their operation; approximately 1.5 $m^3$ of water is required to process a tonne of sugarcane intern, producing approximately 1 $m^3$ of wastewater (Sahu et al., 2015). The process and mill house are responsible for the majority of the water consumed during processing; the wastewater produced by the mill house is characterised by high oil, and solids content, while effluent produced by the process house is characterised by its elevated organic matter content evidenced by its high BOD and COD (Polestya et al., 2008). Figures 2-4 presents the general process outline for sugar production.

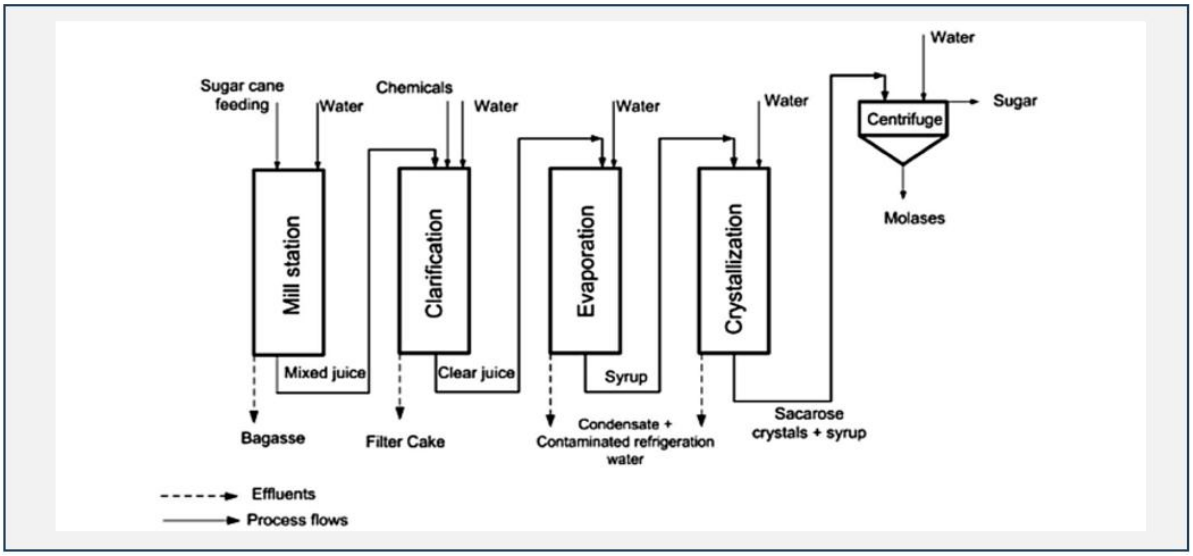


Figure 2-4: Sugar production process outline (Sahu et al., 2015)

The quality of the wastewater produced depends on the chemicals used during processing, the characteristics of the sugarcane, and the soil the sugarcane is grown (Sahu et al., 2015). Table (2-2) below presents the average physiochemical properties of the wastewater produced by the sugar manufacturing process.

Table 2-2: Physiochemical Properties of Sugar industry effluent (Sahu et al., 2015)

| Parameter | Unit | Range |
|---|---|---|
| COD (mg/l) | (mg/l) | 2150 – 1100 |
| BOD (mg/l) | (mg/l) | 1960 – 655 |
| TS (mg/l) | (mg/l) | 3050 – 2452 |
| Chloride | (mg/l) | 860 – 30 |
| Calcium | (mg/l) | 470 – 365 |
| Total Dissolved Solids | (mg/l) | 1915 – 1480 |
| Total Suspended Solids | (mg/l) | 790 – 220 |
| Conductivity (µS/cm) | (mg/l) | 925 – 540 |
| Oil and grease | (mg/l) | 134.4 – 88.7 |
| Alkalinity ($CaCO_3$) (mg/l) | (mg/l) | 100 |
| pH | (mg/l) | 8.4 -6.7 |

### 2.3.1 Traditional methods for the treatment of sugar industry wastewater.

Evaporation, bio-composting, and fertirrigation are common treatment methods.

#### 2.3.1.1 Evaporation

This process involves heating wastewater in specially designed boilers; steam generated from the process is used for energy production, while condensate generated can be treated and reused in the manufacturing process, supplementing the water required for manufacturing. The residue left after evaporation can also be used to prepare livestock feed (Christofoletti et al., 2013).
While this treatment method has its merits, there are several pitfalls to consider: (I) the fowling of the boilers due to the incrustation of the vapours produced, (II) spontaneous crystallisation caused by the increase in solids concentration, and finally (III) the high energy demand of the process, this property is most likely the largest pitfall of this method as it has significant cost implications (Christofoletti et al., 2013; Chopra et al., 2012 ).

#### 2.3.1.2 Bio-composting

Bio-composting involves mixing press mud/filter cake (produced from juice clarification) with sugar industry wastewater to produce organic manure (Latif et al., 2011). This method of treatment has the benefit of supplementing the demand for fertiliser hence reducing operating costs while at the same time reducing waste generation. However, there remain several pitfalls with this treatment method, with the most significant being the inability to deal with large volumes of wastewater due to extended treatment periods. A single treatment requires 15 days or more and large treatment areas (Fito et al., 2019).

#### 2.3.1.3 Fertirrigation

This process employs soil as a treatment medium and involves the irrigation of sugar industry wastewater onto agricultural fields (Chopra et al., 2012). This treatment method has the benefit of reducing fertilizer consumption and the use of irrigation water (Fito et al., 2019). This treatment process only applies to wastewater with low contaminant concentrations and often requires the pretreatment of the wastewater to avoid harm to both the crop and soil. Hence this method is not favoured and is seldom employed (Fito et al., 2019).

### 2.3.2 Biological treatment of sugar industry wastewater.

Sugar industry wastewater (SIWW) biological treatment technologies have been extensively studied. Biological treatment utilises microorganisms to transform the organic portion of the wastewater into $CO_2$ $H_2O$, while simultaneously utilising the contaminants in the wastewater

to promote the growth of microorganisms (Fito et al., 2019; Valderrama et al., 2002; Akpor, 2014).

Aeration and anaerobic digestion are effective SIWW treatments due to its high sugar and volatile acid content (Nacheva et al., 2009).

#### 2.3.2.1 Aerobic treatment

Aerobic treatment entails organic matter degradation in oxygen rich conditions including processes such as the use of trickling filters, activated slime, and aerated bayous have been extensively used to treat SIWW (Velásquez et al., 2019). While the SIWW is easily degraded, the fats and oils present are not degraded due to methane generation during hydrolysis (Kushwaha et al., 2011). Previous research into the aerobic treatment of SIWW has affirmed this process's merits and capacity for effectively removing pollutants. For example, Hamoda and Al-Sharekh reported substantial COD reductions of 67.8 percent in their aerobic reports on laboratory-scale research.

#### 2.3.2.2 Anaerobic treatment

Anaerobic treatment refers to the decomposition of organic substances by microbes in an environment devoid of oxygen. An advantage of this procedure is the production of biogas as a by-product. Various types of reactors are commonly employed, such as batch, fixed-bed (AFR), up-flow anaerobic fixed bed (UAFB) reactors, and up-flow anaerobic sludge bed (UASB) reactors (Ramjeawon and Baguant, 1995).

The anaerobic reports on laboratory-scale testing conducted by revealed decreases in COD (Chemical Oxygen Demand) of 81.8%, 89%, and 74%, respectively (Ramjeawon and Baguant, 1995).

## 2.4 The Generation and Treatment of Municipal Landfill Leachate.

Landfill leachate is generated through physical, chemical, and biological processes during municipal solid waste (MSW) degradation. Rainwater percolation through the waste body resulting in the degraded matter leaching; hence, landfill leachate refers to the effluent generated by the percolation of rainwater through degrading waste disposed of in a landfill (Youcai, 2018; Costa et al., 2019). The leachate's composition depends on several factors, including age, regional climate, site hydrology, and waste composition (Somani et al., 2019). Inorganic compounds (nitrates, ammonium, chlorides), xenobiotic compounds (phthalates,

benzene, phenols), metals (mercury, copper, lead, zinc), and organic matter (fatty acids, organic carbon) are the four main constituents of landfill leachate (Ramakrishnan et al., 2014).

Landfill leachate is categorised into three categories: (I) young, (II) intermediate, and (III) old. Young landfill leachate is generated by landfills between 1-5 years old characterised by high volatile acid and organic matter content, low pH, and high biodegradability, while old landfill leachate generated by landfills between 10 ≤ years old is characterised by high pH, the organic matter present is generally in the fulvic and humic fractions (Mojiri et al., 2020). Table (2-3) below presents the leachate characteristics and biodegradability.

Table 2-3: Physiochemical properties of Landfill leachate (Tejera et al., 2019)

| Parameter | Unit | Young | Intermediate | Old |
|---|---|---|---|---|
| **COD** | **(mg/l)** | ≈ 10 000 | 10 000 - 5000 | ≤ 5 000 |
| **$BOD_5$/COD** | **-** | 1.0 - 0.5 | 0.5 – 0.1 | > 0.1 |
| **$NH_3$ - N** | **(mg/l)** | ≤ 400 | - | ≥ 400 |
| **Biodegradability** | **-** | High | Medium | Low |
| **pH** | **(mg/l)** | 6.5 | 7.5 – 6.5 | > 10 |

### 2.4.1 Traditional methods for the treatment of landfill leachate.

Recirculation, biological, and transfer to WWTPs are well-established treatment techniques for landfill leachate and are favoured for their low treatment cost and convenience, while physical and chemical treatment methods, including membrane separation and coagulation/flocculation, have also been extensively used (Teng et al., 2021).

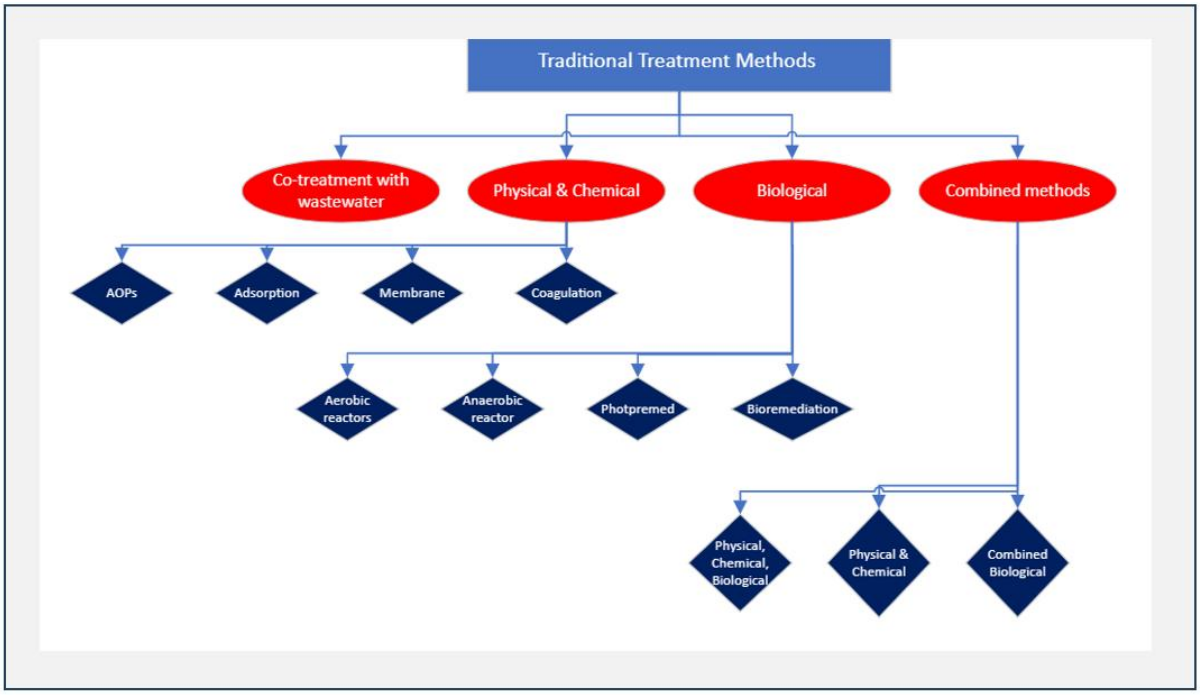


Figure 2-5: Traditional leachate treatment methods (Abdel-Shafy et al., 2024)

2.4.1.1 Recirculation

Leachate recirculation involves the reintroduction of the leachate into the landfill waste body through irrigation and other similar methods and is often used in conjunction with other treatment methods. However, this treatment method's effectiveness depends on the volume and frequency of use, as frequent use results in refractory substance accumulation in the leachate, posing further challenges for subsequent treatment and may also affect the landfill's stability (White et al., 2011).

2.4.1.2 Transfer to WWTPs.

This treatment method involves the discharge of the leachate to municipal WWTPs common for leachate treatment and management (Dereli et al., 2020). Among its merits, combined leachate and domestic wastewater treatment has been shown to increase the biological treatability of the leachate through its ability to balance the nutrient compositions and the dilution of pollutants and toxic compounds. Table (2-4) below summarises this treatment method's merits and disadvantages.

Table 2-4: Transfer to WWTPs merits and disadvantages (Dereli et al., 2020)

| Merits | Disadvantages |
|---|---|
| Dilution increases biological treatability | Increase operational cost at the WWTP due to higher nitrogen and organic matter loading. |
| Enhanced efficiency of biological treatment due to nutrient balancing (COD:TP, etc.) | No compliance with effluent discharge limits |
| Reduced capital investment cost by utilising established infrastructure. | Increase sludge production. |

In light of the challenges faced by this treatment method, much research has been conducted on evaluating potential methods to mitigate the accumulation of inhibitory compounds. Chief among these is the use of additives such as carbon-conductive materials. The adsorptive property facilitates the adsorption of inhibitory substances such as heavy metals.

2.4.1.3 Biological treatment.

This process involves the biodegradation of contaminants via metabolic microorganism activity and is favoured for its cost-effectiveness. This method facilitates organic compounds and nutrient removal from the leachate; however, it is inefficient for the removal of inorganics such as metals and non-biodegradable organics (Mojiri et al., 2020).

Biological treatment is separated into two main categories: (I) aerobic and (II) anaerobic treatments. Aerobic is the most used biological treatment method and is often facilitated by the continuous aeration of leachate in large lagoons with activated sludge. This process relies on the elimination of organic matter by protozoa, bacteria, and fungi and is efficient in ammonia stripping while exhibiting low sensitivity to toxic substances (Torretta et al., 2016).

AD of the leachate is generally selected for young leachate treatment because of its high biodegradability.

2.3.1.4 Coagulation and Flocculation.

Coagulation involves colloidal suspension/solution destabilisation, while flocculation involves the agglomeration of the destabilised particles from the coagulation process into larger flocs (Kamaruddin et al., 2017). The process has been shown to remove heavy metal and organic

pollutants effectively; however, his less effective for ammonium and nitrate removal (Torretta et al., 2016). Aluminium sulphate (Alum) and poly-aluminium chloride are used for landfill leachate treatment. Ghafari et al. 2009 found that poly-aluminium chloride and alum remove 43.1% and 62.8% of COD, respectively, while coagulation/flocculation removes 86%.

One of the major pitfalls is the generation of excessive sludge and the accumulation of trace metals in the effluent stream (Torretta et al., 2016).

## 2.5 Anaerobic Digestion and the Principals of Biogas Formation

AD is a well-studied process that produces biogas by microorganisms degrading and converting organic materials low oxygen conditions. These micro-organisms break down complex organic molecules (proteins, polysaccharides, fats, cellulose, hemicellulose) into biogas; bio-methane (55-70%) and $CO_2$ (30-40%) along with hydrogen sulphide ($H_2S$), nitrogen ($N_2$), and water vapour (Sihlangu *et al.*, 2024).

AD has four main phases. First, hydrolysis, then acidogenesis, acetogenesis, then methanogenesis (Khanh Nguyen et al., 2021). Facultative and obligate anaerobic bacteria facilitate the hydrolysis and acid fermentation steps while the microorganisms, including Methanothrix, Methanosarcina, Methanococcus, Methanobacillus, and Methanobaterium are responsible for methane conversion (Walter et al., 2018). The Methanosarcina and Methanothrix use the acetate produced during the acetogenesis step to produce $CH_4$ and $CO_2$, while the Methanobacterium, Mathanococcus, etc., are responsible for hydrogen oxidisation using $CO_2$ as an electron acceptor (Senés-Guerrero et al., 2019). Figure (2-6) below represents the AD biogas formation pathway schematic.

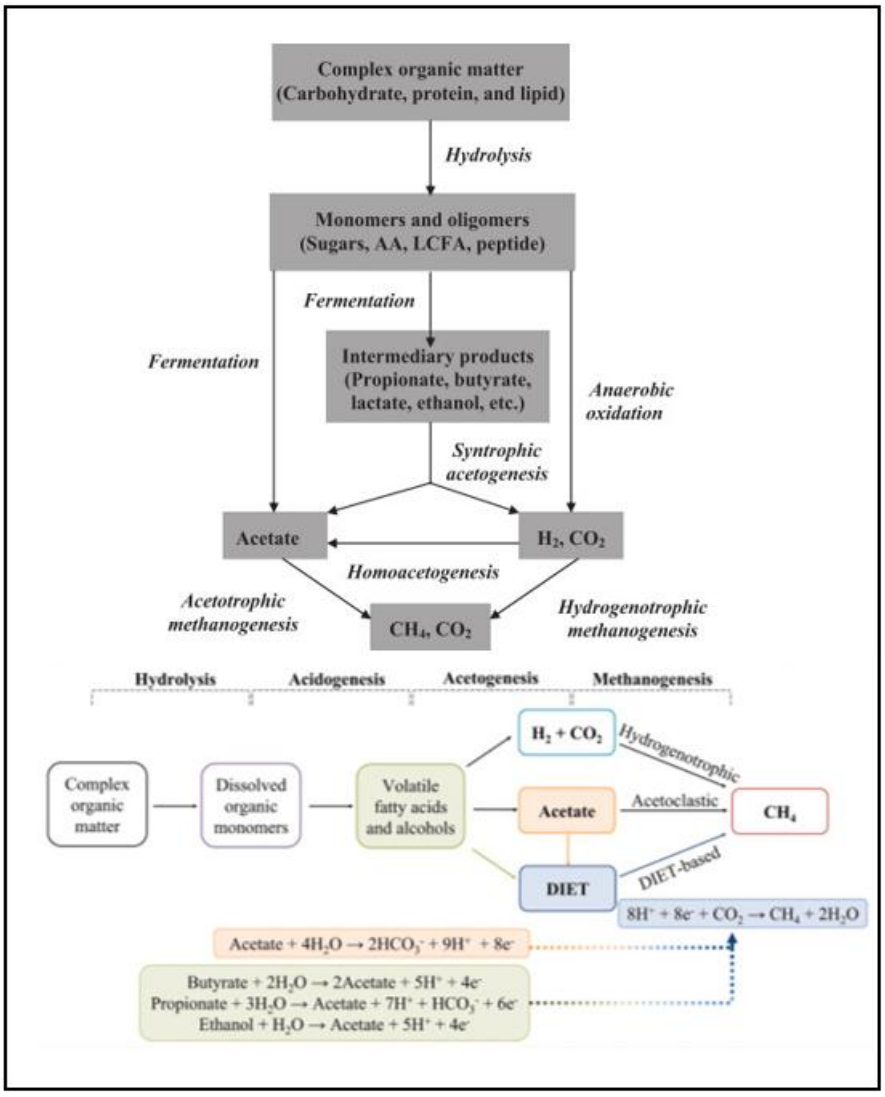


Figure 2-6: AD biogas formation pathway (Kutlar et al., 2022).

### 2.5.1 Anaerobic digestion Mechanism

2.5.1.1 Hydrolysis

The first step of the AD process entails the degradation of complex organic matter into soluble compounds facilitated by extracellular enzymes and water (Wright and Uddin, 2022). Macromolecules such as lipids, proteins, carbohydrates, and proteins are hydrolysed into sugars (monosaccharides and disaccharides), amino acids, alcohols, and LCFA by extracellular proteases, lipases, and cellulases produced by fermentative bacteria (Karrabi et al., 2023). Process conditions, including temperature, biomass particle size concentration, characteristics, and pH, have been shown to affect the solubilisation rate (Wright and Uddin, 2022).

The hydrolysis process is significant in the kinetics of AD and is the rate-limiting step; hence, researchers have placed much focus on evaluating potential enhancement methods for improving the rate of hydrolysis (Luo et al., 2012). Equation 2-1 below details the general hydrolysis reaction.

$$(C_6H_{10}O_5)n+nH_2O \rightarrow nC_6H_{12}O_6+nH_2$$

Equation 2-1

2.5.1.2 Acidogenesis

Acidogenesis (the fermentation step) involves the degradation of the soluble compounds produced during hydrolysis. The acidogenic bacteria (acidogens) absorb monosaccharides and disaccharides, amino acids, and LCFA to produce VFAs, ethanol, ammonia, lactic acid, hydrogen sulphide, carbon dioxide ($CO_2$) and hydrogen ($H_2$). Acetic acid ($CH_3OOH$) is considered the most important of the VFAs produced as it is primarily used by the methanogenic bacteria for methane production ($CH_4$) during the methanogenesis step (Anukam et al., 2019). While LCFA is oxidised using hydrogen ions as electron acceptors, acidogenesis of amino acids and sugars occurs without needing an electron donor or acceptor (Thanarasu, Periyasamy and Subramanian, 2021).

It is challenging to distinguish between the acidogenic and acetogenic reactions as they are both responsible for $H_2$ and $CH_3COO$-(acetate) production. Species including Pepto coccus, desulfomonas micrococcus, Escherichia, and streptococcus have been identified in the AD process; however, the predominant species present is heavily influenced by the feedstock characteristics. Presented in equations 2-2 to 2-4 are the sequence reaction steps for the acidogenesis step.

$$C_6H_{12}O_6 \leftrightarrow 2CH_3CH_2OH+2CO_2$$

Equation 2-2

$$C_6H_{12}O_6+2H_2 \leftrightarrow 2\ CH_3CH_2COOH+\mathbf{2}H_2O$$

Equation 2-3

$$C_6H_{12}O_6 \rightarrow 3CH_3COOH$$

Equation 2-4

2.5.1.3 Acetogenesis

Acetogenesis involves the production of acetate by the conversion of the organic acids produced in the acidogenesis step. The primary by-products of this conversion are $H_2$ and $CO_2$; hence, acetogenesis is also termed the dehydrogenation stage/step (Wright and Uddin, 2022). Due to its inhibitory effects on the acetogenic bacteria metabolism, $H_2$ concentrations must be kept low. Hence, acetogens depend on the consumption of $H_2$ and acetate by the methanogenic bacteria; this syntrophic relationship allows the thermodynamic feasibility of the acetogenesis step.

The transfer of $H_2$ facilitates electron transfer through interspecies hydrogen transfer (IHT); the electron transfer rate is strongly linked to the overall digestion rate (Bajpai, 2017). Presented in equations 2-5 to 2-7 are the sequence reaction steps for the acetogenesis step.

$$CH_3CH_2COO^- + 3H_2O \leftrightarrow CH_3COO^- + H + HCO_3^- + 3H_2$$

Equation 2-5

$$C_6H_{12}O_6 + 2H_2O \leftrightarrow 2\ CH_3COOH + 2\ CO_2 + 4H_2$$

Equation 2-6

$$CH_3CH_2OH + 2\ H_2O \leftrightarrow CH_3COO^- + 3\ H_2 + H^+$$

Equation 2-7

Equation 2-5 to 2-7 depicts acetate production ($CH_3COO^-$) and ($H_2$), which methanogenic bacteria use for $CH_4$ formation in the methanogenesis step; Methanobacterium propionicum and Methanobacterium suboxydans facilitate acid phase product decomposition to ($CH_3COO^-$) and ($H_2$) (Anukam et al., 2019). $CH_3COO^-$ is a crucial intermediary product as its reduction accounts for 70% of the $CH_4$ formed during the AD process; the acetogenesis is responsible for 25% of the $CH_3COO^-$ formed and 11% of the $H_2$ formed (Anukam et al., 2019). Obligate hydrogen-producing acetogens are responsible for the breakdown of VFA formed in the acidogenesis step.

2.5.1.4 Methanogenesis

Methanogenesis is the final step of the AD process and involves the conversion of $CH_3COO$H and $H_2$ to $CH_4$ and $CO_2$ by methanogenic anaerobic bacteria known as methanogens. Methanogens are strict anaerobes and are highly susceptible to even low oxygen concentrations (Anukam et al., 2019). Some of the methanogenic species found in the AD system are M. marinsnigri, Methanogenium cariaci, Methanobrevibacter ruminantium, M. thermoautotrophicum, and M. bryantic; these methanogens are characterised by slow growth and are highly susceptible to environmental changes (Schink, 1997). The preceding AD steps mainly involve converting complex organic molecules to simpler organic molecules, while the methanogenic step involves the removal of organic pollutants, including COD and BOD. Thus, this step's efficiency is measured by organic pollutant removal (Bajpai, 2017). Methanogenesis sequence reaction stages are below.

$$CH_3COOH \rightarrow CH_4 + CO_2$$

Equation 2-8

$$CO_2 + 4H_2 \rightarrow CH_4 + 2H_2O$$

Equation 2-9

$$2CH_3CH_2OH + CO_2 \rightarrow CH_4 + 2CH_3COOH$$

Equation 2-10

Shown in Equation 2-8 is the formation of $CH_4$ and $CO_2$ by the conversion of $CH_3COOH$. Equation 2-9 shows the reduction of $CO_2$ *to* $CH_4$ *by* $H_2$, while Equation 2-10 shows the formation of $CH_4$ through $CH_3CH_2OH$ decarboxylation (Goswami et al., 2016). The main pathways to methanogenesis are: (I) Methylotrophic methanogenesis, which involves the decarboxylation of methyl amines, methyl alcohols, and methyl sulphides (II) Hydrogenotrophic, which involves the production of methane through $CO_2$ reduction by $H_2$ and finally (III) acetotrophic methanogenesis which involves the decarboxylation of acetate or methane formation (Goswami et al., 2016). Figure 2-7 represents the three main pathways of conversion.

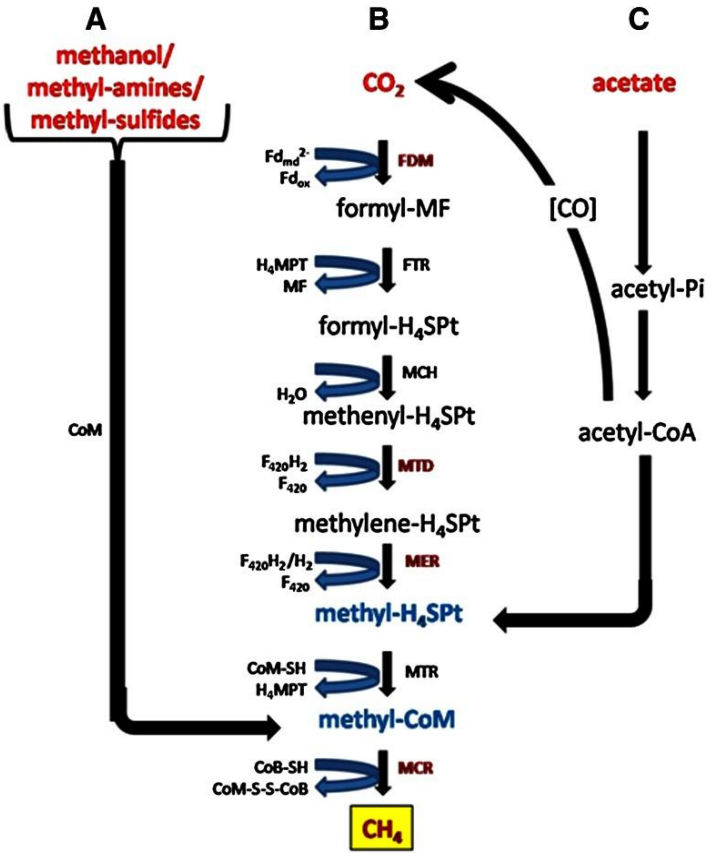


Figure 2-7: An overview of physio-chemical mechanisms of biogas production by microbial communities (Goswami et al., 2016)

Hydrogenotrophic methanogenesis (represented by path B in Figure (2-7)) involves converting $CO_2$ into $CH_4$ and $H_2O$. The $CO_2$ is bound to methanofuran to form a formyl group; three cofactors receive the carbon (I) Tetrahydromethanopterin ($H_4$MPT), (II) Coenzyme F420 (8-hydroxy-5-deazaflavin) and (III) coenzyme M (HS-CoM) (Mercaptoethanesulfonic Acid). Coenzyme B (HS-CoB) acts as the final electron acceptor. The process is dependent on hydrogen ion concentration and sodium serving as an electron donor from $CO_2$. It is responsible for Adenosine Triphosphate (ATP) synthase, which is responsible for methanogen energy production (Goswami et al., 2016). Hence, in contrast to other microbes, sodium ions are required for methanogen growth.

Acteoclastic methanogenesis shows methanogenesis from acetate. Cofactors Coenzyme M (HS-CoM) produce methane and are dependent on Na and $H_2$ concentrations (Goswami et al., 2016). Acetate methanogenesis produce coenzyme M-HTP heterodisulphide (CoM–S–S–CoB). In contrast to hydrogenotrophic methanogenesis, which has $H_2O$ as a by-product.

## 2.6 Factors affecting the Anaerobic digestion.

### 2.6.1 Temperature

The AD process temperature greatly affects biogas quality and quantity. The three main temperature ranges considered for the AD process are psychrophilic (12$^{o}$C to 24$^{o}$C), mesophilic (35$^{o}$C to 42$^{o}$C), and thermophilic (45$^{o}$C to 60$^{o}$C). Likewise, the anaerobes are divided into three categories: (I) Psychrophiles, which are prominent in the psychrophilic digestive regime and are active in temperatures ranging from (12$^{o}$C to 24 $^{o}$C); (II) Mesophiles, which are prominent in the mesophilic digestive regime and are active in temperatures ranging from (22$^{o}$C to 40 $^{o}$C) and (III) Thermophiles which are prominent in the thermophilic digestive regime and are active in temperatures ranging from (50$^{o}$C to 60 $^{o}$C) (Steiniger et al., 2023). Figure (2-8) shows the methanogen activity at each temperature regime.

Because of comparatively low energy demand, anaerobic digesters in WWTPs are typically operated in the mesophilic temperature range (Qasim, 2017). Research has shown digesters operated under mesophilic conditions to be less prone to changes in operating conditions i.e. organic loading rate and temperature (Kim et al., 2002). It exhibits improved process stability compared to digesters operated at thermophilic conditions. However, digesters operated under thermophilic conditions typically show improved pathogen destruction, a higher rate of volatile solids removal, increased anaerobe growth, and biochemical reaction rate. Thermophilic digestion has also been shown to enhance interspecies hydrogen transfer (IHT), increasing methanogenic potential and shorter HRT (Zábranská et al., 2000). Research conducted by De Vrieze et al. (2016) showed increased nutrient and energy recovery when sewage sludge was digested under thermophilic conditions.

While researchers have shown thermophilic digestion to be more efficient with respect to virus and pathogen destruction and biogas yield, thermophilic digestion has also been shown to result in increased VFAs concentrations, affecting process stability and ultimately leading to process failure (Al Sulaimi et al., 2022). Al-Sulaimi et al., 2022 found primary sludge to be more susceptible to VFA accumulation under thermophilic conditions due to its increased mineralised organics concentration compared to secondary sludge. Studies conducted by Blake et al., (2005) found mesophilic conditions produced increased $CH_4$ production rates when compared to other process temperature regimes.

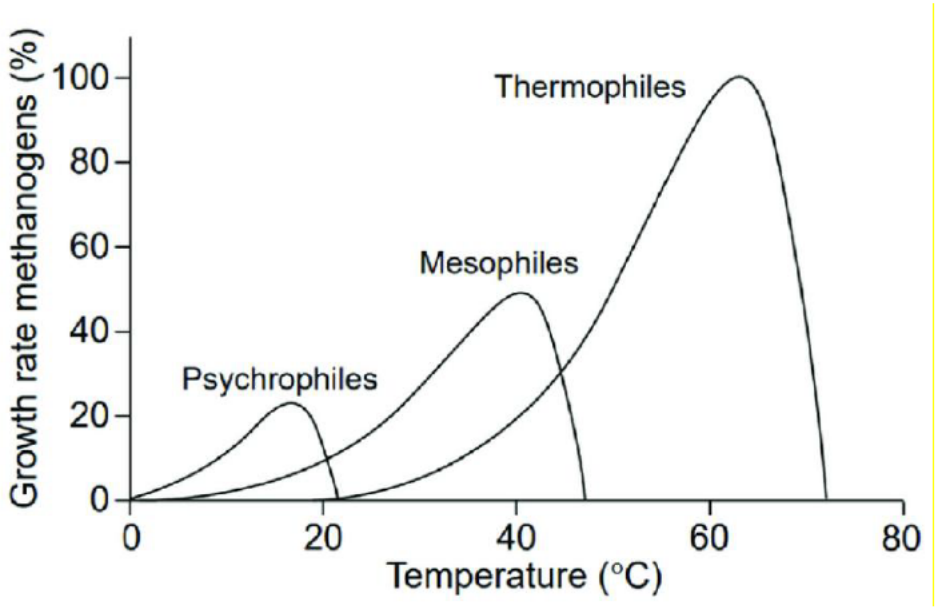


Figure 2-8: Growth rate of methanogenic bacteria vs temperature (Nozhevnikova et al., 2001)

### 2.6.2 pH

The pH at which the AD process is conducted affects biogas production anaerobe growth and anaerobe growth. The pH value depends on the ratio between the digester's alkalinity, acidity, and $CO_2$ in the digester (Chauhan et al., 2018). Methane formation generally occurs between the pH of 6.5 and 8.5, with the optimum between 7.0 to 8.0. In contrast, pH < 6.0 and those exceeding 8.5 have been shown to decrease microbial activity and inhibit digestion, resulting in decreased biogas yield (Weiland, 2009). According to Weiland (2009), the release of free hydrogen ions by fermentation/hydrolysis products (hydrocarbon acidification, VFA, and proteins) affects the pH of the AD process.

A pH increase is often linked to the accumulation of ammonia, while a decreasing pH is often associated with the accumulation of VFAs; increased propionic acid concentration is an early indication of the acidification of the digester and results in a pH decrease and increased $CO_2$ concentration in the biogas produced (Sinervo, 2017).

### 2.6.3 Substrate composition

Studies have identified biomass consisting primarily of proteins, carbohydrates, fats, hemicellulose, and cellulose as suitable feedstock for anaerobic digestion (Bhajani, 2022). The rate of degradation and retention time of AD is feedstock dependent: lignocellulosic biomass (agri-waste) is comprised mainly of lignin, hemicellulose, and cellulose and presents a biomass structure that is highly resistant to biological degradation, resulting in long retentions times and

poor biogas production (Paul & Dutta, 2018). Physiochemical properties such as COD, BOD, TS, VS, and C: N ratio are regarded as key indicators for a feedstock biomethane potential (Bhajani, 2022).

### 2.6.4 Total solids and Volatile solids

The TS and VS content of feedstock are regarded as indicators of the rate of conversion of the AD system; TS is the measure of the total solids content, while VS indicates the organic matter (matter available for biogas conversion) content of the feedstock (Ibro et al., 2022). High TS content is often associated with VFA accumulation and lower biogas yield; in contrast, high VS content is associated with increased biogas yield (Wang et al., 2020).

Ahmadi-Pirlou and Mesri Gundoshmian (2021) discovered that biogas production from anaerobic digestion of sewage sludge increased 64% at 5% TS compared to 25% TS.

### 2.6.5 Organic loading rate (OLR)

The OLR represents the organic content fed to the reactor or digester and is generally expressed in grams VS of COD fed per day or unit time. The optimum OLR of an AD system is dependent on the feed substrate composition and biochemical activity. Past research has shown a strong correlation between OLR and biogas yield; increased OLR is linked to increased biogas yield; however, overloading the reactor/digester results in inhibitory intermediary products accumulating and a decrease in biogas yield (Ibro et al., 2022).

### 2.6.6 Hydraulic Retention Time

HRT is the time the feedstock is held in reactor. Research has shown AD effluent quality improvement with increased HRT; however, increased HRT is also associated with a decreased reaction rate (Ibro et al., 2022). The decreased reaction rate is attributed to the VFA accumulation, while the accumulation of acetic acid has been linked to shorter retention times. The optimal HRT depends on feedstock composition and process parameters like temperature and OLR. Studies reveal that at optimal HRT, most digestive biogas is produced between weeks 3 and 4. The average duration for the AD of sewage sludge is between 10 - 20 days. Based on most research, 90% of methane production can be obtained within 14 days of therapy (Appels et al., 2008).

### 2.6.7 Inoculation

Inoculation is the process of introducing acclimated anaerobes to a digester/reactor in the form of digestate/seed sludge to accelerate the digestion process. An effective inoculum must have a diverse consortium of microbes capable of degrading a broad range of feedstocks; digested WWT sludge is often utilised as inoculum for AD processes. Inoculum serves as a reserve of micronutrients and nitrogen, which balance the C/N while facilitating enzymatic activity. Xu et al. (2013) correlated xylanolytic and cellulolytic bacteria presence in the inoculum and increased biomethane yield when co-digestion corn stover with dairy waste effluent.

The careful determination of an optimal inoculum substrate ratio (ISR) is of utmost importance for mitigating VFA generation throughout the anaerobic digestion process, aiming to maximise methane production. Excessive ISR ratios have been found to exert an overwhelming burden on microbial populations. In contrast, decreased ISR leads to increased reactor volume demands and reduced methane ($CH_4$) production (Dixon et al., 2019). However, compared to ISR ratios of 1:1 and 2:1 during wet AD, the ISR ratio of 0.3 resulted in the lowest $CH_4$ production.

## 2.7 Enhancing the anaerobic digestion process

The intrinsic complexity of AD is associated with diverse bacterial consortia and the precise balance that needs to be maintained during each stage of the digestion process. Enhancing the rates at which complicated substrates degrade has conventionally been linked to the utilisation of pre-treatments. Managing nutrient balance has typically included adding co-substrates through anaerobic co-digestion (ACD) to avoid the build-up of harmful substances and improve the production of biogas.

### 2.7.1 Anaerobic co-digestion

Co-digestion entails combining various substrates to create the feed solution for anaerobic digestion (AD). The justification behind its extensive usage revolves around maximising the anaerobic environment and adjusting the feed's stoichiometry to optimise the degree of degradation achieved (Effenberger et al., 2016). Enhancing digestion efficiency with respect to reducing VS and generating biogas often entails mitigating factors that inhibit anaerobic digestion processes.

The focus of research on anaerobic co-digestion has primarily revolved around optimising biogas generation, economic viability and the cost-to-energy output ratio. Economic viability

of the anaerobic co-digestion heavily depends on optimising energy outputs (Silvestre et al., 2014). Co-digestion typically augments biogas production through beneficial synergistic effects in the digestion medium. This is mainly attributed to the supplementation of deficient nutrients in the feedstock (Mata-Alvarez et al., 2000); furthermore, ACD modifies the C/N ratio. The fundamental principle of ACD is the digestion of a Low C/N ratio substrate and a high C/N ratio (Ward et al., 2008). In their study, Luste and Luostarinen (2010) noted a significant disparity in methane production potential based on VS concentrations of sewage sludge and grease trap waste. Specifically, they measured methane generation levels of 263 $LCH_4$/kg VS added for sewage sludge and 918 $LCH_4$/kg VS added for grease trap waste. The variations in methane potentials associated with volatile solids provide complexity to the optimisation of AD biogas generation. This underscores the importance of carefully selecting diverse substrates for co-digestion. Moreover, it is shown that the kinetics of biological processes, namely the parameters related to them, exhibit significant variations depending on the organic composition of feedstocks. As indicated before, the increased production of biogas facilitated by co-digestion might be attributed to an additional mechanism: the potential reduction of inhibitory conditions. The decrease in efficiency within the microbial group of AD directly influences the decomposition of organic matter, thereby hindering biogas generation. Therefore, it is crucial to avoid circumstances that hinder the biogas production process in order to maximise its efficiency. To prevent inhibitory effects in co-digestion processes, there are two methods that can be employed: either neutralising the inhibitors in one of the substrates or utilising the synergistic interactions between different substances, which can result in positive consequences.

Despite the numerous benefits associated with co-digestion, researchers have found challenges in its implementation, resulting in system disturbances which often arise from inadequate substrate ratios and suboptimal operating circumstances. A study conducted by Wan et al. (2007) demonstrated the challenge of digestive system malfunction. Astals et al. (2018) provided additional evidence supporting this conclusion since their research demonstrated that the introduction of crude glycerol at a concentration of over 4% into the digester decreased methane output. Wan et al. (2007) suggest that using a short HRT.
may cause digestion failure by removing microorganisms during the disposal of treated wastewater.

### 2.7.2 Pretreatment Methods.

The most extensively researched topic in literature pertains to the utilisation of pre-treatments to enhance hydrolysis. Microwave and thermal pre-treatments, acid-alkaline media utilisation, and mechanical techniques, including high pressure, ultrasound, chemical oxidation, and electrooxidation, are a few examples of diverse methods aimed at enhancing the rate of degradation of the substrates (González et al., 2018).

Figure 2-9 illustrates various pre-treatments and their potential combinations to enhance the effectiveness of solubilisation and disruption of organic molecules.

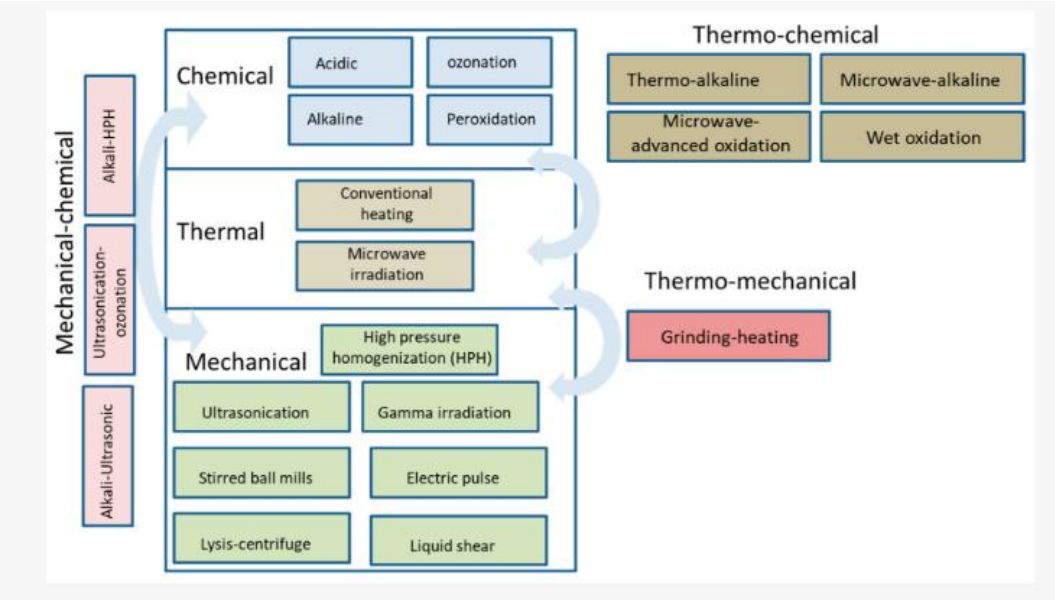


Figure 2-9: Pretreatment methods (Khanh Nguyen et al., 2021)

#### 2.7.2.1. Ultrasonic Pre-treatment

The application of ultrasonication has been thoroughly researched and proven to be a highly effective mechanical pretreatment technique to increase biodegradability of AD feedstock and relies on disruption of the feedstock macrostructure facilitated by hydro-mechanical shear stresses within cavitation (Khanh Nguyen et al., 2021). Ultrasonication has several effects on the feedstock, including particle size reduction, increased organic compounds solubilisation, biological activity stimulation, and the release of enzymes, and has been observed to have an impact on the size distribution of COD particles (Guo et al., 2013). Ultrasonication caused a shift in the peak of the particle size distribution from the particulate fraction, which typically consists of particles > 1600 nm, to the lowest size range, where particles are < 2 nm.

Factors such as sonication time and frequency are crucial factors to be considered. a study by Appels et al (2008). found a 40 and 15% increase in biogas yield when low and moderate-specific energy inputs were applied, respectively. Further, Dewil et al. (2006) found that ultrasonically pretreated WAS presented improved dewaterability, decreased volume and induced the release of COD. Ultrasonication has been identified as the predominant pretreatment method for improving biogas generation during anaerobic digestion of MWW.
Nevertheless, a significant disadvantage of ultrasonication pretreatment is the considerable expenditure of energy (Yusaf & Al-Juboori, 2014). In addition, it should be noted that not all research has reported consistent findings regarding the improvement of biogas generation and VS reduction with the application of ultrasonication; a minimal increase in $CH_4$ generation and VS reduction following the ultrasonication of WAS under mesophilic conditions (Sandino et al., 2005).

#### 2.7.2.2. High-pressure homogenisation (HPH)

The HPH pretreatment method involves the application of a sudden and intense pressure gradient exceeding 500 bar, which leads to cavitation, severe shearing forces, and high turbulence, followed by depressurisation. This process results in increased SCOD concentration and the disintegration of large molecules through hydrolysis (Nabi et al., 2019). Zhang et al. (2015) found that 30 MPa high-pressure homogenization (HPH) was the most energy-efficient. A suspension (SS) with 2.48% total solids (TS) underwent one homogenization cycle. The greatest COD of 43.94% was reached at 80 MPa pressure and four homogenisation cycles for sludge with a TS of 9.58 g/L. HPH has been shown to increase biogas production and reduce volatile sulphur compounds that cause odour in municipal waste sludge digester headspaces, but it has little effect on pathogen elimination during AD (Ariunbaatar et al., 2014).

#### 2.7.2.3. Microwave Irradiation

Microwave irradiation pretreatment occurs within the wavelength range of 1 mm to 1 m, which corresponds to frequencies greater than 300 MHz but less than 300 GHz. This method boosts biogas generation by 50%. Effective organic compound dissolution increases biogas yield (Khanh Nguyen et al., 2021). Gil et al. (2018) found that semi-continuous microwave pretreatment increased methane generation by 20% and SS biodegradability by 70%.

Microwave pre-treatment affects primary and secondary sludge digestion. A 3.2-fold increase in soluble COD to total COD and a 41% decrease in volatile solids yield (Khanh Nguyen et al., 2021).

#### 2.7.2.4. Chemical pretreatment

Chemical pretreatment is a highly effective technique for breaking down complex organic waste. This process involves the use of chemical reagents including alkalis, acids, and oxidants to enhance the hydrolysis of SS. Additionally, it enhances the biodegradability of cellulose, increasing the generation of biogas (Khanh Nguyen et al., 2021). Various chemical procedures have been investigated for AD, such as acid, alkali pretreatment, and ozonation (Wang et al., 2020). Nevertheless, chemical pretreatment is not appropriate for compounds that can be quickly broken down by biological processes (Khanh Nguyen et al., 2021). The chemical pretreatment result mostly relies on the organic component, the procedure employed, and the specific chemical utilised.

### 2.7.3 The use of Carbon Conductive Materials (CCMs).

A wide range of carbon-based materials, including granular activated carbon (GAC), graphene, carbon cloth, graphite, carbon nanofibers (CNT), and biochar, have been used in different studies related to (AD research (Kultar et al., 2022). The most often utilised CCM in wastewater treatment is Granular Activated Carbon (GAC), as Yang et al. (2017) reported; followed by carbon cloth and biochar. Kultar et al., (2022) examined the effects of modifying CCMs under various operational settings, including varied modes of operation and temperatures. When CCMs were added, researchers observed significant improvements in the performance of AD in different key areas: (I) methane produced per gram of organic matter; (ii) rate of $CH_4$ production; (iii) decreased VFA accumulation; (iv) an increased ability to tolerate inhibitory substances; (v) lag phase reduction (Kultar et al., 2022; Yang et al. 2017).

The primary mechanism by which CCMs aid DIET is through high electrical conductivity (EC). Microorganisms conduct extracellular electron transfer (EET) more effectively through CCMs compared to pili because: (i) CCMs, have a significantly higher ECs, compared with the EC of pili (Liu et al., 2012), and (ii) CCMs may eliminate the need for microorganisms expending energy on synthesising conductive pili, for DIET (Yang et al., 2017).

## 2.8 Sewage sludge as a Substrate in AD.

The continuous rise in population is directly linked to the gradual expansion of (WWTPs) functioning globally, resulting in the generation of substantial quantities of sewage sludge. Hazardous compounds in sewage sludge pose a significant environmental risk and issues related to odour and hygiene. Consequently, it is imperative to dispose of them following appropriate treatment (Mitraka et al., 2022). However, treating and disposing of sewage sludge is costly, accounting for over half the overall treatment expenses. Hence, much focus has been given to pursuing sustainable and cost-effective strategies for managing and treating sewage sludge before disposal. An effective method suitable for the intended use is AD, which has been shown to stabilise sludge and eliminate odours and pathogens and provide a solution to the growing concerns about energy scarcity through biogas production.

According to the International Energy Agency (IEA Bioenergy Task 37, 2017), Germany holds a prominent position in global biogas generation, biogas plants that generate an impressive 55,108 GWh/y of power. 1,258 sewage treatment plants produce 3,517 gigawatt-hours of power each year. India currently possesses 83,540 biogas plants, but the generation of bioenergy remains mostly focused on individual households and is predominantly limited to small-scale biogas plants. These smaller plants are primarily utilised by the rural population. The industrial and household wastewater sludge of 48.5 million South Africans has the potential to generate 1,488 MW of power. In 2009, this accounted for 7% of Eskom's total national supply. Municipal WWTPs have the potential to generate around 824 MW of electricity, which can be utilised within the local area to fulfil the energy requirements. The study assumed that all population-generated raw wastewater solids could be converted, exaggerating energy potential (van der Merwe-Botha et al., 2016).

## 2.9 Biochar

### 2.9.1 Biochar Production and Properties

Biochar is a solid material produced by converting biomass through a thermochemical process in an environment with restricted or no oxygen at temperatures 350°C to 1000°C. It is carbonaceous, porous, and has stable carbon properties (Sinervo, R. 2017). Although biochar is a new scientific concept, ancient Amazonians utilised primitive biochar to make soil called Terra Preta (Vieira Novais et al., 2017). Biochar improved agricultural soil qualities (Vieira Novais et al., 2017).

Biochar synthesis involves pre, primary, and carbonaceous product production (Lee et al., 2017). The initial phase is ascribed to the moisture and low-boiling point substances removal. Moisture evaporation leads to the disruption of bonds and the creation of – COOH, – CO groups, and hydroperoxide. Step two involves the rapid devolatilization and decomposition of hemicellulose and celluloses (Ding et al., 2014). The final phase, occurring at temperatures exceeding 500°C, involves the deterioration of lignin and other organic substances characterised by more robust chemical linkages (Cárdenas-Aguiar et al., 2017).

Biochar is derived from organic residues obtained from agricultural and forestry activities (Agri-waste), as well as waste streams such as sewage sludge. Feedstock and process factors including temperature, environment, and heating rate affect BC characteristics (González et al., 2018).

#### 2.9.4.1. Biochar production methods.

Producing biochar typically entails the processes of pyrolysis and hydrothermal carbonisation (HTC). Both processes produce biochar, bio-oil, and syngas in solid, liquid, and gaseous forms, respectively. Pyrolysis, the most common biochar manufacturing process, involves anaerobic thermal degradation of biomass at 200–1000 °C (Demirbas and Arin, 2002). Pyrolysis can be classified into two primary categories depending on the duration of time and the level of heat involved. Fast pyrolysis refers to a process that takes place within a few seconds, whereas slow pyrolysis includes intermediate and long-term pyrolysis, which can last from minutes to days. Fast pyrolysis is characterised by a higher temperature compared to slow, moderate, and long-term pyrolysis.

There are two categories of pyrolysis: Torrefaction, occurring at temperatures between 230 ≤ 300°C, and gasification, which occurs at 800 °C in producing gaseous end products (González et al., 2018).

Table 2-5: Pyrolysis process categorization (González et al., 2018).

| Process Classification | Temperature ($^0$C) | Residence time | Product Yield | | |
|---|---|---|---|---|---|
| | | | Gas (as Syngas) % | Liquid (as Bio-oil) % | Solid (as Biochar) % |
| Fast | ≥300 ≤1000 | ≤ 2 seconds | 75 | 12 | 13 |
| Intermediate | 500 | ≥10 ≤20 Seconds | 50 | 25 | 25 |
| Slow | ≥100 ≤1000 | ≥5 ≤ 30 minutes | 30 | 35 | 35 |
| Gasification | ≥800 | ≥10 ≤20 Seconds | 5 | 10 | 85 |

2.9.4.2. Biochar composition and properties.

Biochar consists primarily of carbon, with smaller amounts of hydrogen, oxygen, nitrogen, and sulphur; the stability of biochar decreases as the Oxygen to Carbon (O: C) ratio increases (Afifah & Priadi, 2017). According to Ippolito et al. (2012), the biochar with the lowest ratio (graphite) exhibits the most stability, whilst highest ratios (biomass) demonstrates the diminished stability. Therefore, O: C or H:C ratios ≤ 0.2 indicate that the BC is made out of graphene layers and demonstrates chemical stability. The H: C and O: C of Biochar generally decrease with increasing temperature. The exceptionally low O: C and H:C ratio observed in Biochar indicates diminished polarity and increase hydrophobicity, resulting in $CO_2$ adsorption in the presence of water (Afifah & Priadi, 2017). Biochar derived from diverse materials through various techniques has distinct characteristics. The characteristics of biochars are primarily influenced by the methods used in their manufacture, which encompass factors such as heat transfer, pyrolysis temperature, heat transfer rate residence time, and feedstock type. The factors determining the utilisation of biochars are their surface area, distribution of pore sizes, and capacity for ion exchange. Typically, higher pyrolysis temperatures promote the production of biochars with enhanced ability to adsorb organic pollutants. This is achieved by increasing, microporosity and surface area, and the hydrophobic nature of the biochars. In contrast, biochars generated at lower temperatures exhibit superior efficacy in eliminating polar organic compounds and inorganic substances through precipitation, ion exchange capacity and electrostatic attraction (González et al., 2018).

### 2.9.2 Effects of pyrolysis temperature on physicochemical properties of BC.

There exists a robust correlation between the temperature at which pyrolysis occurs and the alterations in the physicochemical and structural properties of biochar. The pyrolysis temperature impacts surface functional groups, pH, and surface area. Elevating pyrolysis temperatures enhances the carbonised portions, surface area, volatile matter, and pH, while simultaneously reducing surface functional groups and cation exchange capacity (CEC) (Tomczyk et al., 2020).

#### 2.9.2.1. Specific Surface Area

According to Bonelli et al. (2007), increased temperatures lead to changes in the surface area and porosity of biochar. The probable cause of this phenomenon is the breakdown of organic substances and the subsequent creation of micropores. The SSA is commonly analysed through the use of Brunauer–Emmett–Teller (BET) analysis. Studies have also shown the correlation between the degradation of ester groups and aliphatic alkyls and increased pyrolysis temperatures while exposing the aromatic lignin core and potentially increasing the surface area (Tomczyk et al., 2020). Ghani et al. (2013) demonstrated that when temperatures are below 500 °C, lignin does not transform into a PAH (hydrophobic polycyclic aromatic hydrocarbon), resulting in a decreased hydrophilicity of biochar. When exposed to temperatures exceeding 650 °C, biochar remains chemically stable and has an increased hydrophobicity.

As the pyrolysis temperature increases, chemicals that clog the pores are removed or broken down by thermal cracking, increasing surface area. Pyrolysis gradually breaks down organic materials like cellulose and lignin to create vascular bundles or channel architectures and increase surface area and pore volumes. (Tomczyk et al., 2020). According to Vamvuka and Sfakiotakis (2011), amorphous carbon structures have the ability to create micropores furthermore, increasing the temperature of pyrolysis releases volatile substances and creates micropores.

#### 2.9.2.2. pH

Ding et al. (2014) found that carbonates and inorganic alkalis cause biochars' alkaline pH. Yuan et al. (2011) observed the elevation of carbonates and base cations as temperature increases, resulting in an increase in pH within the range of 6.5 to 10.8. When the temperature rises, pH rises too. Ronsse et al. (2012) and Zhao et al. (2017) found that pyrolysis increases

ash content and oxygen functional groups, which raises pH. The elimination of acidic functional groups and the appearance of simple functional groups also contribute (Al-Wabel et al., 2013). pH rises mainly result from the dissociation of alkali salts from organic substances caused by elevated temperature (Ding et al., 2014). At temperatures exceeding 300 °C, alkali salts undergo a process of separation from the organic matrix, resulting in an elevation of pH. Hemicelluloses and cellulose, unlike other substances, break down at temperatures between 200 and 300 °C. This breakdown results in the generation of phenolic compounds and organic acids, which decrease the pH (Yu et al., 2014). pH stabilises at approximately 600 °C as alkali salts are liberated (Shinogi et al., 2003).

2.9.4.3. Surface Functional Groups.

Heating biomass to 350 to 650 degrees Celsius causes the breaking of chemical bonds, leading to the formation of many new functional groups such as lactol, carboxyl, lactone, anhydride, ether, pyridone, pyrone, quinine (Mia et al., 2017). The FTIR spectra of biochar exhibit oxygenated hydrocarbon functional groups, which correspond to the cellulose and hemicellulose carbohydrate structure (Ghani et al., 2013). Pyrolysis has the ability to eliminate absorption bands from the feedstock and generate distinct bands. In their study, Ghani et al. (2013) discovered sawdust biochar presented a wide range of frequencies between 3000 and 3600 $cm^{-1}$, with the greatest point at 3339 $cm^{-1}$. Additionally, there was a narrower range of frequencies from 2700 to 3000 $cm^{-1}$. The band observed at 3330 $cm^{-1}$ is attributed to OH functional groups presence (Pretsch et al., 2009). Bands observed at 2900 $cm^{-1}$ are attributed stretching of alkyl C-H bonds. Conjugated ketones and quinones display aromatic C–0 and C–c stretching at approximately 1600 $cm^{-1}$ (Ruthiraan et al., 2015), whereas ketones, aldehydes, and esters exhibit C=O stretching at 1735 $cm^{-1}$. C–O–C groups, namely phenolic compounds coupled with lignin, resulted in the band appearance at 1238 $cm^{-1}$ (Kardam et al., 2012).

Biochar that is exposed to high temperatures (600 ≥700°C) become hydrophobic and develops structured carbon layers (Uchimiya et al., 2011). The process of deoxygenation and dehydration of biomass leads to a reduction in the functional groups that contain hydrogen and oxygen. Surface groups have the ability to either donate or accept electrons, resulting in the formation of acidic, basic, hydrophilic, or hydrophobic regions (Amonette & Joseph, 2009). This product may exhibit diminished IEC (Novak et al., 2009).

2.9.4.4. Cation Exchange Capacity (CEC)

The CEC of BC refers to its capacity to attract and absorb cations, which include nutrients and heavy metals. As the temperature of pyrolysis increases, biochar exhibits a greater number of structured carbon layers, similar to graphene, and a reduced amount of surface functional groups (SFGs) (Ahmad et al., 2014). Joseph et al. (2010) found that the elimination of SFGs and the generation of aromatic carbon decrease the cation exchange capacity (CEC). Multiple studies have shown that raising the pyrolysis temperature reduces the CEC of biochar (Tomczyk et al., 2020). According to Banik et al. (2018), carboxylate and phenolate groups can produce negative surface charges, but oxonium groups (heteroatoms in aromatic rings) can generate positive charges. Research has shown that biochars produced at temperatures exceeding 600 $^{0}$C have increased cation exchange capacity (CEC) and surface microporosity (Kasozi et al., 2010). The reason for this is the volatile material reduction (Song and Guo, 2012).

### 2.9.3 The application of biochar as an additive in AD.

Researchers have shown interest in using biochar as an addition in AD because of its potential to augment the AD process. Mumme et al. (2014) noted significant cost associated with producing biochar as the main factor hindering its widespread adoption. One potential solution to this issue is to diversify the applications of biochar, such as utilising it as an additive AD. Activated carbon (AC) has been investigated as an additive in AD, yielding favourable outcomes. According to Luo et al. (2015), biochar may possess comparable characteristics to AC. When comparing biochar to activated carbon (AC), one disadvantage of activated carbon is its cost of production. Biochar is produced at lower temperatures without activation, and hence, it is substantially cheaper to produce. Luo et al. (2015) propose that biochar has the potential to effectively immobilise micro-organisms and mitigate inhibition by adsorption, thanks to its substantial surface area. The leftover biochar in the digestate could function as a soil amender if the digestate is employed as fertiliser (Luo et al., 2015). The potential benefits of incorporating biochar into the process include enhanced process stability, increased methane output, and reduced inhibitory issues (Mumme et al., 2014). Figure 2-10 presents a schematic describing the application of BC in the AD process.

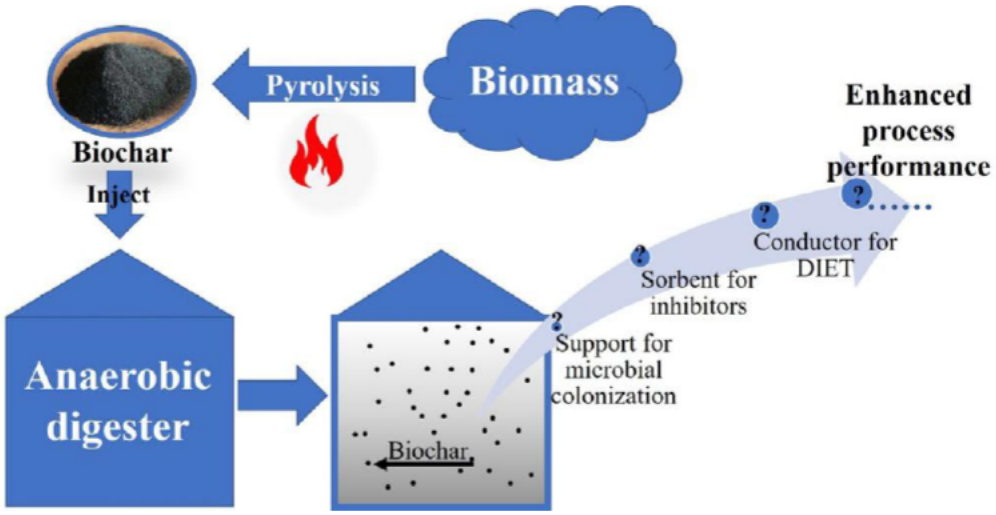


Figure 2-10: Application of biochar in the AD process (Pecchi and Baratieri, 2019).

Represented in the table below is a summary of the research conducted on the impacts of Biochar addition on the AD process. Presented in Table 2-6 is a summary of the impact of BC on the AD process.

Table 2-6: Summary impact of BC addition on the AD process

| **Biochar** | | **AD Process** | **Impact on AD process** | **Reference** |
|---|---|---|---|---|
| **Biomass** | **Biochar loading rate** | | | |
| **Pine sawdust** | **30, 20, 10 (g/L)** | OFMSW | Increased biogas production rate and yield. | Rasapoor et al. (2020) |
| **Wheat straw** | **10, 5, 8 (g/L)** | Poultry litter | Increased biomethane yield. Increase system buffering capacity | Indren et al. (2020) |
| **Saw dust** | **15 g/L** | Sewage sludge | Increased biomethane yield. Increase DIET. | Wang et al. (2020) |

| | | | | |
|---|---|---|---|---|
| **corn stover** | **1.82 - 3.06 g/gTS** | primary sludge (PS) | Increase biomethane production rate and yield. Increased VS and COD removal | Wei et al. (2020) |

### 2.9.4 Impacts of BC Addition and its Potential Enhancement Mechanisms.

2.9.4.1. BC as an inhibitor adsorber.

Inhibition is typically the main reason for decreased bio-methane production in AD. An inhibitor halts the growth of bacteria; direct inhibitors encompass a range of substances, including heavy metals ($Zn^{2+}$, Ni, Cd, $Pb^{4+}$, $Mg^{2+}$), organic compounds including halogenated aliphatics, lignocellulose hydrolysate, pesticides, antibiotics, while indirect inhibitors include VFAs, ammonium, hydrogen, sulphides, and long chain fatty acids (Chiappero et al., 2020). The presence of ammonia ($NH_3$) and ammonium ($NH^{4+}$) concentrations, together known as total ammonia nitrogen (TAN), can strongly impede or hinder some processes. Optimal regulation of ammonia/ammonium levels can stabilise microbial growth and improve buffer capacity.

Studies have investigated zeolites and GAC/BC adsorbents as potential methods for alleviating ammonia ($NH_3$) and ammonium ($NH^{4+}$) inhabitation. Research indicates the potential of BC to impede ammonia production; however, the specific mechanisms by which this occurs are not yet understood (Shen et al., 2017). BC can reduce ammonia levels through direct mechanisms such as cation exchange capacity, surface functionality, and adsorption. BC may also indirectly decrease ammonia concentrations through DIET and microbe immobilisation (Lü et al., 2018). The effectiveness of BC in reducing ammonia depends on the specific features of the BC and the feedstock, as well as temperature and pH of the AD system.

2.9.4.2. Enhancing Bio-methane Yield.

A study conducted be Wei et al. (2020), found biochar addition increased $CH_4$ generation by 8.6–17.8% during the AD of sludge. Pan et al. (2019) noted an increase of 32-36% increase

in $CH_4$ generation during the AD of chicken manure. Sugiarto et al. (2021) discovered that biochar increased $CH_4$ production 46.9% during food waste AD. BC can enhance the rate of complex organic decomposition, perhaps increasing the production of $CH_4$ by improving activity of glucanase, lipase protease, and protease enzymes, potentially leading to increased COD in AD of sludge (Khalid et al., 2021). Biochar enhances microorganisms' density, facilitating their interaction with substrates effectively addressing the inherent issue (Khalid et al., 2021). Excessive BC loading can impede mass transfer and organic matter decomposition; this is attributed to the BC's absorption of dissolved organic matter, restricting the availability of substrates for methanogenesis. The merits of biochar addition in AD are broadly recognised. However, it is important to mitigate its disadvantages.

#### 2.9.4.3. Lag-phase Reduction.

Shi et al. (2022) discovered that the lag phase, was reduced by 7.82 hours when 0.6 grams of biochar per gram of VS were added. In addition, Wang et al. (2018) showed that biochar led to a reduced lag time of sludge by 27.5%. Sunyoto et al. (2016), found that the addition of biochar resulted in a simultaneous reduction of the lag period for $CH_4$ synthesis and $H_2$ production. Luo et al. (2015) discovered that biochar (pyrolytic) reduces methanogenesis lag phase and increases the rate at which $CH_4$ is produced. However, the impact of biochar on total $CH_4$ generation, as observed by (Lü et al. 2016), is restricted.

#### 2.9.4.4. Direct Interspecies Electron Transfer.

The metabolic equilibrium in AD relies on the exchanging electrons between syntrophic bacteria. Research has found that hydrogen and interspecies formate transfer are the dominant mechanisms (Chen et al., 2022). In the DIET electrons are transferred from bacteria that donate electrons to microorganisms that take electrons (Summers et al., 2010). DIET circumvents the thermodynamic constraint by not utilising hydrogen as the electron carrier (Baek et al., 2016) and exhibits a significantly higher electron transfer capacity (Storck et al., 2015). When DIET is facilitated by biochar, biochar can behave as conductive pili, allowing for enhanced syntrophic bacteria growth as less enzymatic reactivity is required. A recent study found that the rate of $CH_4$ synthesis was directly associated with the presence of functional groups containing oxygen. This correlation was observed to be stronger than the influence of electrical

conductivity (Ren et al., 2019). Figure 2-11 presents the effect of BC on DIET during the digestion process.

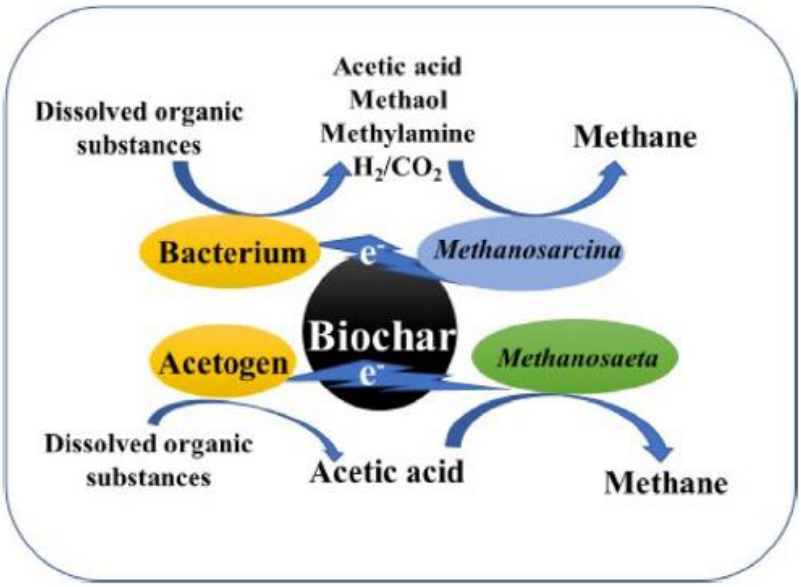


Figure 2-11: BC DIET impact (Pan et al., 2019)

## 2.10 Ultrasonic Pre-treatment and its application in AD.

The hydrolysis stage is typically the phase that limits the rate of AD. Thus, the anaerobic process is improved by discovering a pretreatment method that speeds up hydrolysis. When compared to other pretreatment procedures, ultrasonic pretreatment shows promise in terms of being environmentally friendly and potentially economically viable. However, no data has been produced yet to support this claim.

Ultrasonic waves have a frequency range that spans from 20 kilohertz to 10 megahertz. Applying acoustic energy to a liquid leads to the creation and enlargement of gas bubbles as the liquid absorbs gas and vapour that were previously dissolved in it. Cavitation is a phenomena when bubbles implode, leading to extremely high temperatures and pressures within the cavity. The localised rise in temperature and pressure is enough to enhance chemical reactivity, break down polymers, and generate chemical free radicals. Dewil et al., (2016) determined that cavitation can lead to several effects: 1) increased chemical reaction rates due to localised high pressure and temperature; 2) intense shear forces, causing mechanical damage to components; 3) generation of reactive radicals facilitating chemical reactions; and 4) further degradation of compounds, allowing volatile and hydrophobic substances to react with.

## 2.11 Design of Experiments (DOE).

DOE is a statistical technique employed in the process of experimental design for laboratory research and the development of new products or formulas. DOE is widely utilised across several industries to identify the most effective parameter among multiple variables or factors, with the goal of enhancing process yield, minimising variation, and reducing total cost (Montgomery, 2013). DOE enables concurrent consideration of several factors or variables, resulting in more precise outcomes and speedier experimentation compared to the old One Factor at a Time (OFAT) approach. Therefore, the utilisation of DOE results in reduced expenses (Roy, 2001). DOE is a potent technique used for quantitative analysis in experimental design. It is applied through several methods, such as Central Composite Design (CCD) Response Surface Method (RSM), Taguchi design, full factorial analysis, etc.

### 2.11.1 Response Surface Methodology (RSM).

The primary objective of RSM is to achieve optimisation, even when the position of the optimal point is not known beforehand. Therefore, it is logical to employ a design that ensures equal accuracy of estimation in all directions. CCD and Box-Behnken design are extensively utilised experimental design methods for three-level, three-factor investigations.

The CCD, RSM design, is effective for conducting experiments in a sequential manner and provides a sufficient data to analyse for lack of fit. This design requires the incorporation of five levels for each factor and includes combinations where all factors are simultaneously set at their highest or lowest level.

The utilisation of the BBD should be limited to circumstances where one does not have a concern about forecasting excessive reactions. Furthermore, this design has the ability to rotate or almost rotate, suggesting the model can provide a stable distribution of scaled prediction variance across the experimental design region (Montgomery, 2005) requiring three levels for each factor, as opposed to the five levels in the CCD. This reduces the experimental trials needed to assess multiple variables and their interactions. Additionally, it is convenient and cost-effective to implement compared to the CCD when the number of factors is less than five ($k < 5$)

# Chapter 3: Methodology

## 3.1. Introduction.

This chapter presents the experimental methodology employed to accomplish the objectives of this investigation. It details the procedures followed for the collection and characterisation of samples and analyses conducted. Furthermore, it provides a comprehensive description of the experimental design for the BMP tests and the methods used for the synthesis of Biochar from sugarcane bagasse.

Section 3.2 describes the collection of the IWW, sludge and inoculum samples. Section 3.3 details the analytical equipment employed in this study. Section 3.4 describes the characterisation methods employed for the characterization of the IWW, sludge and inoculum samples. Section 3.5 describes the methodology employed for the synthesis of biochar derived from sugarcane bagasse. Section 3.6 describes the characterisation methods utilized for the characterization of the synthesised biochars, and finally, Section 3.7 outlines the optimisation of the BMP system, a comparative study between the optimised IWW and BC systems.

## 3.2. Collection of industrial wastewater, sludge and inoculum.

Two types of industrial wastewater were considered in this study: (i) sugar industry wastewater (final effluent) and (ii) landfill leachate source from a local waste management facility. The primary sewage sludge utilized in this study was sourced from the Amanzimtoti WWTP in Durban and was collected from the primary settling tanks (PSTs), with the inoculum collected from the secondary anaerobic digesters. The industrial wastewater, primary sludge and inoculum were characterized prior to anaerobic digestion for pH, Volatile Solids (VS), Total Solids (TS), and Chemical Oxygen Demand (COD) using the standard analytical methods outlined in APHA 2005. The samples were then stored at a temperature of $5^0$C.

### 3.3. Analytical Equipment.

The list of analytical equipment utilized in this study are listed in Table 3-1

Table 3-1: List of equipment used in this study.

| Parameter | Instrumentation | Analysis Methodology |
|---|---|---|
| **COD (mg/L)** | DR 3900 HACH Spectrophotometer | Method 8000 (HACH®, Loveland, Colorado) |
| **Total Solids (TS)** | HCB602H Analytical Balance | APHA (2005) |
| **Volatile Solids (VS)** | HCB602H Analytical Balance | APHA (2005) |
| **$CH_4$ (%)** | GC-2014 Schimadzu | Standard Method |
| **$CO_2$ (%)** | GC-2014 Schimadzu | Standard Method |
| **pH** | Hanna pH meter | Standard Method |

### 3.4. Primary sludge, inoculum, and industrial wastewater characterisation.

The TS, pH, COD, and VS of both the raw (undigested) and processed (digested) samples were analyzed to compare and evaluate the efficiency of the treatment process. The analysis was conducted following the standardised technique defined by APHA (2015). Gas chromatography was employed to examine the gas composition in the biogas (Yang, Zhang, & Wang, 2015). Equation (3-1) below was used to determine the removal efficiency of the anaerobic digestion/treatment process.

$$Removal\ Effiency\ (\%) = \frac{Initial\ Concentation\ \ (Ic) - Final\ Concetration\ (Fc)}{Initial\ Concentation\ \ (Ic)} \times 100$$

Equation 3-1

Where:

$I_c$ = is the initial concentration.

$F_c$ = is the final concentration.

### 3.4.1. pH

As discussed in Chapter 2, pH is a crucial process parameter in AD and has a marked impact on the performance of the AD system as such, the pH was measured to quantify the degree of alkalinity and or acidity of the primary sludge inoculum and industrial wastewater. The pH of the samples was determined using a pH meter, following the standard methodology outlined in AHPA 2005.

### 3.4.2. TS

The total solids content is an important process parameter in AD and is defined as the residues left after the drying of the sample at $105^0$C. The TS of each was analysed by measuring 20 ml of each sample into a crucible and drying it for 24 hours in a drying oven set to $105^0$C according to APHA (2005) section 2540B.

The residue left after drying was then measured, and the TS was determined using the equation below:

$$Total\ Solids\ \left(\frac{gm}{L}\right) = \frac{B-A}{Vs} \times 1000$$

Equation 3-2

Where:

A = is the weight of crucible (mg).

B = is the weight of crucible + residue (mg).

Vs = is the sample volume in mL.

### 3.4.3. VS

VS content refers to the reduction in weight that occurs when a sample is heated in a muffle furnace at 550°C for 1 hour and when liquids (slurry or wastewaters) are heated for a duration of 30 minutes and is conducted in accordance with the APHA 2005 standard methodology. The determination of volatile solids (VS) is crucial both before and following the anaerobic

co-digestion process, as numerous biogas calculations rely on VS, organic loading rate, and the percentage decrease in VS.

The VS was determined using the equation 3-3:

$$Volatile\ Solids\ \left(\frac{mg}{L}\right) = \frac{B-C}{Vs} \times 1000$$

Equation 3-3

where:

B = is the weight of crucible + residue (mg) after drying at ($105^0$C).

C = weight of crucible + residue after combustion (mg).

Vs = is the sample volume in mL

### 3.4.4. COD

The chemical oxygen demand (COD) measurements for both the industrial-wastewater and sewage sludge samples were conducted by diluting 1 mL of substrate with 9 mL of deionized water. The solution was agitated to achieve homogeneity, thereafter, 0.2 mL of the solution was introduced into the prepared COD vials. A blank sample consisting of a COD vial containing 0.2 mL of deionized water was also prepared. The COD vials were agitated and placed in the thermoreactor for a duration of 2 hours, during which they are subjected to heating at a temperature of $120^0$C. Subsequently, the vials are extracted and allowed to cool at ambient temperature. By utilising the 432 HR programme on the HACH 3900 Spectrophotometer the blank sample is assessed, followed by the measurement of the samples.

## 3.5. Synthesis of biochar from sugarcane bagasse.

Sugarcane bagasse (SCB) is the fibrous lignocellulosic byproduct remaining after the processing of sugarcane for the manufacturing of sugar. Biochar is a solid substance composed of carbon and mineral components. Biochar is produced through the pyrolysis of biomass materials in an environment with limited oxygen (Iwuozor et al., 2023).

To fully exploit the capabilities of Biochar for enhancing the AD process, the pyrolysis technique of production was utilised. The following is a description of the method utilized to synthesise of BC from sugar cane bagasse.

Sugarcane bagasse was obtained as the raw material from The Sugar Mill Research Institutes (SMRI) at the University of Kwa-Zulu Natal in Durban.

i. The bagasse was washed to remove soil and other impurities and milled to a size of 3 cm; the milled bagasse was subsequently dried in a drying oven set to $105^0$C for 24 hours.
ii. The sugarcane bagasse was pyrolysed at three different temperatures, $350^0$C, $450^0$C and $550^0$C, for 30 minutes in a muffle furnace to produce biochar in a 1L lab-scale pyrolysis reactor.
iii. The biochar yield was obtained by quantifying the difference in mass of the bagasse sample prior to and during pyrolysis.
iv. The biochar was pulverised into fine particles ranging from 0.8 to 2.0 mm in size, and the particle size was determined by particle size analysis.


Figure 3-1: Biochar synthesis process outline.

### 3.6. Biochar Characterisation.

The synthesised biochars were characterised to validate synthesis by examining the pH, conductivity, surface area, surface morphology, and elemental composition. This was achieved through the use of Fourier-transform infrared spectroscopy (FTIR), scanning electron microscopy (SEM), and energy dispersive X-ray (EDX) analysis.

#### 3.6.1. pH

Comprehending the pH of biochar is crucial due to its potential impact on the pH of the AD system and other characteristics and processes when biochar is applied as an additive in AD. Biochars generated at temperatures over 400°C are expected to exhibit higher pH levels compared to biochars produced at temperatures below 400°C (Mukherjee et al. 2011).

The pH of the biochar produced at each pyrolysis temperature was determined as follows:

i. 5.0 g of dried biochar was weighed and added into a 100 mL centrifuge tube.
ii. 50 mL of Deionised Water (DIW) was added to the centrifuge tube and shaken vigorously.
iii. The samples were placed in the mechanical orbital shaker for 1 hr at 25°C.
iv. The suspension was allowed to rest for approximately 30 min.
v. The pH of the suspension was analysed using a pH meter.
vi. The pH values were recorded once the reading stabilised.
vii. The pH meter was rinsed with DIW after each reading.

### 3.6.2. Electrical Conductivity (EC).

Biochars generated through pyrolysis at elevated temperatures typically exhibit greater EC values (Claoston et al., 2014). The observed phenomenon can be ascribed to the accumulation of ash resulting from material volatilisation during pyrolysis (Cantrell et al., 2012).
The EC of the biochar produced at each pyrolysis temperature was determined as follows:

i. 5.0 g of dried biochar sample was weighed and added into a 100 mL centrifuge tube.
ii. 50 mL of Deionised Water (DIW) was added to the centrifuge tube and shaken vigorously.
iii. The samples were placed in the Mechanical orbital shake for 1 hr at 25°C.
iv. The suspension was allowed to stand for approximately 30 min.
v. The EC was measured using an EC meter as per the OEM methodology.
vi. The EC values were recorded once the reading stabilised.
vii. The EC meter was rinsed with DIW after each reading.

### 3.6.3. Fourier-transform infrared spectroscopy (FTIR).

The functional groups and molecular structures of the biochars, including organic, polymeric, and inorganic components, were analysed using a Fourier Transform Infrared (FTIR) spectrometer. The analysis was conducted within the range of 400 to 4000 cm1 using a Shimadzu FTIR 8400 instrument.

### 3.6.4. Energy Dispersive X-ray (EDX) and Scanning Electron Microscopy (SEM) analysis.

The morphology and elemental composition of the biochars were analysed at Capetown University of Technology (CPUT) using SEM/EDX techniques. The analysis was conducted using Nova Nano SEM, combined with EDT and TLD detectors. The task was performed using a magnification range of 10–50 thousand times and an acceleration voltage of 5 kilovolts.

## 3.7.Experimental Set-up

### 3.7.1. Biochemical Methane Potential (BMP) test.

The initial AD experiments were conducted utilising 1L Schott bottles as bioreactors. The bioreactors were securely sealed using screw caps equipped with ports. The bioreactor utilised in this study was a graded Schott bottle having a total capacity of 1000 mL. The bottle was clearly marked with graduations up to 950 mL. The screw caps were equipped with silicone tubes to ensure no liquid would escape, while the remaining openings were sealed with small screw caps. Prior to completely sealing the apertures, a purging operation was carried out using $N_2$ gas to induce anaerobic conditions in the bioreactors, allowing the anaerobes to function successfully (Wu et al., 2016). The bioreactors were purged for a minimum duration of 4 - 5 minutes (Yukesh Kannah et al., 2017). The downward water displacement approach was employed to collect biogas into a cylinder using silicone tubing. The digesters were agitated using a magnetic stirrer for a duration of two hours prior to quantifying the volume of biomethane generated (daily). The BMP tests were duplicated, with a duplicate of a control sample. Figure 3-2 displays the schematic diagram of the bioreactors utilised. The bioreactors were placed in the water bath and operated at the mesophilic conditions ($37^0$C). The hydraulic retention time (HRT) was set at 21 days to simulate real-world conditions.

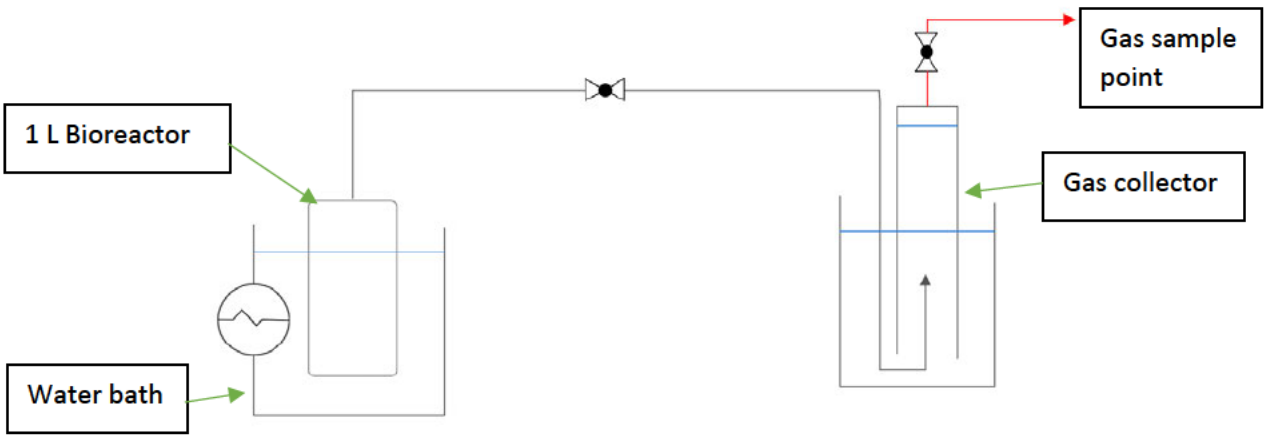


Figure 3-2: BMP system schematic.


Figure 3-3: BMP experimental set-up.

### 3.7.2. Biogas collection and characterization.

The study utilised the downward water displacement approach (Tetteh et al., 2017) to quantify the volume of gas produced. Shimadzu GC-2014 instrument to analyse the biogas produced; instrument that was fitted with a thermal conductivity detector and a Poropak column. The flow rate in both the left and right columns was 8 mL/min, with a column temperature of 40°C. The pressure on the right and left-hand side of the column was maintained at a range of 108-1086 KPa. The temperature at the injection port was 120 degrees Celsius, whereas the temperature at the detector was 250 degrees Celsius. Nitrogen gas ($N_2$) was utilised as the carrier gas.

The gas chromatograph (GC) was calibrated by utilising neat samples of methane ($CH_4$), Nitrogen ($N_2$), and carbon dioxide ($CO_2$) to determine the period of retention for each individual component. The gas was gathered for analysis on the gas chromatograph (GC) with a syringe with a diameter of 100 (µm).

### 3.7.3. IWW Screening tests.

The BMP test was conducted to assess two types of wastewaters: Intermediate landfill leachate (ILL) and sugar industry effluent/wastewater (SIWW). This was implemented as a discriminative approach to pick the optimal industrial wastewater among the two based on their performance during the digesting process.

The batch AD experiments were conducted utilising 1L Schott bottles as bioreactors BMP test was duplicated, with a duplicate of a control sample and control containing primary sludge and

inoculum. The bioreactors were placed in the water bath and operated at the mesophilic conditions (37 $^0$C). The hydraulic retention time (HRT) was set at 21 days. The study examined biomethane yield and quality, as well as COD and VS reduction. The inoculum-substrate ratio (ISR) employed was 1:1 (gVS) at a co-substrate loading rate of 1:5 (Volume IWW: Total Volume).

Table 3-2 shows the volumes required for each substrate (IWW, primary, sludge and inoculum) were determined using the ISR equation below:

$$ISR = \frac{VS_{inoc}}{VS_{sub}}$$

Equation 3-4

where:

$VS_{inc}$ is the volatile solids content of the inoculum g/l.

$VS_{sub}$ is the sum of the volatile solids content of the substrate and co-substrate g/l.

Table 3-2: IWW BMP test bioreactor loading.

| Bioreactor | Inoculum Substrate ratio | Co-substrate loading rate | Inoculum (ml) | Primary Sludge (ml) | Landfill Leachate (ml) | Sugar Industry Wastewater (ml) |
|---|---|---|---|---|---|---|
| **R1** | N/A | N/A | 800 | 0 | 0 | 0 |
| **R2** | 1:1 | 1:5 | 270 | 530 | 0 | 0 |
| **R3** | 1:1 | 1:5 | 230 | 440 | 130 | 0 |
| **R4** | 1:1 | 1:5 | 495 | 175 | 0 | 130 |

### 3.7.4. Biochar Selection Tests.

To determine the efficacy of the synthesised biochars in enhancing the functionality of the anaerobic digestion system, a feasibility test was conducted. This test utilised biochar synthesised from sugarcane bagasse produced at three different pyrolysis temperatures, i.e., 350, 450 and 500 degrees Celsius and was conducted to ascertain the suitability of biochar in AD and to select the best-performing biochar. The investigation was conducted by introducing primary sludge (PS), the best performing IWW identified in the IWW screening test, and inoculum into eight (8) bioreactors. After being filled, the bioreactors were flushed with

nitrogen gas to induce anaerobic conditions. The optimum operation conditions determined in the IWW optimisation runs were employed.

### 3.7.5. IWW and Biochar BMP system optimisation

Response Surface Methodology (RSM) is a valuable method that is utilised to optimise and gain insight into the mechanisms of processes. RSM was employed to identify the optimum process parameters (temperature, ISR and co-substrate loading rate) and model the system for the IWW system and the optimum process parameters (temperature, BC loading and co-substrate loading rate) for the BC system.

### 3.7.6. Design of Experiment (DOE)

The Box-Behnken design from the Design-Expert software (version 11.1.2.0) was used to evaluate three process parameters. The response variables assessed for evaluating the process performance were the percentage removal (%) of COD, VS, and biogas yield. The response variables statistically analysed using RSM to assess the influence of interactions between the process components on the Biological Methane Potential (BMP) process. The experimental data generated from the BBD runs were used to create regression models for the process by fitting a generic model, as reported by Ghaleb et al. (2020).

*T*able 3-3: Box-Behnken design; Process Factors and coded levels (IWW system)

| **Process parameter** | **Factor Code** | **Coded Level** | | |
|---|---|---|---|---|
| | | **-1** | **0** | **1** |
| **Temperature ($^0$C)** | A | 25 | 37 | 55 |
| **ISR** | B | 1:2 | 1:1 | 1.5:1 |
| **Co-substrate loading** | C | 1:20 | 1:10 | 1:5 |

Table 3-4: DOE factors and coded levels (IWW system)

| Process parameter | Factor Code | Coded Level | | |
|---|---|---|---|---|
| | | -1 | 0 | 1 |
| Temperature ($^0$C) | A | 25 | 37 | 55 |
| ISR | B | 1:2 | 1:1 | 1.5:1 |
| Biochar loading (g/L) | C | 2.5 | 5 | 10 |

The experimental results were then fitted to the generic multi-varied regression model equation represented below:

$$Y = \beta_0 + \beta_1 A + \beta_2 B + \alpha_3 C + \beta_4 D + \beta_{11} A^2 + \beta_{22} B^2 + \beta_{33} C^2 + \beta_{44} D^2 s + \beta_{12} AB + \varepsilon$$

Equation 3-5

Where:

$Y$ represent the responses, A, B, and C represent the input variables, and finally, the $\beta$ terms represent the coefficients of the models.

### 3.7.7. System Optimisation

The BMP process for the IWW and BC systems were optimised using the numerical method optimization tool in Design Expert. This was done by processing the variables acquired for the dependent responses and maximising the response. The input parameters were kept within the range shown in Tables 3-5 and 3-6. The four responses were optimised, and the optimal solutions were generated. The optimisation process yielded solutions with a confidence level of 95%.

Table 3-5: Numerical optimization of IWW BMP system

| Factor | Goal | Lower Limit | Upper Limit |
|---|---|---|---|
| **A: Temperature** | is in range | 25 $^0$C | 55 $^0$C |
| **B: ISR** | is in range | 1:2 | 1.5:1 |
| **C: Co-substrate Ratio** | is in range | 1:20 | 1:5 |
| **Response** | | | |
| **Biogas Yield (ml/gVS$_{added}$)** | maximize | 13.5 | 91.3679 |
| **COD removal (%)** | maximize | 13.9191 | 40.6436 |
| **VS removal (%)** | maximize | 21.9813 | 41.15 |

Table 3-6: Numerical optimization of BC BMP system

| Factor | Goal | Lower Limit | Upper Limit |
|---|---|---|---|
| **A: Temperature** | is in range | 25 $^0$C | 55 $^0$C |
| **B: Co-substrate loading ratio** | is in range | 1:2 | 1.5:1 |
| **C: Biochar loading rate (g/L)** | is in range | 2.5 | 10 |
| **Response** | | | |
| **Biogas Yield (ml/gVS$_{added}$)** | maximize | 0.629247 | 59.7589 |
| **COD removal (%)** | maximize | 14.7541 | 46.0496 |
| **VS removal (%)** | maximize | 4.32971 | 52.1756 |

### 3.7.8. Model Validation

The validity of the response models was verified by comparing the expected responses to the experimentally generated responses. The projected models were then verified under the optimal conditions to verify the dependability and appropriateness of the models with a 95% confidence level. Three experimental trials were carried out under the optimal conditions. The average of the outcomes from each trial was thereafter compared to the predicted value

# Chapter 4: Results & Discussion

## 4.1. Introduction

This chapter presents the results acquired from the research investigation. The results include the characterisation of both the wastewater samples employed and the biochars that were synthesised. The following studies were conducted: the screening and selection study for the IWW BMP system, the optimisation study for the IWW BMP system, the screening and selection study for the Biochar BMP system, the optimisation study for the Biochar BMP system, the BMP study for the ultrasonic pretreated IWW, and the comparative study between the optimised IWW and Biochar systems.

## 4.2. Characterisation of Industrial Wastewater (IWW), Primary Sludge and Inoculum.

The objective of characterising the IWW, primary sludge, and inoculum was to assess the composition of the substrates before conducting the experiments, as they have an impact on the anaerobic process and, consequently, the quantity and quality of biogas produced. Table 4-1 presents the descriptions of the inoculum and substrates. Appendix A1 contains a set of illustrative calculations for the inoculum prior to digestion.

Table 4-1: Characterisation of IWW, sewage sludge and inoculum

| Parameter | Units | Sugar Industry Wastewater | Intermediate Landfill Leachate | Primary Sludge | Inoculum |
|---|---|---|---|---|---|
| **pH** | n/a | 5.5 | 7.85 | 5.05 | 7.83 |
| **COD** | mg/L | 202 650 ± 27.5 | 5 346 ± 46 | 59 040 ± 31,5 | 42 080 ± 24,5 |
| **TS** | gTS/L | 168.46 ± 8.8 | 2.56 ± 0.5 | 39.02 ± 7.1 | 53.4 ± 6.5 |
| **VS** | gVS/L | 115.36 ± 10.7 | 4.385 ± 9.8 | 29.72 ± 6.6 | 27.96 ± 5.8 |
| **VS/TS** | n/a | 0.68 | - | 0.76 | 0.52 |

As per the findings of Li et al. (2017), the theoretical total solids (TS) and volatile solids (VS) range for primary sludge are between 30 and 60 (gTS/L) and 30 and 50 (gVS/L), respectively.

The TS for PS was 39.02 (gTS/L), and VS was 29.72 (gVS/L), falling within the expected range. The results also suggest that the sludge exhibits excellent biodegradability, as seen by a VS/TS ratio over 50%.

Furthermore, the SIWW sample exhibited a VS/TS ratio of 0.68, indicating a greater presence of organic substances compared to insoluble substances. The inoculum had the lowest VS/TS value, measuring 0.52, indicating a higher concentration of microorganisms compared to the organic materials. Therefore, it demonstrates its potential use as an inoculum rather than as a substrate.

The results indicate that all the Industrial wastewater exceeds the discharge limit set by the Department of Water Affairs (DWA, 2020).

## 4.3. Characterisation of Biochar.

### 4.3.1. pH

Presented in table 4-2 below are the results obtained from the pH analysis of each BC.

Table 4-2: pH of synthesised BC

| Parameter | Biochar (350 $^0$C) | Biochar (340 $^0$C) | Biochar (550 $^0$C) |
|---|---|---|---|
| **pH** | 7.0 ± 0.2 | 9.0 ± 0.1 | 9.1 ± 0.1 |

The BC synthesised at a pyrolysis temperature of 350 °C (BC350) exhibited the lowest recorded pH (7.0 ± 0.2), while the BC synthesised at a temperature of 550 °C (BC550) exhibited the highest recorded pH (9.1 ± 0.1). This result is expected and correlates with the scientific literature. According to Ding et al. (2014), there is a relationship between the pH values of biochars and the presence of carbonates and inorganic alkalis; these groups are mostly responsible for the alkaline pH. Yuan et al. (2011) observed that the levels of total base cations and carbonates rise as the temperature increases, resulting in an increase in pH within the range of 6.5 to 10.8. The relationship between temperature and pH is such that when temperature increases, biochar pH also increases. This increase in pH is linked to the rise in oxygen functional groups and ash content that takes place during pyrolysis, (Zhao et al. 2017). However, pH rises mainly result from the dissociation of alkali salts from organic substances caused by elevated pyrolysis temperature (Yuan et al., 2011). At temperatures exceeding 300

°C, alkali salts undergo a process of separation from the organic matrix, resulting in an elevation of the product's pH.

### 4.3.2. Electrical Conductivity (EC).

Presented in Table 4-3 below are the results obtained from the EC analysis of each BC.

Table 4-3: EC of synthesised BC

| Parameter | Units | De-ionised water | Biochar (350 $^0$C) | Biochar (340 $^0$C) | Biochar (550 $^0$C) |
|---|---|---|---|---|---|
| **Electrical Conductivity** | Micro-Siemens ($\mu S\ cm^{-1}$) | 13.2 ± 0.1 | 210 ± 5 | 220 ± 5.5 | 300 ± 10 |

BC 350 exhibited the lowest recorded EC (210 ± 5 $\mu S\ cm^{-1}$), while BC550 exhibited the highest recorded EC (300 ± 10 $\mu S\ cm^{-1}$). literature has found Biochar EC values ranging from 100 $\mu S\ cm^{-1}$ to 54.2 Deci-siemens ($dS\ m^{-1}$) (Cantrell et al., 2012). The EC is influenced by the temperature at which pyrolysis occurs and type of feedstock, similar to the pH. Biochars generated at elevated temperatures typically exhibit greater EC values (Claoston et al., 2014). The observed phenomenon is reported to be a result of the rising accumulation of ash due to the volatile substance evaporation (Cantrell et al. 2012). At elevated temperatures, the presence of certain inorganic salts, including potassium (K), sodium (Na), magnesium (Mg), and calcium (Ca), as well as carbonates such as $CaCO_3$ and $MgCO_3$, increase resulting in EC increase. Additionally, the formation of inorganic alkalis occurs (Yuan et al., 2011).

### 4.3.3. SEM (Scanning electron Micrography) and EDX (Energy Disperse X-ray) analysis.

4.3.3.1. Effect of pyrolysis temperature on BC surface morphology.

SEM micrographs (20 and 50 kx) of biochars produced at various temperatures are depicted in Figure 4-1 (a-f). The BC350 image revealed that the biomass had undergone a process of softening, melting, and merging into a cohesive mass of vesicles. Figure 4-1 (a). The vesicles formed as a consequence of the emission of volatile gases from the biomass. With the rise in temperatures, additional volatile gases were emitted from the biomass. Subsequently, the vesicles on the surface of BC450 ruptured upon cooling. Consequently, the morphology of BC450 displayed various pore configurations as displayed in Figure 4-1 (f) .

The SEM images unambiguously demonstrate that the biochar materials possess a morphology resembling flakes, with sizes ranging in the micrometre scale. However, the disintegration of the permeable framework was detected at elevated temperatures and is evident in the BC550 sample. This phenomenon may be attributed to the heightened and increased process of carbonisation (Niju et al., 2019). Hence, BC450 exhibited the greatest formation of micropores on its surface at a field view of 4.13 μm.

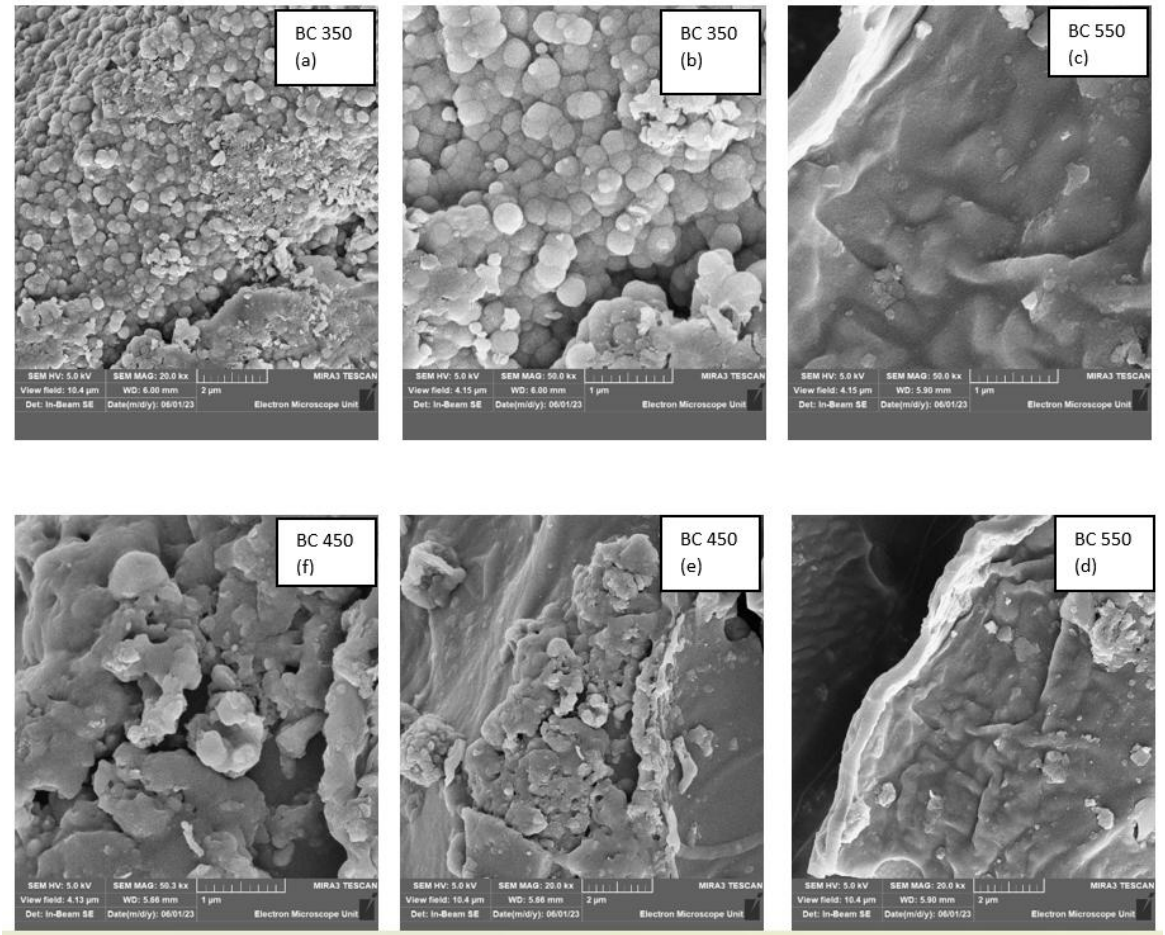


Figure 4-1 (a-f): SEM image analysis of synthesised BCs.

4.3.3.2 Effect of pyrolysis temperature on the elemental composition of the synthesised BCs.

Table 4-4 presents the elemental composition of each synthesised biochar.

Table 4-4: Elemental composition of synthesised BCs

| Element | BC 350 | | BC 450 | | BC 550 | |
|---|---|---|---|---|---|---|
| | Weight % | Std. Dev | Weight % | Std. Dev | Weight % | Std. Dev |
| **C** | 54.49 | 5.76 | 73.83 | 3.56 | 78.33 | 5.28 |
| **0** | 34.97 | 3.72 | 19.5 | 2.09 | 13 | 6.02 |
| **Mg** | 0 | n/a | 0.19 | 0.03 | 0.14 | 0.05 |
| **Al** | 1.91 | 0.59 | 1.15 | 0.32 | 1.64 | 0.61 |
| **Si** | 7.18 | 5.51 | 3.69 | 1.51 | 4.1 | 2.12 |
| **K** | 0 | n/a | 0.43 | 0.12 | 0.94 | 0.68 |
| **Ti** | 0 | n/a | 0 | n/a | 0.16 | 0.15 |
| **Fe** | 1.45 | 1.16 | 0.93 | 0.3 | 1.69 | 0.97 |
| **Ca** | 0 | n/a | 0.28 | 0.08 | 0 | n/a |

EDX analysis showed that the elemental composition of the synthesised biochars changed depending on the pyrolysis temperature. The C content increased from 54.49% (BC350) to 78.33% (BC550), while oxygen (O) content decreased from 34.97% (BC350) to 13.00% (BC550) as the pyrolysis temperature increased. These findings correspond with prior studies (Sun et al., 2018; Wang et al., 2015; Cantrell et al., 2012). The drop in the oxygen content at higher temperatures can be attributed to the dissolution of oxygenated bonds, releasing low molecular weight byproducts containing hydrogen and oxygen (Zhao et al., 2017). Furthermore, the H/C ratios (an indication of the degree of aromaticity) and O/C ratios (an indication of the degree of polarity) changed with pyrolysis temperature (Wang et al., 2015). Furthermore, the O/C and H/C ratios indicate the changes in structure and surface hydrophilicity. A higher degree of carbonisation and the subsequent loss of functional groups containing oxygen and hydrogen (such as hydroxyl and carboxyl groups) at elevated temperatures lead to lower O/C and H/C ratios. This suggests that the surface of biochar becomes more aromatic and less hydrophilic, as observed in a study by Tan et al., 2015.

Furthermore, the levels of nutrients potassium (K) and iron (Fe) also exhibited an increase as the pyrolysis temperature increased. The BC550 sample had the highest quantity of Fe, indicating the possibility of metal volatilisation at elevated temperatures (Sun et al., 2018).

Figures 4-2 and 4-3 present graphical representations of elemental composition of each synthesised biochar.

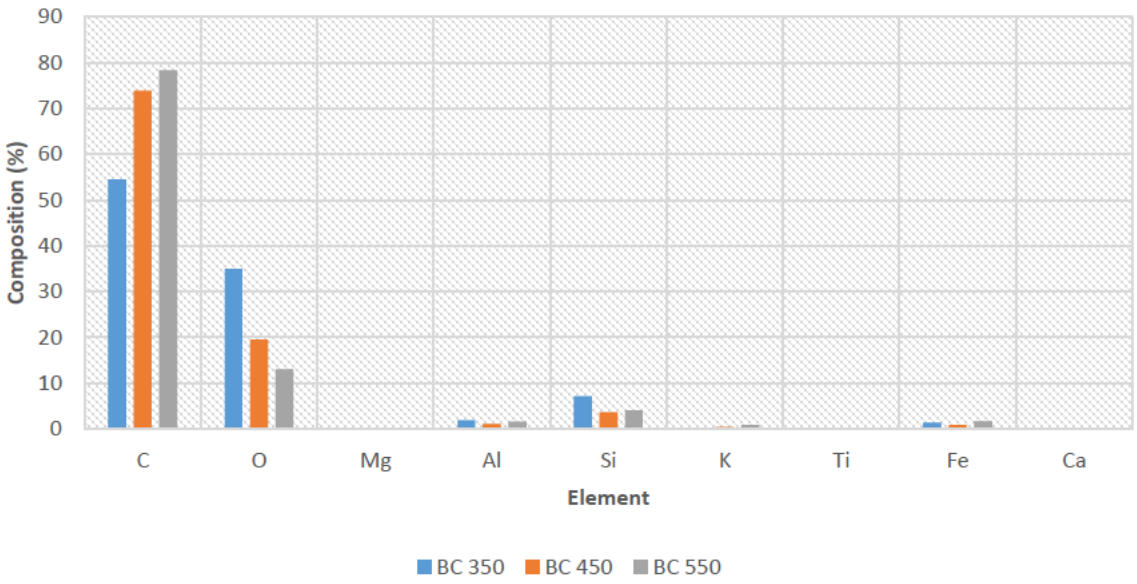


Figure 4-2: Elemental composition of synthesised BCs

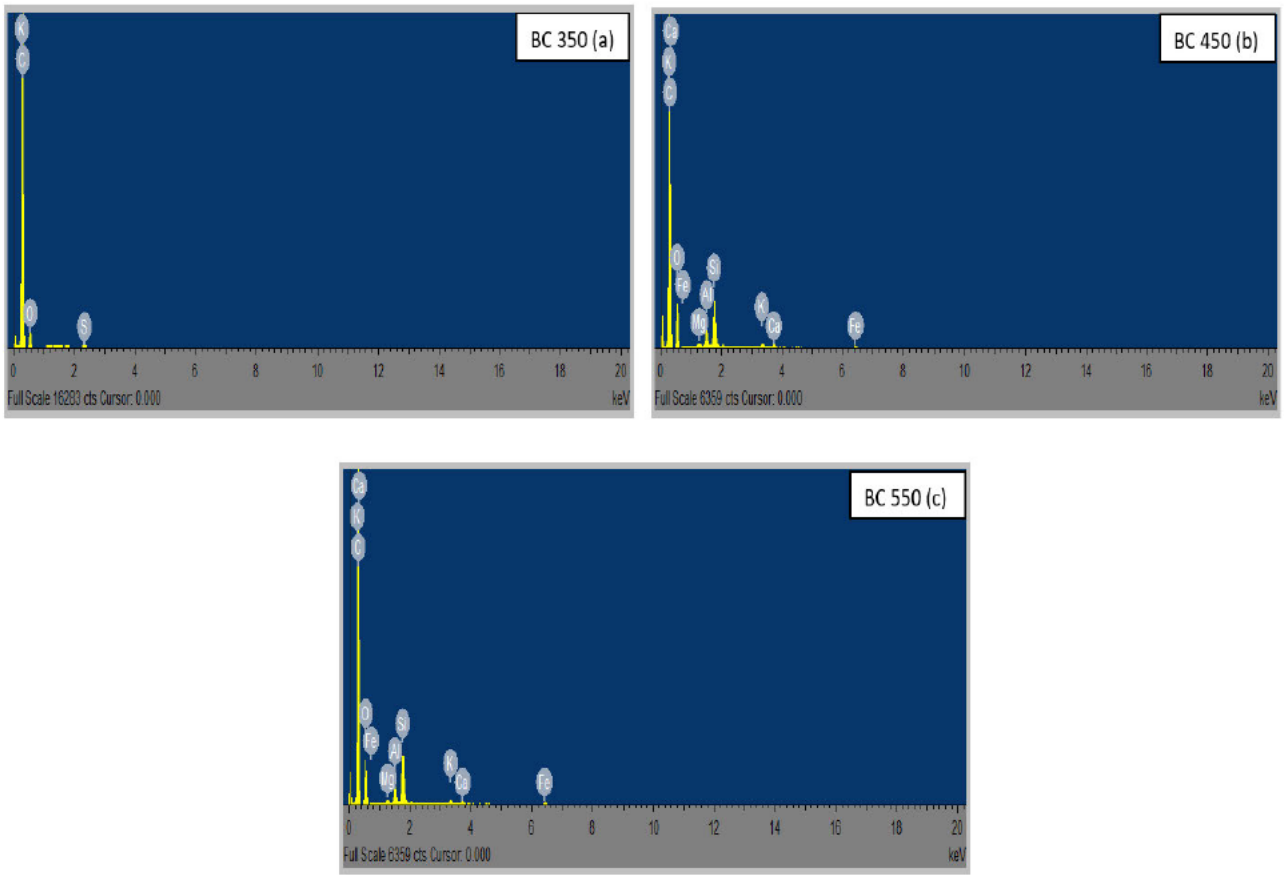


Figure 4-3: EDX graphical results; a- (BC 350), b- (BC450), c- (BC550)

### 4.3.4 FTIR analysis Effect of pyrolysis temperature on the functional group characteristics of synthesised BCs.

The surface functional groups of biochar were identified using FTIR spectroscopy to investigate the impact of temperature on the chemical composition of biochar.

The band allocations for the synthesised biochars are outlined in Table 4-5, revealing the presence of ether, carbonyl, hydroxyl carboxyl, and aromatic C=N bond functional groups

Table 4-5: Identified surface functional groups.

| Functional Group | Wave number ($cm^{-1}$) |
|---|---|
| O-H Stretching | 3200 – 3400 |
| C≡C Stretching | 2190 - 2260 |
| C=O stretching | 1700 - 1740 |
| N-H Band | 1550 - 1650 |
| Carboxylic Acid | 1550 - 1610 |
| Methyl C-H asymmetric | 1430 - 1470 |
| Nitro compound stretching | 1350 - 1380 |
| Primary alcohol C-O stretch | 1050 |
| Aliphatic iodo compounds C-I Stretch | 500 - 600 |

The temperature effect on biochar was successfully investigated using FTIR spectroscopy. The mid-infrared spectrum is categorised into distinct regions: (1) the region of single bonds (2500 to 4000 $cm^{-1}$), (2) the zone of triple bonds (2000 to 2500 $cm^{-1}$), and (3) the fingerprint region. The spectral band at wave number 3300 $cm^{-1}$ is attributed to the elongation of hydroxyl groups, indicating alcohols and phenols (Cantrell et al., 2012). With an increase in pyrolysis temperature, the intensity of the stretching band associated with hydrogen-bonded hydroxyl groups progressively diminished. This outcome was anticipated as a result of increased mass loss during the process of thermal breakdown and the subsequent release of gas products. The N–H band was observed at all temperatures and is associated with the carboxylate functional

group. The peaks seen at 1400 to 1600 $cm^{-1}$ indicate the existence of C–O or O–H stretching vibrations of phenol and C=O stretching vibrations of aromatic rings (Yao et al., 2012). Nitro-compound stretching spectrum detected at around 1367 $cm^{-1}$. Observation of tertiary amine C–N stretches occurred at a frequency of 1150 $cm^{-1}$, while primary amine C–N stretches were found at a frequency of 1025 $cm^{-1}$. All biochars exhibited the presence of C–N lengths of secondary amines. According to the FTIR spectra, pyrolysis at lower temperatures caused dehydration, the initiation of bond breaking, and the generation of transformational products (Cantrell et al., 2012). The disappearance of the asymmetric stretching (at 1150 $cm^{-1}$) of C–O bonds with increasing pyrolysis temperature indicates the breakdown and depolymerization of hemicellulose, celluloses, and lignin, as suggested by Cantrell et al. (2012). The biochars exhibited a little peak at 1090 $cm^{-1}$, may be attributed to the stretching of aliphatic ether C–O or alcohol C–O bonds. The C–N extending peaks of secondary amines are more prominent. The peak may also suggest asymmetric stretching of Si-O-Si, which can be attributable to the elevated Si content (Qian and Chen, 2013). The occurrence of bands with wavenumbers ≤ 600 $cm^{-1}$ could be attributed to the stretching variation of inorganic substances like $CaCl_2$ and KCl (Hossain et al., 2011).

Figure 4-4 presents the FTIR spectra analysis graphs for each synthesised biochar.

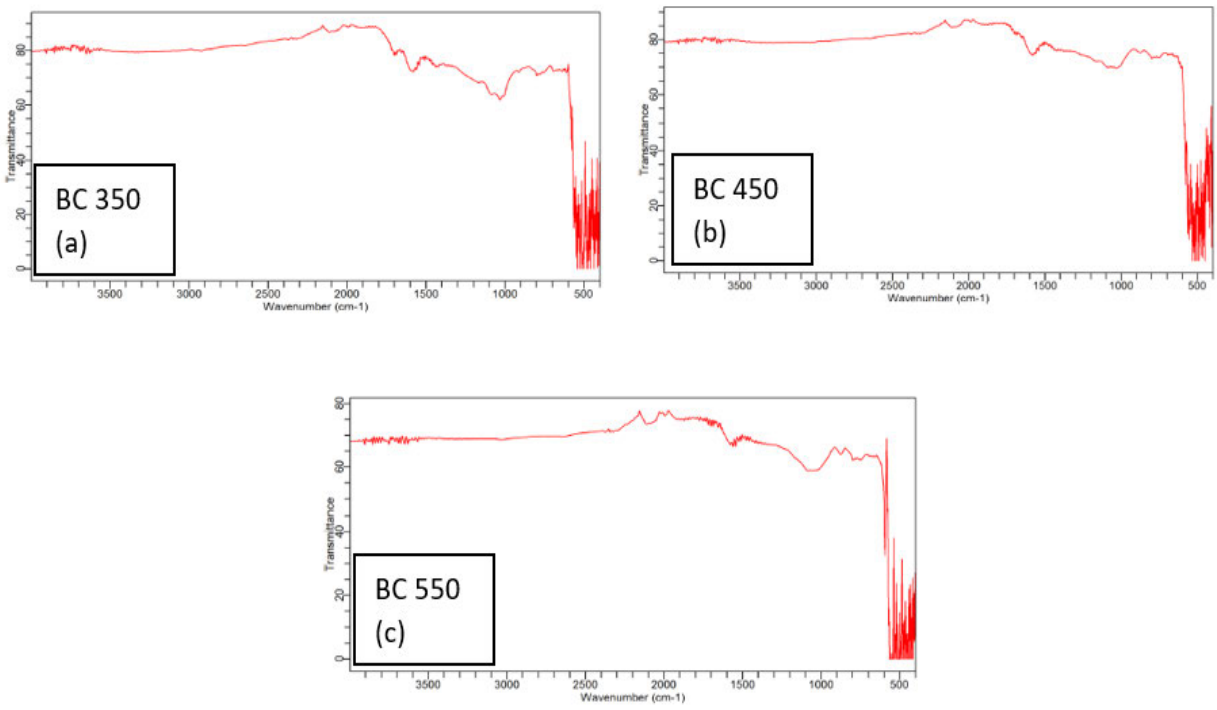


Figure 4-4 (a-c) FTIR spectra for synthesised BCs.

### 4.4.Industrial Wastewater Selection BMP tests.

The BMP test was conducted to assess two types of wastewaters: intermediate landfill leachate (ILL) and sugar industry wastewater (SIWW). This was implemented as a discriminative approach to pick the most optimal industrial wastewater among the two based on their performance during the digesting process.

The batch AD experiments were conducted utilising 1L Schott bottles as bioreactors BMP test was conducted in duplicate, with an additional duplicate of a blank control sample. The bioreactors were placed in the water bath and operated at mesophilic conditions (37 $^{0}$C). The hydraulic retention time (HRT) was set at 21 days to mimic the industry standard. The study examined four parameters: biomethane yield and quality ($CH_4$ and $CO_2$ content), and COD and VS reduction. The inoculum-substrate ratio (ISR) employed was 1:1 (gVS) at a co-substrate loading rate of 1:5 (Volume IWW: Total Volume). The loading of each bioreactor is detailed in the table 4-6. R2 was used as a baseline control to compare the performance of each IWW.

Table 4-6: IWW BMP test bioreactor loading.

| Bioreactor | Inoculum Substrate ratio (gVS) | Co-substrate loading rate | Inoculum (mL) | Primary Sludge (mL) | Landfill Leachate (mL) | Sugar Industry Wastewater (mL) | Total Volatile Solid loaded (g) |
|---|---|---|---|---|---|---|---|
| **R1** | 1:1 | N/A | 800 | 0 | 0 | 0 | 22.13 |
| **R2** | 1:1 | N/A | 270 | 530 | 0 | 0 | 20.84 |
| **R3 (SIWW)** | 1:1 | 1:5 | 230 | 440 | 0 | 130 | 35.04 |
| **R4 (ILL)** | 1:1 | 1:5 | 495 | 175 | 130 | 0 | 17.48 |

Table 4-7: IWW BMP test results

| Bioreactor | Average TS (g) (before digestion) | Average VS (g) (before digestion) | COD (mg/L) | pH (before digestion) | pH (after digestion) | Biogas Yield (mL) | Biogas Yield ($ml/gVS_a$) |
|---|---|---|---|---|---|---|---|
| **R1** | 42,80 | 22.13 | 38 800,00 | 7.5 | 8.0 | 270 | 12,20 |
| **R2 (CNTRL)** | 31,93 | 20.84 | 48 050,00 | 5.93 | 7,23 | 800 | 38.39 |
| **R3** (SIWW) | 51,66 | 35.04 | 71 950,00 | 4.93 | 6.5 | 440 | 12.55 |
| **R4** (ILL) | 27,70 | 17.48 | 35 500,00 | 5.63 | 7.23 | 950 | 54,35 |

Table 4-7 presents the reactor loading in terms of TS, VS, COD and pH pre- and post-digestion. R3 exhibited the highest VS content. This was expected as SIWW contained the highest VS content compared with that of ILL. Similarly, R4 exhibited the lowest VS content as a result of the low VS content of ILL. R4 exhibited the lowest initial pH at 5.5 this was expected given the recorded pH of SIWW.

### 4.4.1. Effect of IWW on biogas and biomethane yield.

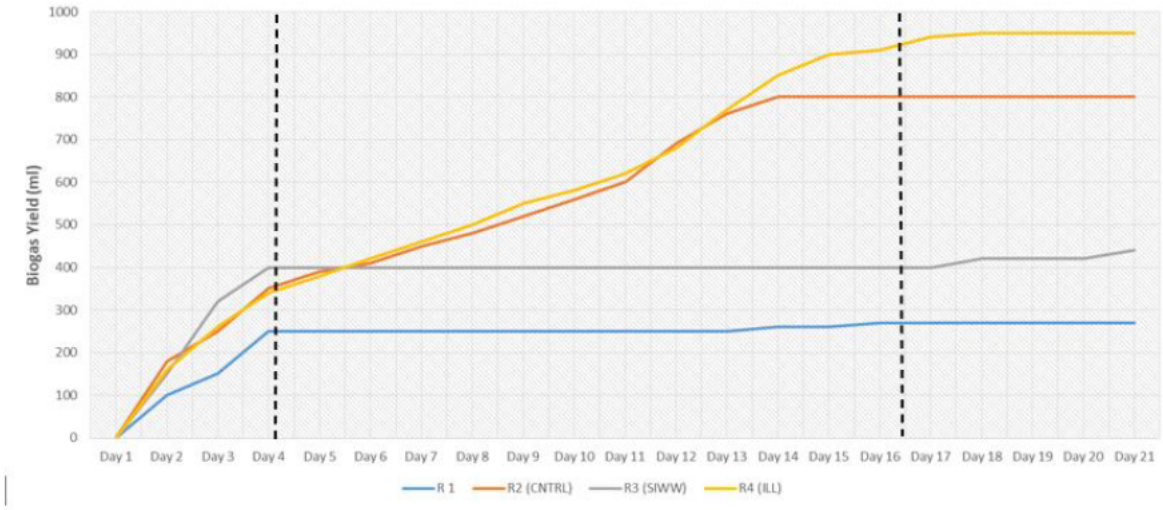


Figure 4-5: Accumulative biogas yield (IWW BMP)

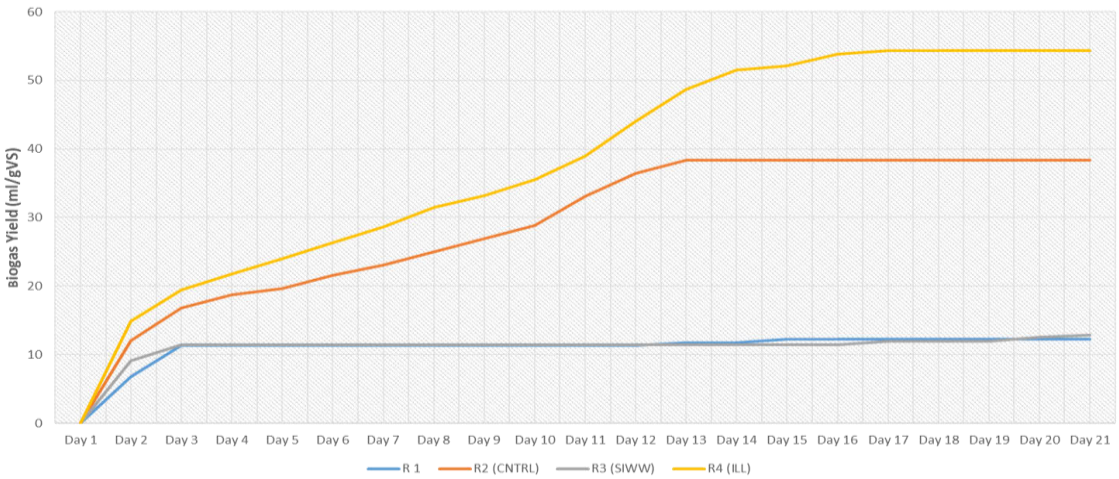


Figure 4-6: Accumulative biogas yield mL/gVS (IWW BMP)

Figure 4-5 depicts the accumulative biogas yield for each bioreactor. R3 exhibited the highest rate of biogas production between days 1 – 4, where biogas production ceased at day 4 for R1 and R3. The halt in biogas production for R3 was attributed to the high VFA content of the SIWW, resulting in the accumulation of VFAs. This is evidenced by the final pH of R3 of 6.5. R4 exhibited the longest sustained biogas production (BP), with BP halting after day 17; R4 also exhibited the highest biogas yield of 54,35 mL/gVS. R2 (CNTRL) exhibited a similar biogas production trend to that of R4. The addition of IIL resulted in a 29 % increase in biogas yield when compared to the control (R2) these results correlate well with previous studies conducted (Montusiewicz and Lebiocka, 2011). The biogas yield in decreasing order was as follows: R4 (54,35 mL/gVS) >R2 (CNTRL) (38.39 mL/gVS) > R3 (12.55mL/gVS) > R1 (12,20 mL/gVS). R4 exhibited the highest $CH_4$ yield of 76.4% $CH_4$ followed by R3 at 71.40 % $CH_4$, R2 at 67.7 % $CH_4$ and lastly 40.71 % $CH_4$ for R1. R4 exhibited an 11.39 % increase in $CH_4$ yield when compared to the CNTRL (R2).

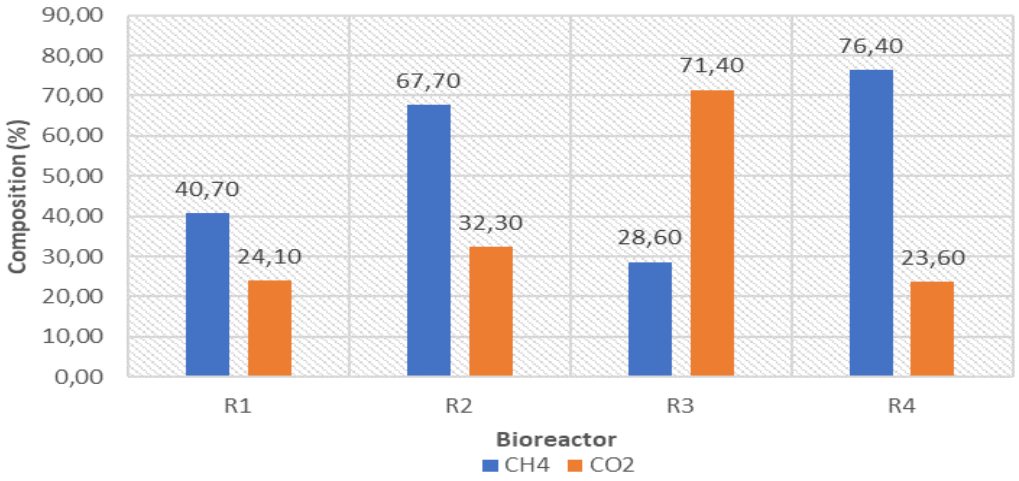


Figure 4-7: Biomethane yield (IWW selection BMP)

Figure 4-7 depicts the average $CH_4$ and $CO_2$ concentrations of the biogas produced by each bioreactor. The biomethane yield in decreasing order was as follows: R4 (76.40 % $CH_4$) >R3 (71.40 % $CH_4$) > R2 (67.70 % $CH_4$) > R1 (40.70 % $CH_4$). IWW streams were found to increase the $CH_4$ concentration when compared to the CNTRL (R2). According to Mata-Alvarez et al. (2000), co-digestion typically augments biogas production and quality through beneficial synergistic effects in the digestion medium. This is mainly attributed to the supplementation of deficient nutrients in the feedstock. The addition of ILL was found to have the greatest impact on $CH_4$ content, achieving an 11.39% increase in $CH_4$ content when compared to the CNTRL (R2)

### 4.4.2. Effect of IWW on COD and VS removal.

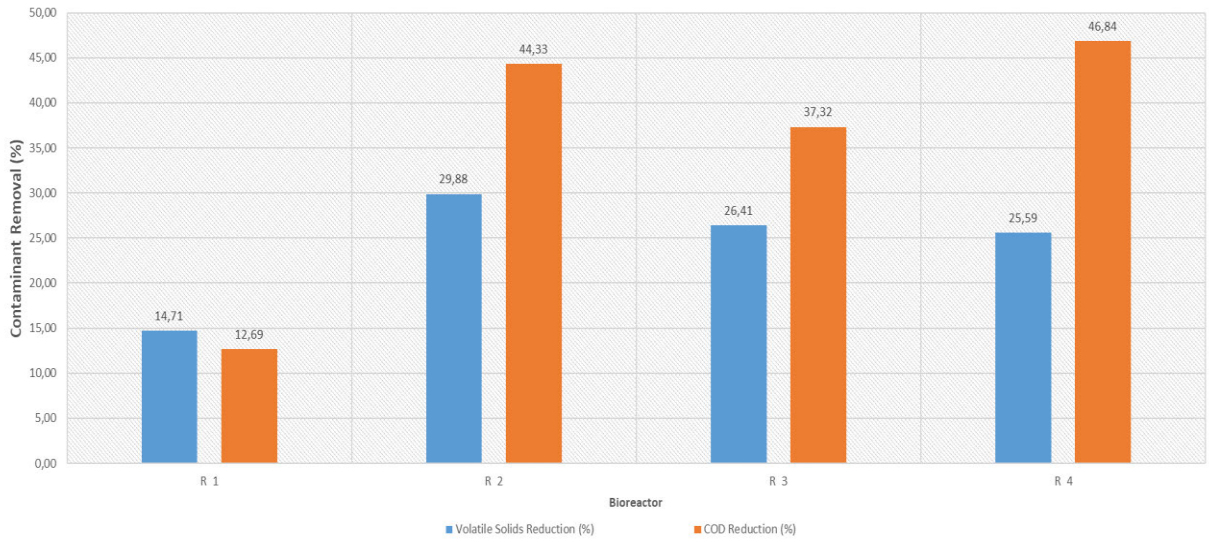


Figure 4-8: Effect of IWW on contaminant removal.

Figure 4-8 depicts the effect of each IWW on COD and VS removal for each assay. The highest VS removal was observed in R2 (29.88%), followed by R3 (26.41 %), R4 (25.59%) and lastly, R1 (14.71%). The highest COD removal was observed in R4 (46.84%) followed by R2 (44.33 %), R3 (37.32%) and lastly R1 (12.69%). ILL (R4) was found to increase the COD removal % by 5.36%, presenting a marginal increase in COD removal. However, IIL exhibited a 14.36 decrease in VS removal when compared to the CNTRL (R1).

### 4.4.3. Summary.

The effects of each IWW were evaluated with respect to their impact on four key performance indicators (biogas yield, biomethane yield and COD and VS removal). ILL was found to increase the biogas yield by 29 % when compared to the control; ILL was also found to increase the COD removal by 5.36% compared to the control. However, ILL exhibited a 14.36 % decrease in VS removal. The ILL also exhibited an 11.39 % increase in biomethane yield compared to the CNTRL. Hence, ILL was identified as the best-performing IWW and was selected for further evaluation in terms of process optimisation.

## 4.5. Optimisation of the IWW BMP system using RSM.

The main purpose of optimization was to establish the optimal operating conditions for ACD of intermediate landfill leachate with primary sewage sludge. The findings consist of the investigated factors in coded form, the experimental results, and the model-predicted response factor results. The experimental biogas yield, COD and VS removal values were collected and evaluated using the methods described in Chapter 3, whereas the predicted values were determined from the model equations generated for each response. The model's statistical significance was assessed through ANOVA. A numerical optimisation technique was employed to optimise the desired goals, including maximum Biogas yield (mL/gVSadded), COD, and VS removal (%). Finally, model validation was conducted. The model's fit was assessed by the adjusted $R^2$, coefficient of determination ($R^2$), coefficient of variance (CV), standard deviation (SD), and appropriate precision (AP). Furthermore, Fisher's F-values and corresponding p-values at a 95% confidence level were employed to assess the significance of the model equations for each output parameter. These results may be found in Tables 4-9 to 4-11

The experimental results were modelled using a second-order polynomial equation for all three responses. Design Expert software proposed a quadratic model for response variables, which were represented as functions of the Temperature (A), ISR (B), and Co-substrate loading (C). Additionally, the model included the sum of the constants, three linear effects (A, B, C), three quadratic effects ($A^2$, $B^2$, $C^2$), and three interaction effects (AB, AC, BC). The optimal sequence of interacting factors for maximising Biogas yield is determined to be (AC > AB > BC). For COD removal, the preferred order is (AB > AC > BC), while for VS removal, the recommended order is (AB > AC > BC). The first order terms demonstrate the primary impact of input factors while the third and second terms demonstrate the relationships among the predictor factors.

The model equations are formulated using coded values for Biogas Yield, COD and VS removal are described.

**Biogas Yield** = 59.9696 + 3.33743 A + 6.57608 B - 0.192024 C - 9.97907 AB - 4.1192 AC - 25.0815 BC -24.005 $A^2$ - 1.9206 $B^2$ + 1.75371 $C^2$

Equation 4-1

**COD Removal (%)** = 31.8143 + 2.70051A - 2.14382B + 1.71722C + 8.65452AB + 6.825AC - 2.03937BC - 7.12343$A^2$ + 1.98463$B^2$ + 1.13413$C^2$

Equation 4-2

**VS Removal (%)** = 26.3367 + 5.1165A + 1.82245B - 0.111514C + 2.29363AB - 3.77627AC - 1.25255BC - 1.90203$A^2$ + 6.20249$B^2$ + 5.9890 $C^2$ - 3.17536$A^2$B

Equation 4-3

Table 4-8 BBD matrix for the ILL system

| | | | | | Experimental Results | | | Predicted Values | | |
|---|---|---|---|---|---|---|---|---|---|---|
| Std | Run | Factor 1 A: Temperature | Factor 2 B: ISR | Factor 3 C: Co-substrate Ratio | Response 1 Biogas Yield | Response 2 COD Removal | Response 3 VS Removal | Response 1 Biogas Yield | Response 2 COD Removal | Response 3 VS Removal |
| | | Degrees Celsius | | | (ml/gVS) | % | % | % | % | % |
| 2 | 1 | 1 | -1 | 0 | 42.0463 | 22.1229 | 34.7057 | 40.78 | 22.87 | 34.81 |
| 13 | 2 | 0 | 0 | 0 | 61.5787 | 31 | 27.18 | 59.97 | 31.81 | 26.34 |
| 3 | 3 | -1 | 1 | 0 | 46 | 13.9191 | 21.9813 | 47.26 | 13.18 | 21.87 |
| 14 | 4 | 0 | 0 | 0 | 58.3301 | 30.9 | 26.3401 | 59.97 | 31.81 | 26.34 |
| 10 | 5 | 0 | 1 | -1 | 91.3679 | 33.3013 | 41.15 | 91.65 | 33.11 | 41.71 |
| 9 | 6 | 0 | -1 | -1 | 27.4424 | 33.046 | 35 | 28.34 | 33.32 | 35.56 |
| 1 | 7 | -1 | -1 | 0 | 13.5 | 35.9799 | 29.2744 | 14.15 | 34.77 | 29.17 |
| 4 | 8 | 1 | 1 | 0 | 34.63 | 34.6801 | 36.5871 | 33.98 | 35.89 | 36.69 |
| 15 | 9 | 0 | 0 | 0 | 60 | 33.5429 | 25.4899 | 59.97 | 31.81 | 26.34 |
| 5 | 10 | -1 | 0 | -1 | 32 | 27.3 | 22.1 | 30.45 | 28.23 | 21.64 |
| 12 | 11 | 0 | 1 | 1 | 42 | 32.7414 | 39.5514 | 41.11 | 22.87 | 38.99 |
| 7 | 12 | -1 | 0 | 1 | 38.6751 | 17 | 28.3 | 38.31 | 31.81 | 28.97 |
| 6 | 13 | 1 | 0 | -1 | 45 | 21 | 40.1 | 45.37 | 13.18 | 39.43 |
| 8 | 14 | 1 | 0 | 1 | 35.1983 | 38 | 31.1949 | 36.74 | 31.81 | 31.65 |
| 11 | 15 | 0 | -1 | 1 | 78.4006 | 40.6436 | 38.4116 | 78.12 | 33.11 | 37.85 |

### 4.5.1. ANOVA analysis.

The response models underwent ANOVA analysis to determine the relevant elements that were accurately incorporated into the models, shown in Table 4-9 to Table 4-11. All models were determined to have a confidence level of 95%. The regression sum of squares, F-values, P-values, adeq precision, and LOF values all satisfied the necessary requirements for determining the model significance. P-values below 0.05 indicate great significance of the model terms, whereas values > 0.05 and < 0.1 suggest minor significance of the models. The P-values achieved were < 0.05 indicating the regression model equations significance and the significant fit of the experimental data to the model equation. LOF values > 0.1 suggest goodness of fit. However, the analysis revealed several model terms in the models had minimal significance, since their P-values were > 0.05. Nevertheless, the model incorporated specific terms to meet the criteria set by the parent terms of interaction.

The regression coefficient of determination ($R^2$), adjusted $R^2$, and predicted $R^2$ were used to evaluate the models. $R^2$ measured the fit between experimental data and models. All of the $R^2$ values were determined to be in close proximity to 1, indicating a strong correlation between the data and the linear regression model depicted in Figure 4-9.

The discrepancy between the observed $R^2$ and the corrected $R^2$ was determined to be smaller than 0.2, hence confirming the importance of the models. The $R^2$ values for Biogas yield, COD removal %, and VS removal % were determined to be 0.9971, 0.9853, and 0.9932, respectively. The adep accuracy, quantifies the ratio of the signal to noise, met the acceptable criterion of being > 4. The ratios for Biogas Yield, COD removal, and VS removal were 52.85, 21.39, and 23.23, respectively.

Table 4-9: ANOVA regression model (quadratic) \ for biogas yield (mL/gVS)

| Source | Sum of Squares | df | Mean Square | F-value | p-value | |
|---|---|---|---|---|---|---|
| **Model** | 5594.10 | 9 | 621.57 | 192.73 | **< 0.0001** | **significant** |
| **A-Temperature** | 89.11 | 1 | 89.11 | 27.63 | 0.0033 | |
| **B-ISR** | 345.96 | 1 | 345.96 | 107.27 | 0.0001 | |
| **C-Co-substrate Ratio** | 0.2950 | 1 | 0.2950 | 0.0915 | 0.7745 | |
| **AB** | 398.33 | 1 | 398.33 | 123.51 | 0.0001 | |
| **AC** | 67.87 | 1 | 67.87 | 21.04 | 0.0059 | |
| **BC** | 2516.33 | 1 | 2516.33 | 780.24 | < 0.0001 | |
| **$A^2$** | 2127.65 | 1 | 2127.65 | 659.72 | < 0.0001 | |
| **$B^2$** | 13.62 | 1 | 13.62 | 4.22 | 0.0950 | |
| **$C^2$** | 11.36 | 1 | 11.36 | 3.52 | 0.1194 | |
| **Residual** | 16.13 | 5 | 3.23 | | | |
| **Lack of Fit** | 10.85 | 3 | 3.62 | 1.37 | 0.4483 | **not significant** |
| **Pure Error** | 5.28 | 2 | 2.64 | | | |
| **Cor Total** | 5610.22 | 14 | | | | |

| Std. Dev | Mean | C.V. % | $R^2$ | Adjusted $R^2$ | Predicted $R^2$ | Adeq Precision |
|---|---|---|---|---|---|---|
| 1.80 | 47.08 | 3.81 | 0.9971 | 0.9920 | 0.9669 | 52.8547 |

Table 4-10: ANOVA regression model (quadratic) for COD removal %

| Source | Sum of Squares | df | Mean Square | F-value | p-value | |
|---|---|---|---|---|---|---|
| **Model** | 840.86 | 9 | 93.43 | 37.28 | 0.0005 | **significant** |
| **A-Temperature** | 58.34 | 1 | 58.34 | 23.28 | 0.0048 | |
| **B-ISR** | 36.77 | 1 | 36.77 | 14.67 | 0.0122 | |
| **C-Co-substrate Ratio** | 23.59 | 1 | 23.59 | 9.41 | 0.0278 | |
| **AB** | 299.60 | 1 | 299.60 | 119.56 | 0.0001 | |
| **AC** | 186.32 | 1 | 186.32 | 74.35 | 0.0003 | |
| **BC** | 16.64 | 1 | 16.64 | 6.64 | 0.0496 | |
| **$A^2$** | 187.36 | 1 | 187.36 | 74.77 | 0.0003 | |
| **$B^2$** | 14.54 | 1 | 14.54 | 5.80 | 0.0609 | |
| **$C^2$** | 4.75 | 1 | 4.75 | 1.90 | 0.2271 | |
| **Residual** | 12.53 | 5 | 2.51 | | | |
| **Lack of Fit** | 8.04 | 3 | 2.68 | 1.19 | 0.4858 | **not significant** |
| **Pure Error** | 4.49 | 2 | 2.24 | | | |
| **Cor Total** | 853.39 | 14 | | | | |

| Std. Dev | Mean | C.V. % | $R^2$ | Adjusted $R^2$ | Predicted $R^2$ | Adeq Precision |
|---|---|---|---|---|---|---|
| 1.58 | 29.68 | 5.33 | 0.9853 | 0.9589 | 0.08374 | 21.3978 |

Table 4-11: ANOVA regression model (quadratic) for VS removal %

| Source | Sum of Squares | df | Mean Square | F-value | p-value | |
|---|---|---|---|---|---|---|
| **Model** | 598.09 | 10 | 59.81 | 58.75 | 0.0007 | **significant** |
| **A-Temperature** | 209.43 | 1 | 209.43 | 205.73 | 0.0001 | |
| **B-ISR** | 13.29 | 1 | 13.29 | 13.05 | 0.0225 | |
| **C-Co-substrate Ratio** | 0.0995 | 1 | 0.0995 | 0.0977 | 0.7702 | |
| **AB** | 21.04 | 1 | 21.04 | 20.67 | 0.0104 | |
| **AC** | 57.04 | 1 | 57.04 | 56.03 | 0.0017 | |
| **BC** | 6.28 | 1 | 6.28 | 6.16 | 0.0680 | |
| **$A^2$** | 13.36 | 1 | 13.36 | 13.12 | 0.0223 | |
| **$B^2$** | 142.05 | 1 | 142.05 | 139.54 | 0.0003 | |
| **$C^2$** | 132.44 | 1 | 132.44 | 130.10 | 0.0003 | |
| **$A^2B$** | 20.17 | 1 | 20.17 | 19.81 | 0.0112 | |
| **Residual** | 4.07 | 4 | 1.02 | | | |
| **Lack of Fit** | 2.64 | 2 | 1.32 | 1.85 | 0.3508 | **not significant** |
| **Pure Error** | 1.43 | 2 | 0.7142 | | | |
| **Cor Total** | 602.16 | 14 | | | | |

| Std. Dev | Mean | C.V. % | $R^2$ | Adjusted $R^2$ | Predicted $R^2$ | Adeq Precision |
|---|---|---|---|---|---|---|
| 1.01 | 31.82 | 3.17 | 0.9932 | 0.9763 | 0.8191 | 23.2314 |

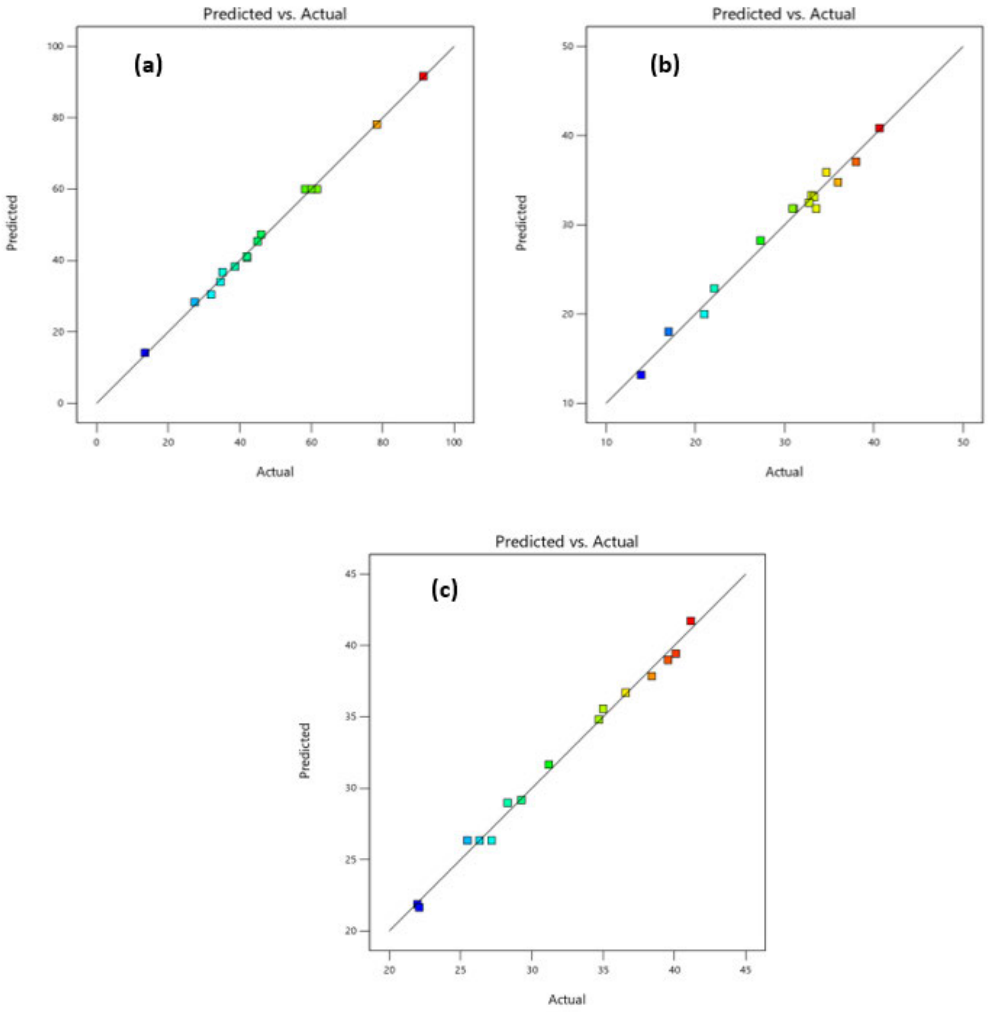


Figure 4-9 (a-b) Biogas yield, COD removal, and VS removal predicted vs actual plots.

#### 4.5.1.1. Residual Plot analysis

The residual plots represent the discrepancy between the observed and anticipated data values generated by the model. The normal probability plot was employed to assess the residuals distribution. The data distribution was determined to be normal, with all data points conforming to a linear pattern (Design Expert 2017). Furthermore, the plot depicting the relationship between residual and predicted values demonstrates that the data points were inside the designated range of the models, indicating that no data omissions. These are depicted in Figure 4-10 and Figure 4-12.

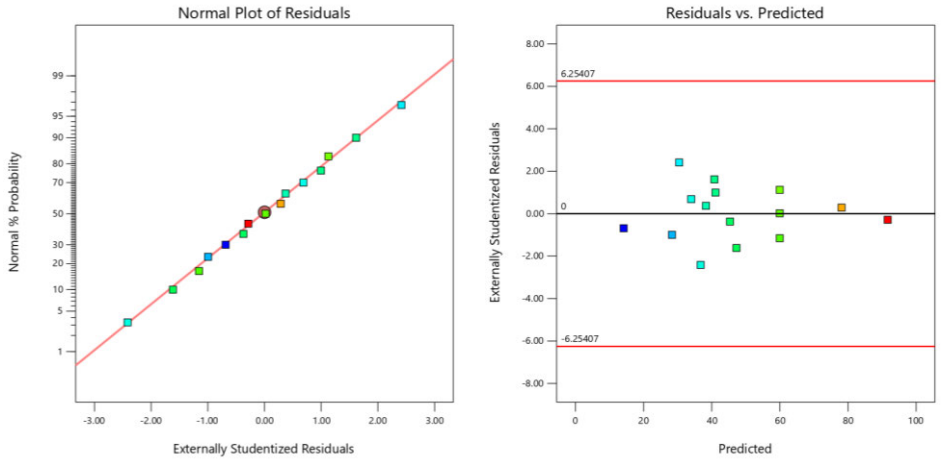


Figure 4-10: Normal plot for biogas yield.

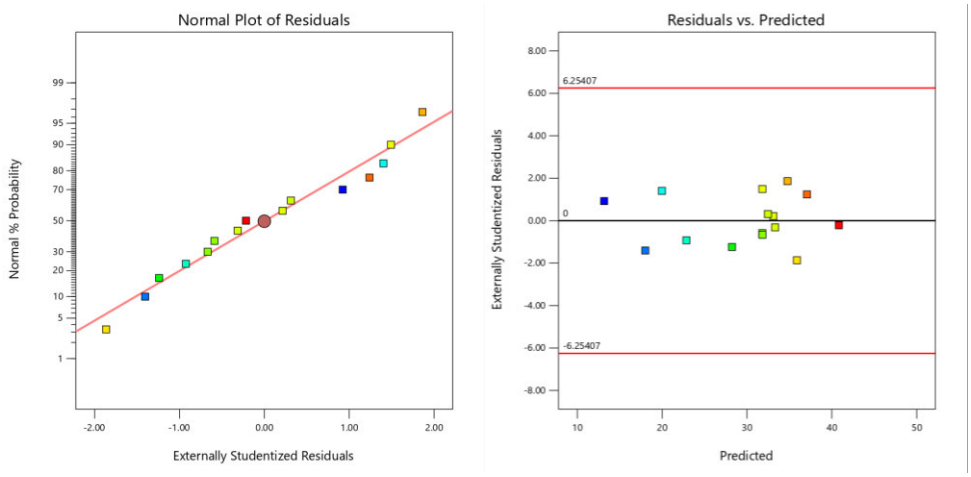


Figure 4-11: Normal plot for COD removal %

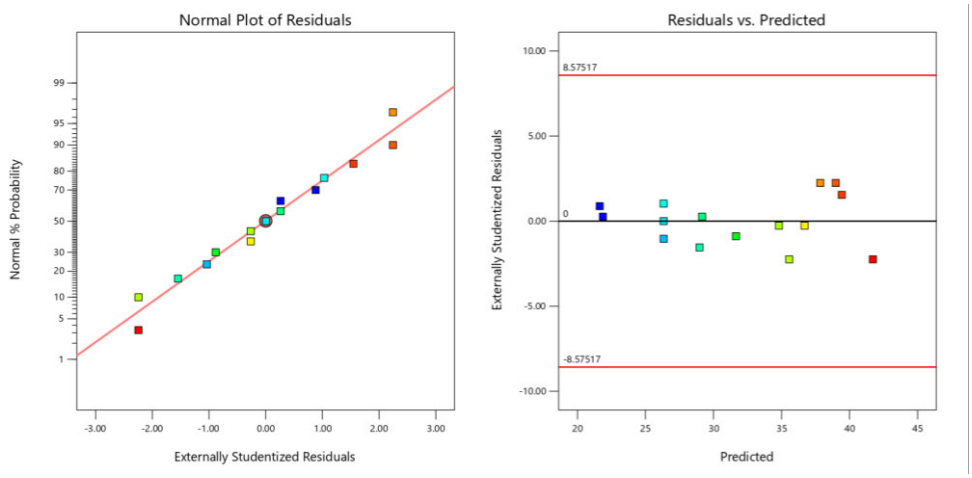


Figure 4-12: Normal plot for VS removal %

### 4.5.2 3D Plot analysis.

The 3D and contour plots in Figure 4-13 to 4-15 are graphical representations of the impact of the factors on each individual responses, specifically in relation to each response regression model. The temperature and ISR were shown to be the most influential parameters, with co-substrate loading also having a significant impact.

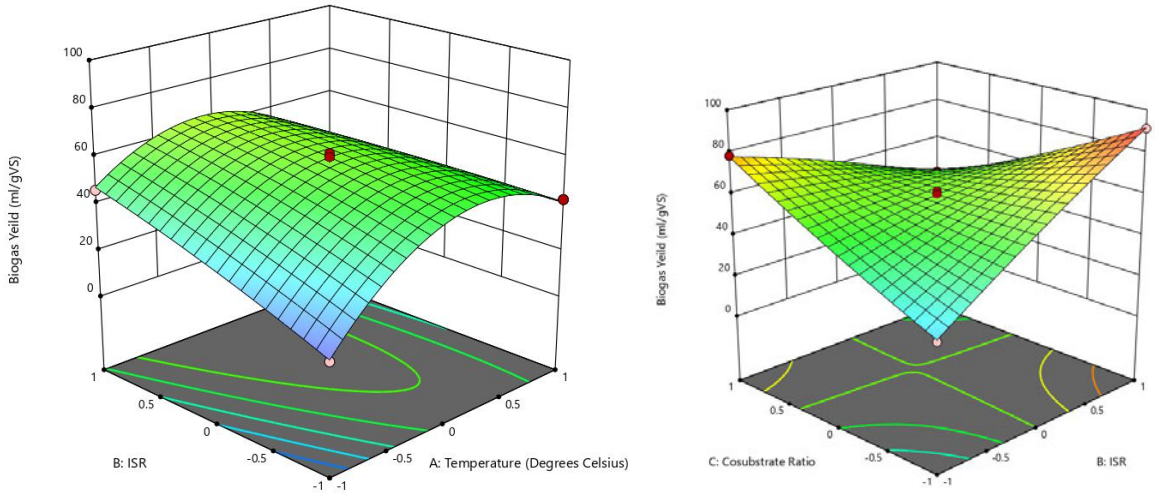


Figure 4-13: Impact of input factor on biogas yield (mL/gVS)

From figure 4-13 the relationship between ISR, Temperature and Co-substrate loading rate on biogas yield are represented graphically. Biogas yield is seen to increase with the increase in ISR with the peak biogas yield recorded at the maximum ISR (1.5:1). Optimal inoculum substrate ratio (ISR) is of utmost importance to avoid the formation of volatile fatty acids (VFA) throughout the anaerobic digestion process, aiming to maximise methane production (Dixon et al., 2019). Inoculum also serves as a source of micronutrients and nitrogen, which balance the C/N ratio during digestion while facilitating enzymatic activity and hence enhancing biogas yield. The increase in temperature was seen to increase biogas yield between 25 – 37 $^{0}$C, however a decreasing trend was observed between 37 and 55 $^{0}$C (representing the thermophilic region). Thermophilic has been shown to result in increased VFAs concentrations, affecting process stability and ultimately leading to process failure (Al-Sulaimi et al., 2022). Increase in biogas yield was observed with increase co-substrate loading this was attributed to the supplementation of nutrients by the leachate were deficient in the initial substrate (Mata-Alvarez et al., 2000).

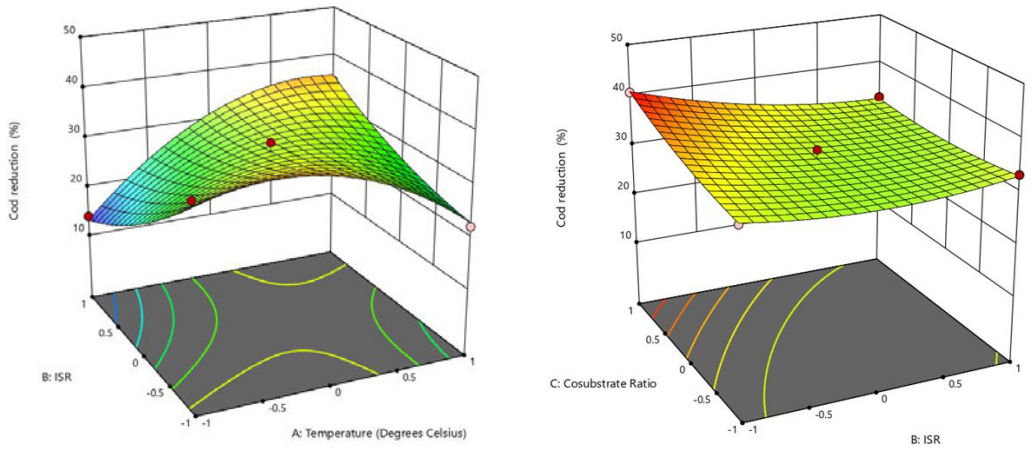


Figure 4-14: Impact of input factors on COD removal %

From Figure 4-14, the relationship between ISR, temperature and co-substrate loading rate on COD removal % yield are represented graphically. An increase in ISR was shown to decrease COD removal. This was attributed to BOD introduced by the increased inoculum loading. COD removal was observed to increase with increasing co-substrate loading.

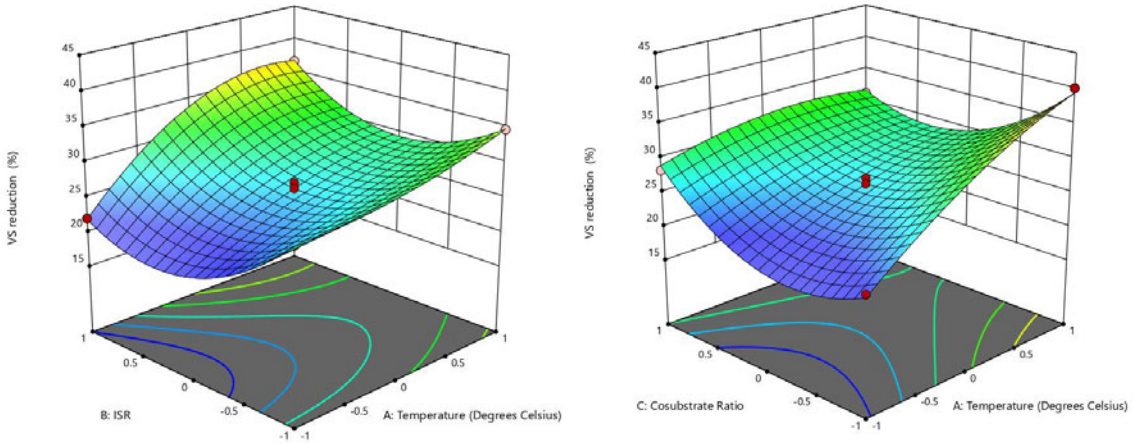


Figure 4-15: Impact of input factors on VS removal%

From Figure 4-15, the relationship between ISR, temperature and co-substrate loading rate on VS removal % yield are represented graphically. An increase in ISR was shown to decrease VS removal. This was attributed to BOD introduced by the increased inoculum loading. VS removal was observed to increase with increasing co-substrate loading.

### 4.5.3. Optimization

To optimize the three input variables, the numerical optimization tool in RSM was used. Table 4-12 demonstrates that all process responses were maximized whereas the input variables (temperature, ISR, and co-substrate loading remained within the range. Figure 4-16 shows the ramp graphs that indicate the optimal operating parameters and the desirability gained. It was discovered that with a temperature of 39 $^{0}$C, a ISR 1.5:1, co-substrate loading ratio of 1:20, at a desirability performance of 90.10%, biogas yield of 90.76 mL/gVS, COD removal of 33.62 % and a VS removal of 43.25 % achieved. The model for each response was validated using the determined optimum condition; three experimental runs were conducted and are described in Table 4-12.

Table 4-12 Optimum conditions for ILL BMP system

| Factor | Goal | Lower Limit | Upper Limit |
|---|---|---|---|
| **A: Temperature** | is in range | 25 | 55 |
| **B: ISR** | is in range | 1:2 | 1.5:1 |
| **C: Co-substrate Ratio** | is in range | 1:20 | 1:5 |
| **Response** | | | |
| **Biogas Yield (ml/gVS$_{added}$)** | maximize | 13.5 | 91.3679 |
| **COD removal (%)** | maximize | 13.9191 | 40.6436 |
| **VS removal (%)** | maximize | 21.9813 | 41.15 |

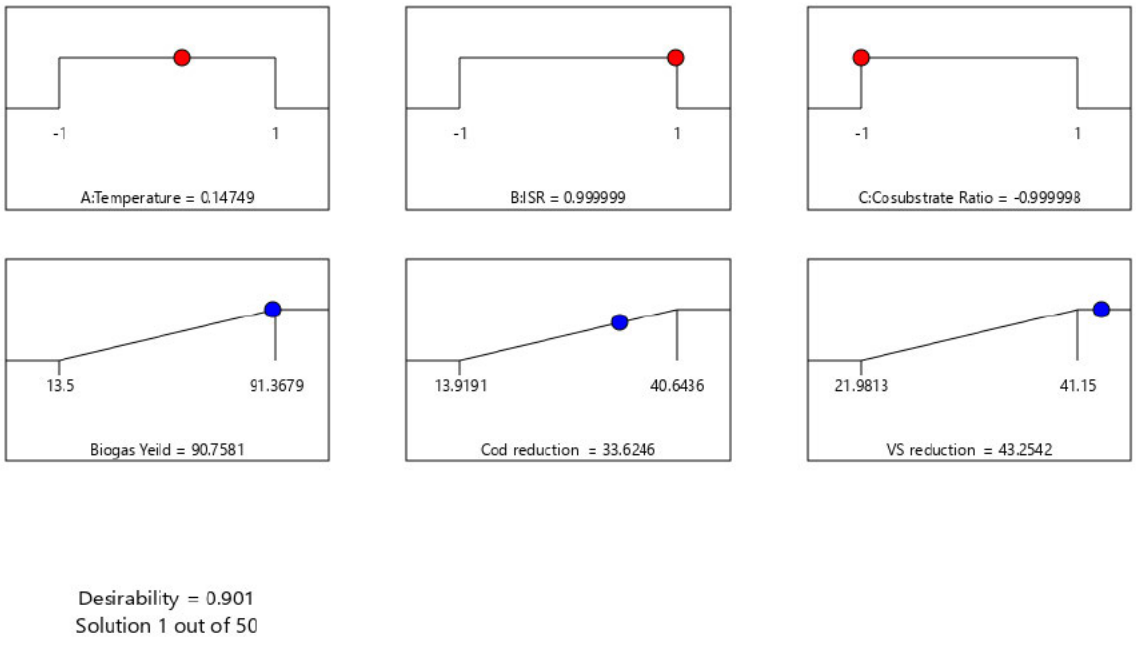


Figure 4-16: Ramp plot for optimum operating conditions for IIL BMP system.

### 4.5.4. Model Validation.

Table 4-13 presents the three experimental runs for each process that were performed under optimal operating parameters to test the appropriateness and validity of the suggested models. The experiment runs yielded mean, biogas, COD, and VS removals of 87.90 mL/gVS, 35.16%, and 39.90%. The observed values closely aligned with the anticipated values, with a discrepancy of less than 5%. This suggests that the models are able to accurately represent the connection between observed and projected outcomes. Therefore, the models demonstrated satisfactory predictive accuracy.

Table 4-13: Model validation experiments

| Run | Biogas Yield ($ml/gVS_{added}$) | COD Removal (%) | VS Removal (%) |
|---|---|---|---|
| 1 | 87.92 | 2.97 | 38.45 |
| 2 | 88.23 | 35.87 | 40.32 |
| 3 | 87.55 | 36.65 | 39.14 |

| | Predicted | | Observed | | | | | |
|---|---|---|---|---|---|---|---|---|
| Analysis | Predicted Mean | Predicted Median | Std Dev | n | SE Pred | 95% PI low | Data Mean | 95% PI high |
| Biogas Yield ($ml/gVS_{added}$) | 91.6524 | 91.6524 | 1.79585 | 3 | 1.86918 | 86.8475 | 87.9 | 96.4572 |
| COD Removal (%) | 33.1114 | 33.1114 | 1.58299 | 3 | 1.64763 | 28.876 | 35.1633 | 37.3468 |
| VS Removal (%) | 41.7148 | 41.7148 | 1.00895 | 3 | 1.10908 | 38.6355 | 39.3033 | 44.7941 |

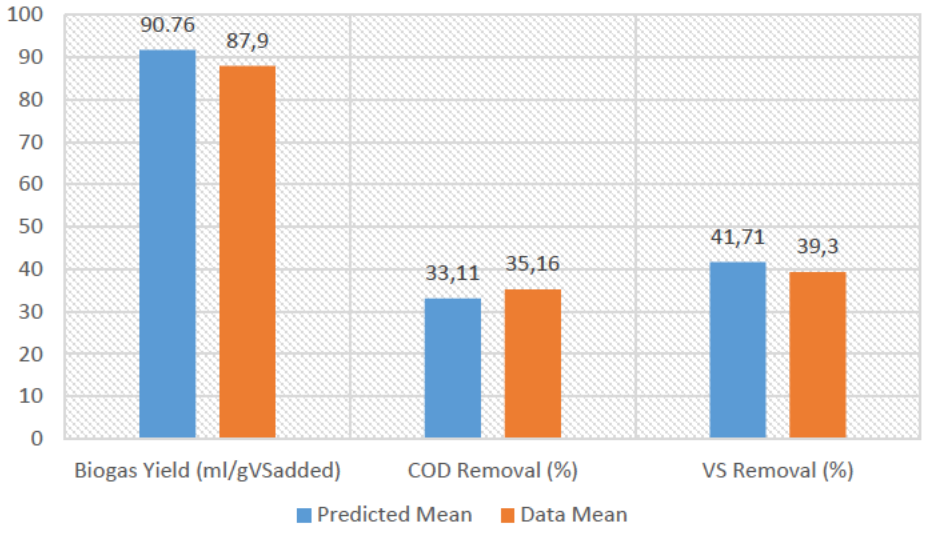


Figure 4-17: Model validation predicted vs experimental results contaminant removal.

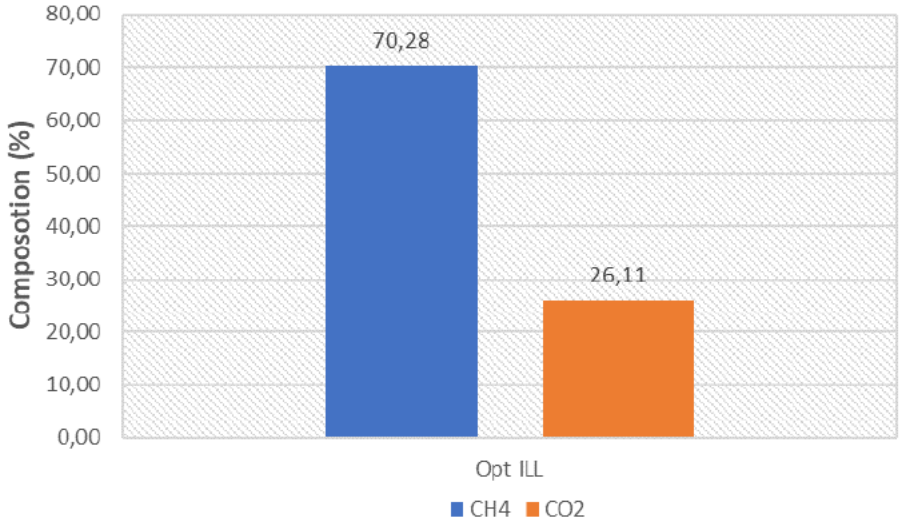


Figure 4-18: Model validation biomethane yield.

Represented in Figure 4-18 is the biomethane yield achieved by the validation experimental runs; the mean $CH_4$ content of 70.28 % was recorded; this value correlates well with the results achieved in the optimization experimental runs.

## 4.6. Biochar Selection BMP tests.

The BMP test was conducted to assess Biochar synthesised from sugarcane bagasse at three pyrolysis temperatures: 350$^0$C, 450$^0$C and 550$^0$C. The synthesised biochars were denoted as follows: BC 350, BC 450, and BC 550. This was implemented as a discriminative approach to

pick the most optimal biochar among the three based on their performance during the digesting process.

The batch AD experiments were conducted utilising 1L Schott bottles as bioreactors BMP test was duplicated, with an additional duplicate of a blank control sample. The bioreactors were placed in the water bath and operated. The hydraulic retention time (HRT) was set at 21 days. The study examined four parameters: biomethane yield and quality, and COD and VS reduction. The optimum process parameters identified in the optimisation of the IWW BMP system were employed and are as follows: temperature (37 $^{0}$C), ISR (1.5:1). However, the maximum co-substrate loading ratio of (1:5) was employed at a biochar loading of 5 (g/L). The bioreactor loading is presented in Table 4-14.

Table 4-14: BC selection BMP tests bioreactor loading.

| Bioreactor | Inoculum Substrate ratio | Co-substrate loading rate | Inoculum (ml) | Primary Sludge (ml) | Landfill Leachate (ml) | Biochar Loading (g/l) |
|---|---|---|---|---|---|---|
| **R1** | 1.5:1 | N/A | 800 | 0 | 0 | - |
| **R (CNTRL 2)** | 1.5:1 | 1:5 | 230 | 440 | 130 | - |
| **R3 (BC 350)** | 1.5:1 | 1:5 | 230 | 440 | 130 | 5 |
| **R4 (BC 450)** | 1.5:1 | 1:5 | 230 | 440 | 130 | 5 |
| **R5 (BC 550)** | 1.5:1 | 1:5 | 230 | 440 | 130 | 5 |

| Bioreactor | TS (g) | VS (g) | COD (mg/l) | Biogas Yield (ml) | Biogas Yield (ml/gVS$_a$) |
|---|---|---|---|---|---|
| **R1** | 42,80 | 22.13 | 38 800,00 | 270 | 12,20 |
| **R (CNTRL 2)** | 31,02 | 18,68 | 36 150,00 | 800 | 42.83 |
| **R3 (BC 350)** | 32.24 | 17,49 | 38 000,00 | 820 | 46,88 |
| **R4 (BC 450)** | 33,04 | 17,86 | 40 700,00 | 900 | 50,38 |
| **R5 (BC 550)** | 33.53 | 18,06 | 40 550,00 | 480 | 26,57 |

### 4.6.1. Effect of BC on biogas and biomethane yield.

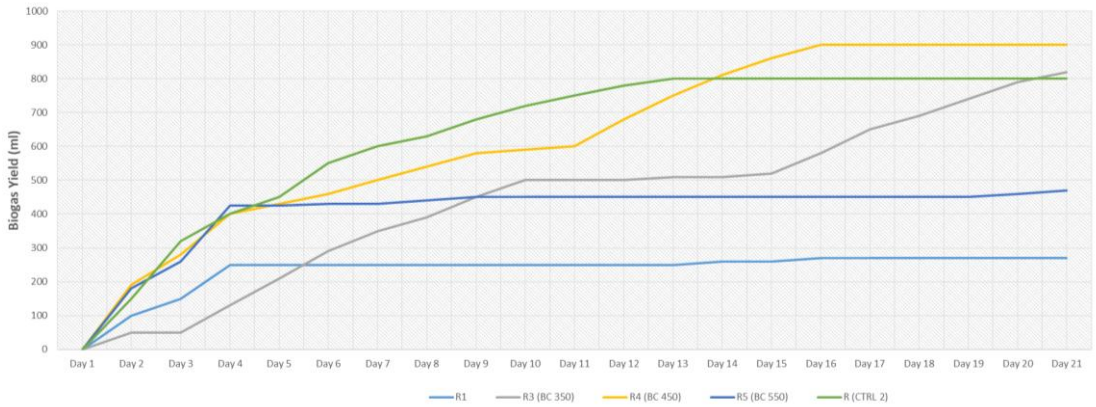


Figure 4-19: Accumulative biogas yield (mL) (BC BMP tests)

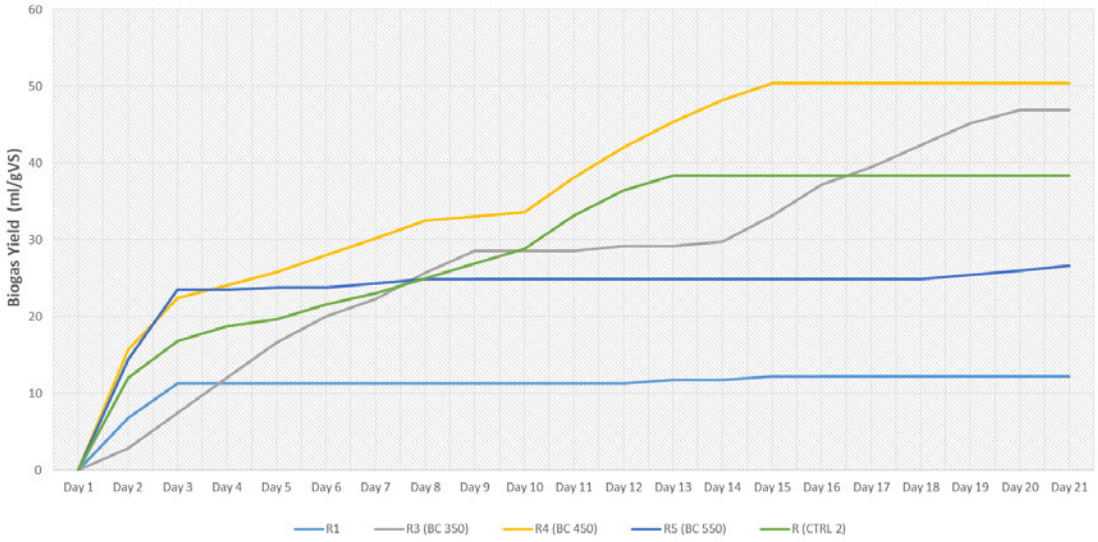


Figure 4-20: Accumulative biogas yield (mL/gVS) (BC BMP test)

Figure 4-(19-20) depicts the accumulative biogas yield for each bioreactor. R4 (BC 450) and R5 (BC 550) exhibited the highest rate of biogas production between days 1 – 3; this observation is confirmed by Shi et al. (2022) reported that the initial period of slow growth, known as the lag phase, was reduced by 7.82 hours when 0.6 grams of biochar per gram of VS were added. The order of biogas yield if descending order is as follows: R4 (BC 450) > R3 (BC 350) > R (CNTRL 2) > R5 (550) > R1 producing 50.38; 46.88; 42.83; 26.57 and 12.20 mL/gVS respectively. Biochar enhances microorganisms' density, facilitating their interaction with substrates effectively addressing the inherent issue (Khalid et al., 2021). The halt in biogas

production for R5 (550) was attributed to the hydrophobic nature of the synthesised BC, as result constant agitation as required to keep the BC particles suspended in the solution (Ding et al. 2014). R4 (BC 450) exhibited the longest sustained biogas production (BP), with BP halting after day 17; R4 also exhibited the highest biogas yield of 50,38 mL/gVS. R (CNTRL 2) exhibited a similar biogas production trend to that of R4. The addition of BC 450 resulted in a 14.34 % increase in biogas yield when compared to the control. These results correlate well with previous studies conducted and are attributed to the reduction of the lags phase as a result of BC addition (Chiappero et al., 2020). R4 (BC 4500) exhibited the highest $CH_4$ yield of 79.5% $CH_4$, followed by R3 at 68.71.% $CH_4$, R (CNTRL) at 67.7 % $CH_4$ and lastly 40.71 % $CH_4$ for R1. R4 (BC 450) exhibited a 14.84 % increase in $CH_4$ yield when compared to R (CNTRL).

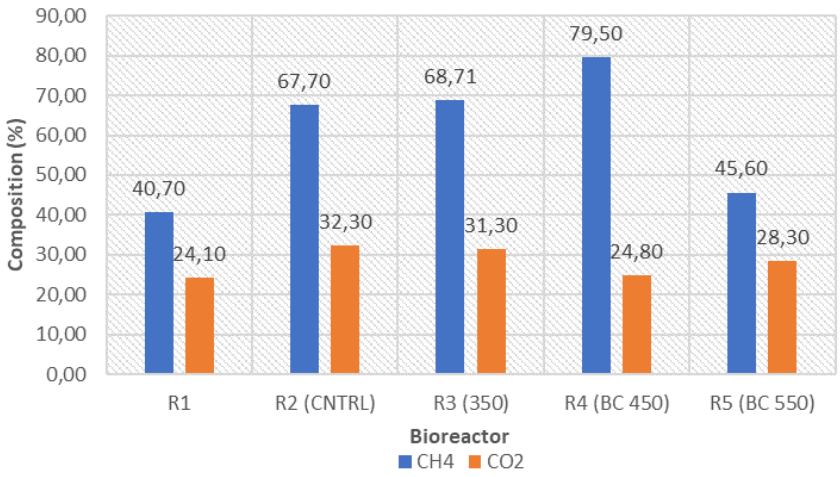


Figure 4-21: Biomethane yield (BC selection BMP)

### 4.6.2. Effect of BC on COD and VS removal

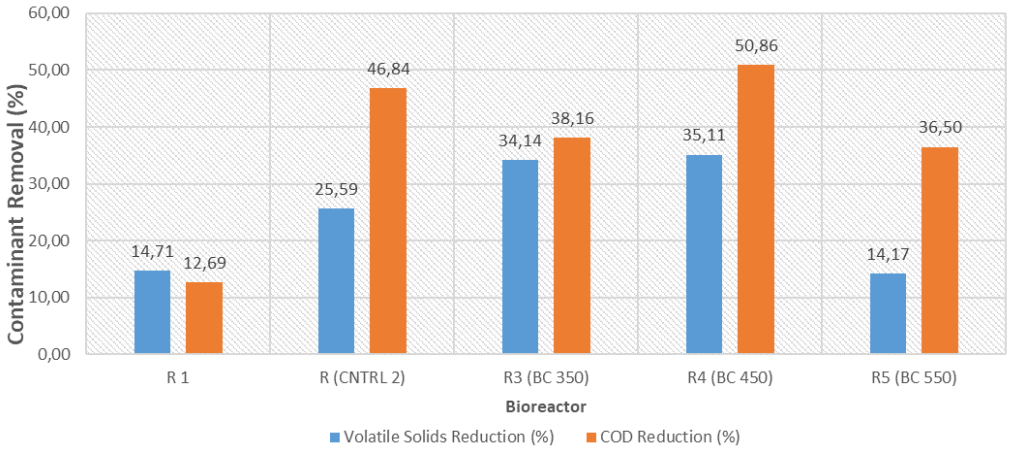


Figure 4-22: Effect of BC on contaminant removal (BC BMP system)

Table 4-22 depicts the effect of each BC on COD and VS removal for each assay. The highest VS removal was observed in R4 (BC 450) (35.11%), followed by R3 (BC 350) (34.14 %), R (CNTRL 2) (25.59%) and lastly, R5 (BC 550) (14.17%). The highest COD removal was observed in R4 (BC 450) (50.86%), followed by R (CNTRL 2) (46.84 %), R3 (BC 350) (38.16%) and lastly, R1 (12.69%). BC 450 was found to have the greatest impact on the performance of the AD system, increasing the COD removal % by 8%, presenting a marginal increase in COD removal. However, BC 450 addition exhibited a 27.11 increase in VS removal when compared to the CNTRL.

### 4.6.3. Summary

The effects of each BC were evaluated with respect to their impact on four key performance indicators (biogas yield, biomethane yield and COD and VS removal). BC 450 was found to increase the biogas yield by 15 % when compared to the control these results correlate well with previous studies conducted and are attributed to the reduction of lag phase as a result of BC addition (Chiappero et al., 2020), BC 450 was also found to increase the COD removal by 8 % compared to the control. The addition of BC 450 exhibited a 27.11 % increase in VS removal. BC 450 also exhibited a 14.84 % increase in biomethane yield compared to the CNTRL. Hence BC 450 was identified as the best performing IWW and was selected for further evaluation in terms of process optimization.

### 4.7. Optimisation of the BC BMP system using RSM.

The main purpose of optimization was to establish the optimal operating conditions for ACD with biochar addition. The findings consist of the investigated factors in coded form, the experimental results, and the model-predicted response factor results. The experimental Biogas, COD and VS values were collected and evaluated using the methods described in chapter 3 whereas the predicted values were determined from the model equations generated for each response (Equation 4-4 to 4-6). The model's statistical significance was assessed through ANOVA. A numerical optimisation technique was employed to optimise the desired goals, including maximum Biogas yield (mL/gVSadded), COD, and VS removal (%). Finally, model validation was conducted. The model's fit was assessed by the adjusted $R^2$, coefficient of determination ($R^2$), coefficient of variance (CV), standard deviation (SD), and appropriate precision (AP). Furthermore, Fisher's F-values and corresponding p-values at a 95% confidence level were employed to assess the significance of the model equations for each output parameter. These results may be found in Tables 4-15 to 4-17.

The experimental results were modelled using a second-order polynomial equation for the biogas model and linear for COD and VS removal. The Design Expert software proposed a quadratic model for response 1 (Biogas yield), which were represented as functions of the Temperature (A), ISR (B), and biochar loading (C). Additionally, the model included the sum of the constants, three linear effects (A, B, C), three quadratic effects ($A^2$, $B^2$, $C^2$), and three interaction effects (AB, AC, BC). The optimal sequence of interacting factors for maximising Biogas yield is determined to be (AC > BC > AB).

The model equations were formulated using coded values for Biogas Yield, COD and VS removal are described in Equation 4-4 to 4-6.

**Biogas Yield =** 3.529 + 18.7166A - 5.37982B + 7.53929C - 0.837095 AB + 9.01348AC + 0.725124BC + 3.63431$A^2$ + 20.6419$B^2$ + 15.0254$C^2$

Equation 4-4

**COD Removal (%)** = 34.8223 + 7.32989 A + -5.33295B + 2.92113C

Equation 4-5

**VS Removal (%) =** 26.2317 + 18.0958 A - 1.76598B - 5.90941

Equation 4-6

Table 4-15: BBD matrix for the BC system

| | | | | | Experimental Results | | | Predicted Values | | |
|---|---|---|---|---|---|---|---|---|---|---|
| Std | Run | Factor 1 A: Temperature | Factor 2 B: Co-substrate Ratio | Factor 3 C: Biochar loading rate | Response 1 Biogas Yield | Response 2 COD Removal | Response 3 VS Removal | Response 1 Biogas Yield | Response 2 COD Removal | Response 3 VS Removal |
| | | Degrees Celsius | | (gBC/l) | (ml/gVS) | % | % | % | % | % |
| 14 | 1 | 0 | 0 | 0 | 3.15418 | 30.6667 | 7.09059 | 3.53 | 34.82 | 26.23 |
| 11 | 2 | 0 | -1 | 1 | 47.4379 | 40.2078 | 12.4633 | 51.39 | 43.08 | 22.09 |
| 6 | 3 | 1 | 0 | -1 | 23.6892 | 36.7293 | 41.9712 | 24.35 | 39.23 | 50.24 |
| 12 | 4 | 0 | 1 | 1 | 43.0692 | 37.2093 | 27.4583 | 42.08 | 32.41 | 18.56 |
| 4 | 5 | 1 | 1 | 0 | 37.0159 | 38.6957 | 40.2278 | 40.30 | 36.82 | 42.56 |
| 8 | 6 | 1 | 0 | 1 | 59.7589 | 41.4847 | 43.5253 | 57.46 | 45.07 | 38.42 |
| 3 | 7 | -1 | 1 | 0 | 2.89419 | 14.7541 | 4.32971 | 4.55 | 22.16 | 6.37 |
| 5 | 8 | -1 | 0 | -1 | 2.6455 | 19.6522 | 9.10053 | 4.95 | 24.57 | 14.05 |
| 10 | 9 | 0 | 1 | -1 | 29.5045 | 31 | 38.9246 | 25.55 | 26.57 | 30.38 |
| 13 | 10 | 0 | 0 | 0 | 0.629247 | 38.7931 | 24.3108 | 3.53 | 34.82 | 26.23 |
| 9 | 11 | 0 | -1 | -1 | 36.7737 | 40.3782 | 47.8794 | 37.76 | 37.23 | 33.91 |
| 1 | 12 | -1 | -1 | 0 | 16.9203 | 37.6871 | 12.5498 | 13.63 | 32.83 | 9.90 |
| 15 | 13 | 0 | 0 | 0 | 6.80356 | 36.8 | 24.3152 | 3.53 | 34.82 | 26.23 |
| 2 | 14 | 1 | -1 | 0 | 54.3904 | 46.0496 | 52.1756 | 52.74 | 47.49 | 46.09 |
| 7 | 15 | -1 | 0 | 1 | 2.66127 | 32.2268 | 7.1535 | 2.00 | 30.41 | 2.23 |

### 4.7.1. ANOVA analysis

The response models underwent ANOVA analysis to determine the relevant elements that were accurately incorporated into the models, shown in Table 4-15 to Table 4-17. All models were determined to have a confidence level of 95%. The regression sum of squares, F-values, P-values, adeq precision, and LOF values all satisfied the necessary requirements for determining the model significance. P-values below 0.05 indicate great significance of the model terms, whereas values > 0.05 and < 0.1 suggest minor significance of the models. The P-values achieved were < 0.05 indicating the regression model equations significance and the significant fit of the experimental data to the model equation. LOF values > 0.1 suggest goodness of fit. However, the analysis revealed several model terms in the models had minimal significance, since their P-values were > 0.05. Nevertheless, the model incorporated specific terms to meet the criteria set by the parent terms of interaction.

The regression coefficient of determination ($R^2$), adjusted $R^2$, and predicted $R^2$ were used to evaluate the models. $R^2$ measured the fit between experimental data and models. All of the $R^2$ values were determined to be in close proximity to 1, indicating a strong correlation between the data and the linear regression model depicted in Figure 4-18.

The discrepancy between the observed $R^2$ and the corrected $R^2$ was determined to be smaller than 0.2, hence confirming the importance of the models. The $R^2$ values for Biogas yield, COD removal %, and VS removal % were determined to be 0.9852, 0.7606, and 0.7431 respectively. The adep accuracy, which quantifies the ratio of the signal to the noise, met the acceptable criterion of being more than 4. The ratios for Biogas Yield, COD removal, and VS removal were 15.9195, 10.7625, and 9.6993 respectively.

Table 4-16: ANOVA regression model (quadratic) \ for biogas yield (mL/gVS)

| Source | Sum of Squares | df | Mean Square | F-value | p-value | |
|---|---|---|---|---|---|---|
| **Model** | 6066.99 | 9 | 674.11 | 37.03 | 0.0005 | **significant** |
| **A-Temperature** | 2802.50 | 1 | 2802.50 | 153.94 | < 0.0001 | |
| **B-Co-substrate loading ratio** | 231.54 | 1 | 231.54 | 12.72 | 0.0161 | |
| **C-Biochar loading rate** | 454.73 | 1 | 454.73 | 24.98 | 0.0041 | |
| **AB** | 2.80 | 1 | 2.80 | 0.1540 | 0.7109 | |
| **AC** | 324.97 | 1 | 324.97 | 17.85 | 0.0083 | |
| **BC** | 2.10 | 1 | 2.10 | 0.1155 | 0.7477 | |
| **$A^2$** | 48.77 | 1 | 48.77 | 2.68 | 0.1626 | |
| **$B^2$** | 1573.25 | 1 | 1573.25 | 86.42 | 0.0002 | |
| **$C^2$** | 833.59 | 1 | 833.59 | 45.79 | 0.0011 | |
| **Residual** | 91.03 | 5 | 18.21 | | | |
| **Lack of Fit** | 71.75 | 3 | 23.92 | 2.48 | 0.3001 | **not significant** |
| **Pure Error** | 19.27 | 2 | 9.64 | | | |
| **Cor Total** | 6158.02 | 14 | | | | |

| Std. Dev | Mean | C.V. % | $R^2$ | Adjusted $R^2$ | Predicted $R^2$ | Adeq Precision |
|---|---|---|---|---|---|---|
| 4.27 | 24.49 | 17.42 | 0.9852 | 0.9586 | 0.8065 | 15.9195 |

Table 4-17: ANOVA regression model (linear) \ for COD removal %.

| Source | Sum of Squares | df | Mean Square | F-value | p-value | |
|---|---|---|---|---|---|---|
| **Model** | 725.60 | 3 | 241.87 | 11.65 | 0.0010 | **significant** |
| **A-Temperature** | 429.82 | 1 | 429.82 | 20.70 | 0.0008 | |
| **B-Co-substrate loading ratio** | 227.52 | 1 | 227.52 | 10.96 | 0.0070 | |
| **C-Biochar loading rate** | 68.26 | 1 | 68.26 | 3.29 | 0.0972 | |
| **Residual** | 228.41 | 11 | 20.76 | | | |
| **Lack of Fit** | 192.53 | 9 | 21.39 | 1.19 | 0.5365 | **not significant** |
| **Pure Error** | 35.88 | 2 | 17.94 | | | |
| **Cor Total** | 954.01 | 14 | | | | |

| Std. Dev | Mean | C.V. % | $R^2$ | Adjusted $R^2$ | Predicted $R^2$ | Adeq Precision |
|---|---|---|---|---|---|---|
| 4.56 | 34.82 | 13.09 | 0.7606 | 0.6953 | 0.5257 | 10.7625 |

Table 4-18: ANOVA regression model (linear) for VS removal

| Source | Sum of Squares | df | Mean Square | F-value | p-value | |
|---|---|---|---|---|---|---|
| **Model** | 2923.98 | 3 | 974.66 | 10.61 | 0.0014 | **significant** |
| **A-Temperature** | 2619.66 | 1 | 2619.66 | 28.51 | 0.0002 | |
| **B-Co-substrate loading ratio** | 24.95 | 1 | 24.95 | 0.2715 | 0.6126 | |
| **C-Biochar loading rate** | 279.37 | 1 | 279.37 | 3.04 | 0.1090 | |
| **Residual** | 1010.69 | 11 | 91.88 | | | |
| **Lack of Fit** | 812.95 | 9 | 90.33 | 0.9136 | 0.6246 | **not significant** |
| **Pure Error** | 197.74 | 2 | 98.87 | | | |
| **Cor Total** | 3934.67 | 14 | | | | |

| Std. Dev | Mean | C.V. % | $R^2$ | Adjusted $R^2$ | Predicted $R^2$ | Adeq Precision |
|---|---|---|---|---|---|---|
| 9.59 | 26.23 | 36.54 | 0.7431 | 0.6731 | 0.5443 | 9.6993 |

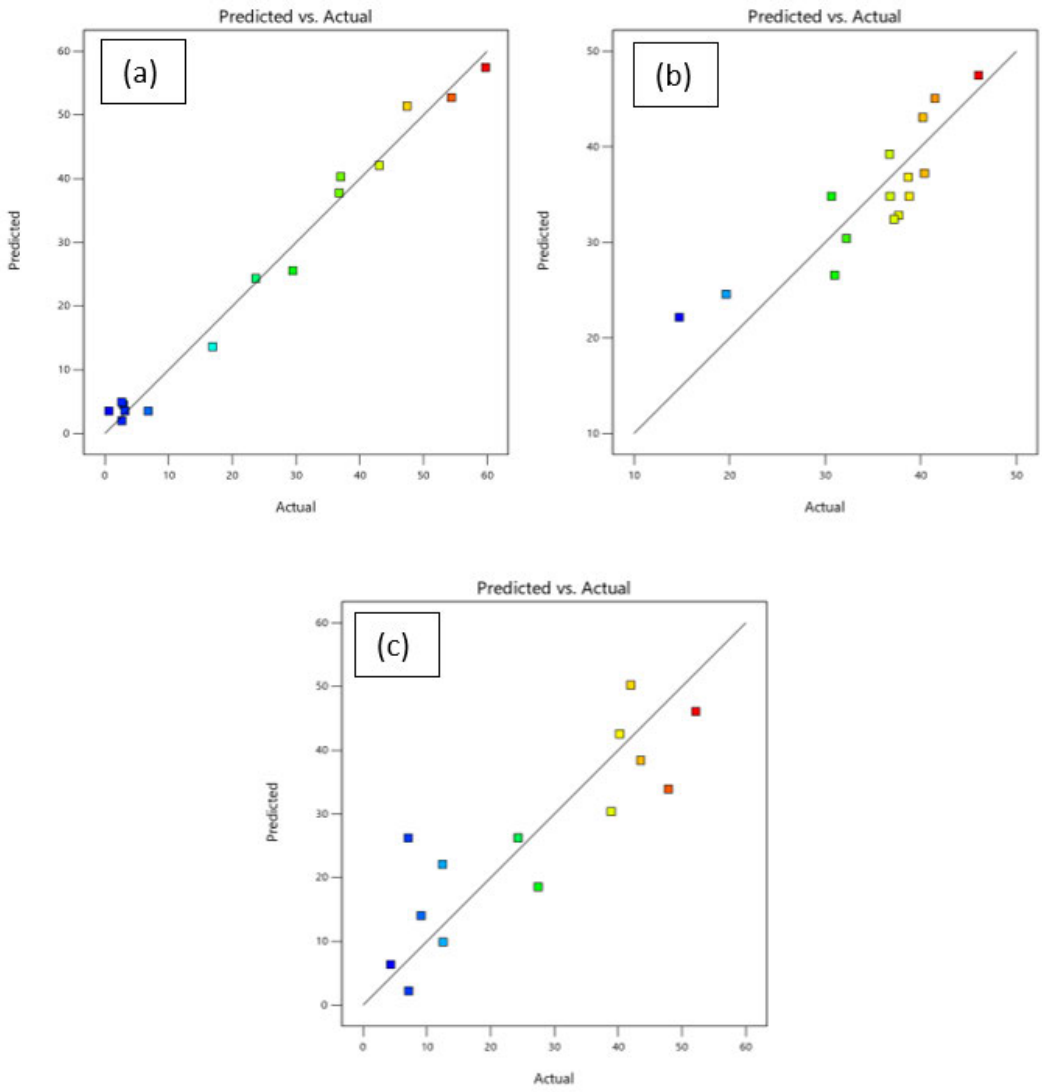


Figure 4-23 (a) Biogas yield, (b) COD removal, and (c) VS removal predicted vs actual plots.

### 4.7.1.1. Residual Plot analysis

The residual plots represent the discrepancy between the observed and anticipated data values generated by the model. The normal probability plot was employed to assess the residuals distribution (figure 4-25 to 4.27. The data distribution was determined to be normal, with all data points conforming to a linear pattern (Design Expert 2017). Furthermore, the plot depicting the relationship between residual and predicted values demonstrates that the data points were inside the designated range of the models, indicating that no data omissions. These are presented in Figure 4.25 to Figure 4.27.

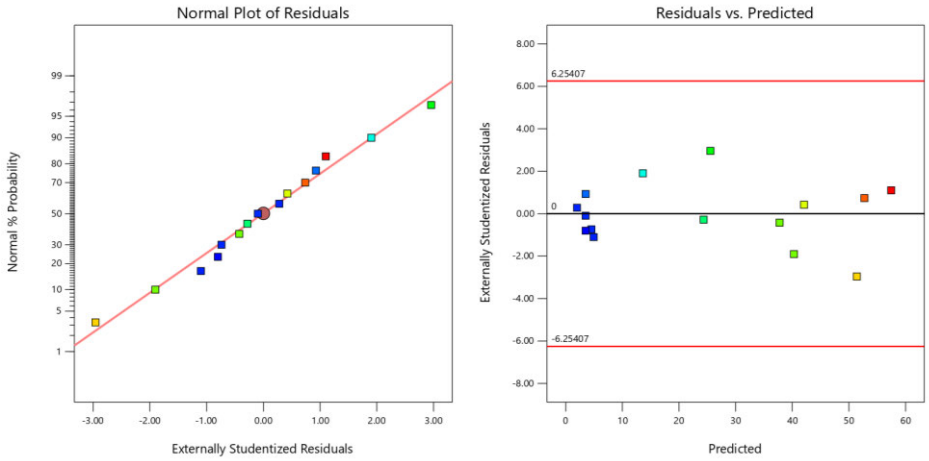


Figure 4-24: Normal plot for biogas yield.

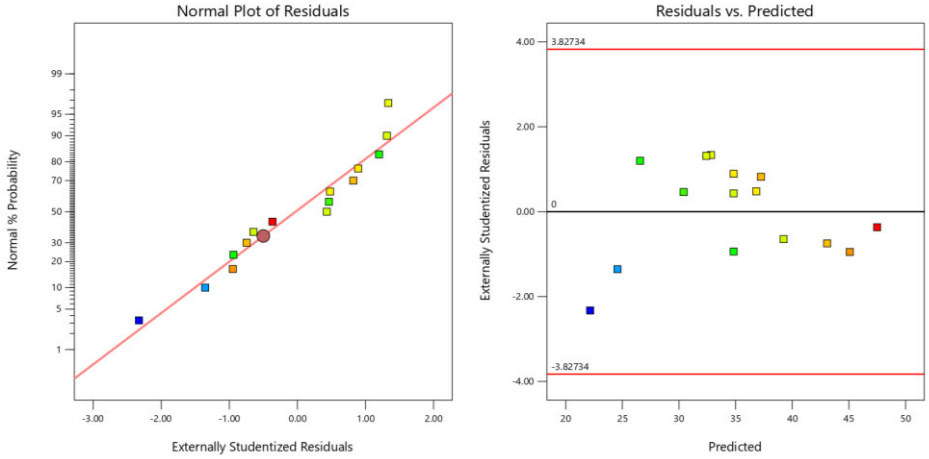


Figure 4-25: Normal plot for COD removal.

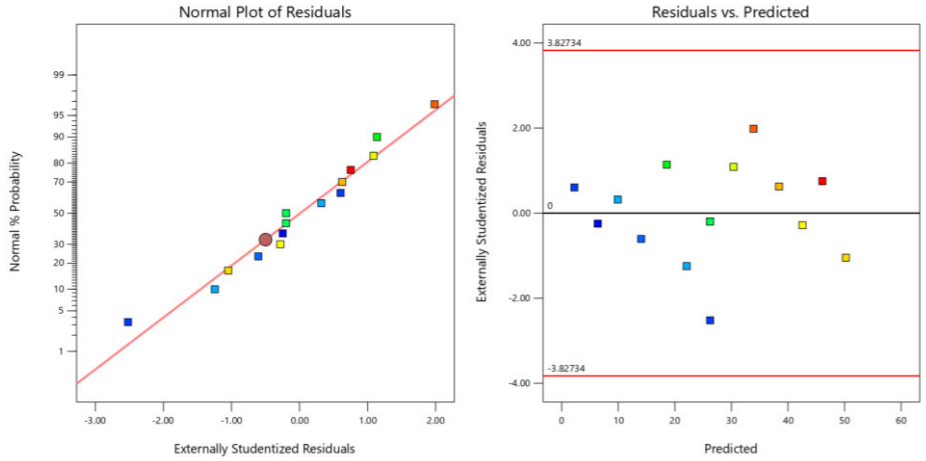


Figure 4-26: Normal plot for VS removal.

### 4.7.2. 3D plot analysis.

The 3D and contour plots in Figure 4-27 to 4-29 are graphical representations of the impact of various factors on each individual responses, as per the regression models for each response. The temperature and BC loading were shown to be the most sensitive parameters, with co-substrate loading being the next most influential.

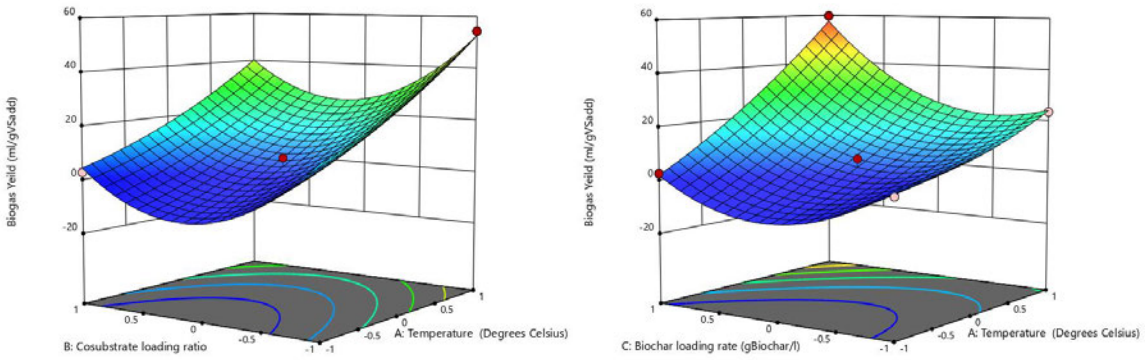


Figure 4-27: Impact of input factor on biogas yield (mL/gVS)

Figure 4-27 the relationship between Temperature, Co-substrate and Biochar loading rate on biogas yield are represented graphically. Biogas yield is seen to increase with the increase in temperature with the peak biogas yield recorded at the maximum temperature of 55 $^{0}$C (coded factor 1) researchers have shown thermophilic digestion to be more efficient with respect to virus and pathogen destruction and biogas yield, thermophilic digestion has also been shown to result in increased VFAs concentrations, affecting process stability and ultimately leading to process failure (Al-Sulaimi et al., 2022). Increase in biogas yield was observed with increase biochar loading with yield peaking at a loading of 10g/L. Biochar has been found to enhance the rate of complex organic decomposition, perhaps increasing the production of $CH_4$ by improving the activity of glucanase, protease, and lipase enzymes, potentially leading to an increase in soluble (COD) in anaerobic digestion systems for sludge (Zhai et al., 2020; Khalid et al., 2021).

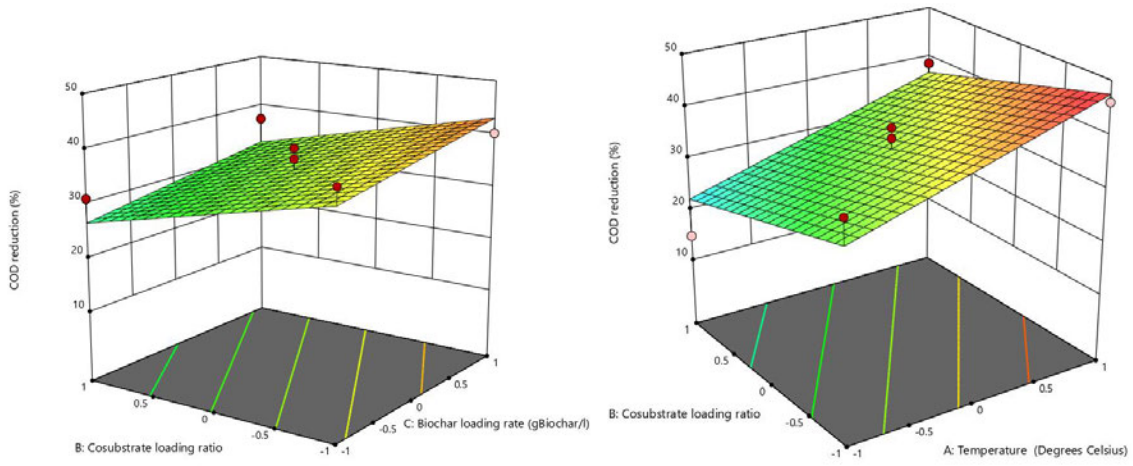


Figure 4-28: Impact of input factor on COD removal.

COD removal was found to increase with an increase in BC loading, similar COD removal increase with temperature increase.

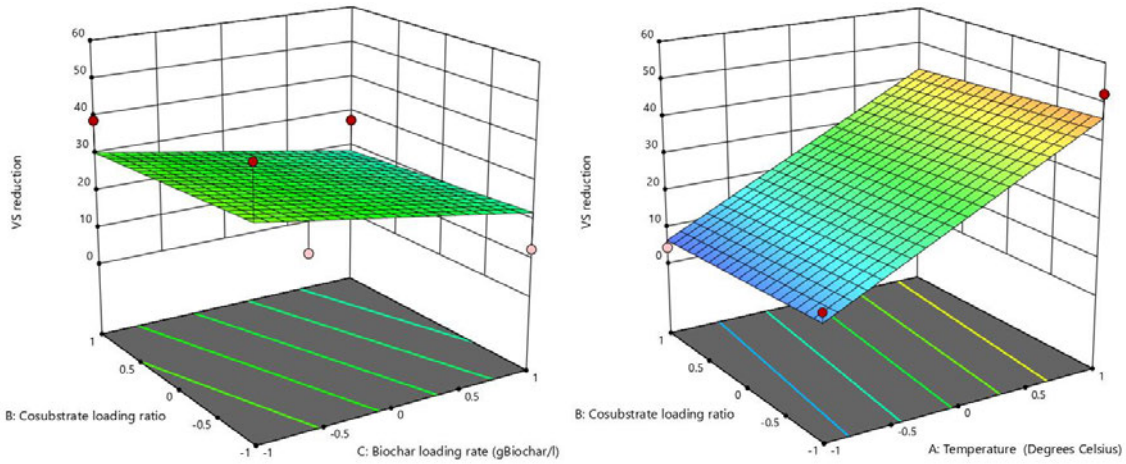


Figure 4-29: Impact of input factor on VS removal.

VS removal was found to decrease with increased BC loading, this could be attributed to the inference of the BC particle as the BC was no separated from the digestate post AD.

### 4.7.3. Optimisation

To optimize the three input variables, the numerical optimization tool in RSM was used. Table 4-19 demonstrates that all process responses were maximized, whereas the input variables (temperature, Co-substrate loading, and BC loading remained within the range. Figure 4-30 shows the ramp graphs that indicate the optimal operating parameters and the desirability gained. It was discovered that with a temperature of 54.99 $^{0}$C, co-substrate loading ratio of 1:20 and a BC loading rate of 6.7 g/L at a desirability performance of 94.00%, biogas yield of 59.75 mL/gVS, COD removal of 48.47 % and a VS removal of 44.11 % achieved. The model for each response was validated using the determined optimum condition; three experimental runs were conducted and are described in Table 4-19.

Table 4-19: Optimum conditions for BC BMP system

| Factor | Goal | Lower Limit | Upper Limit |
|---|---|---|---|
| **A: Temperature** | is in range | 25 | 55 |
| **B: Co-substrate loading ratio** | is in range | 1:20 | 1:5 |
| **C: Biochar loading rate (gBC/L)** | is in range | 2.5 | 10 |
| **Response** | | | |
| **Biogas Yield (ml/gVS$_{added}$)** | maximize | 0.629247 | 59.7589 |
| **COD removal (%)** | maximize | 14.7541 | 46.0496 |
| **VS removal (%)** | maximize | 4.32971 | 52.1756 |

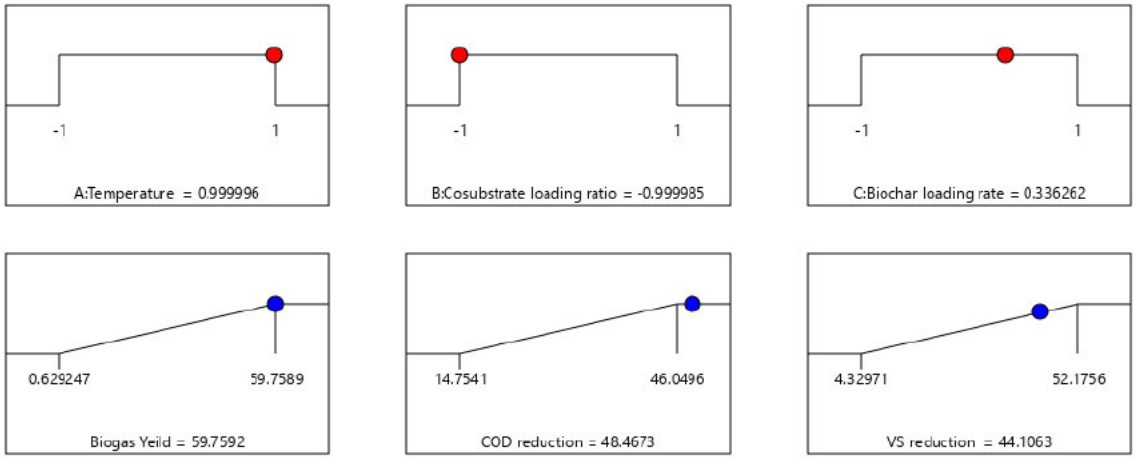


Figure 4-30: Ramp plot for optimum operating conditions for BC BMP system.

### 4.7.4. Model Validation

Table 4-20 presents the three experimental runs for each process that were performed under optimal operating parameters to test the appropriateness and validity of the suggested models. The experiment runs yielded mean, biogas, COD, and VS removals of 60.45 mL/gVS, 47.99%, and 50.88%. The observed values closely aligned with the anticipated values, with a discrepancy of less than 5%. This suggests that the models are able to accurately represent the connection between observed and projected outcomes. The observed results are also within the low and high predicted interval values (PI)Therefore, the models demonstrated satisfactory predictive accuracy.

Table 4-20: Model validation BC BMP experiments

| Biogas Yield ($ml/gVS_{added}$) | COD Removal (%) | VS Removal (%) |
|---|---|---|
| 60.22 | 45.56 | 43.55 |
| 58.35 | 46.28 | 52.8 |
| 62.78 | 52.14 | 56.29 |

| | Predicted | | Observed | | | | | |
|---|---|---|---|---|---|---|---|---|
| Analysis | Predicted Mean | Predicted Median | Std Dev | n | SE Pred | 95% PI low | Data Mean | 95% PI high |
| Biogas Yield ($ml/gVS_{added}$) | 52.7388 | 52.7388 | 4.26676 | 3 | 4.44099 | 41.3229 | 60.4501 | 64.1547 |
| COD Removal (%) | 47.4851 | 47.4851 | 4.55682 | 3 | 3.67382 | 39.3991 | 47.9933 | 55.5712 |
| VS Removal (%) | 46.0935 | 46.0935 | 9.58545 | 3 | 7.72804 | 29.0842 | 50.8821 | 63.1028 |

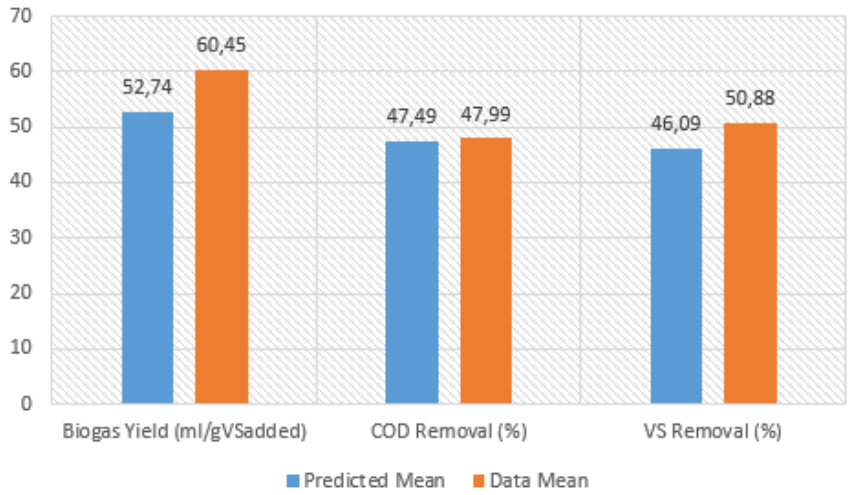


Figure 4-31: Model validation predicted vs experimental results contaminant removal.

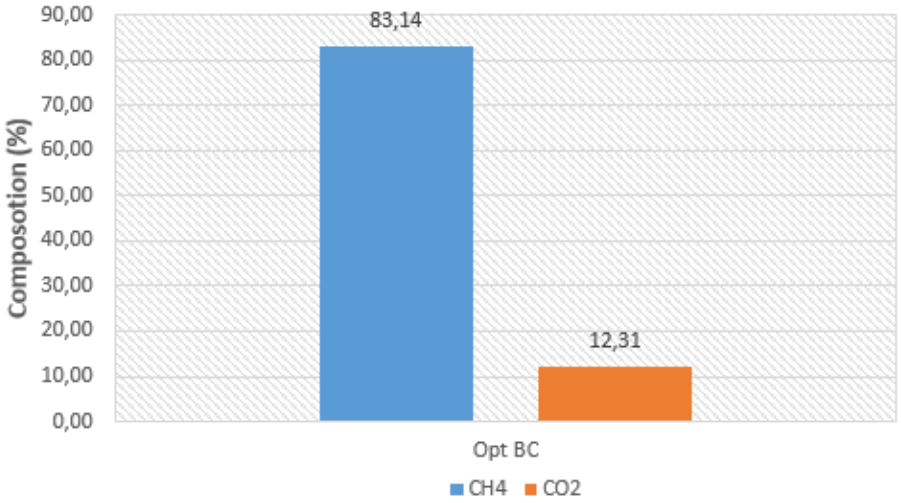


Figure 4-32: Model validation biomethane yield.

## 4.8. Comparative study of optimized IWW and biochar BMP systems.

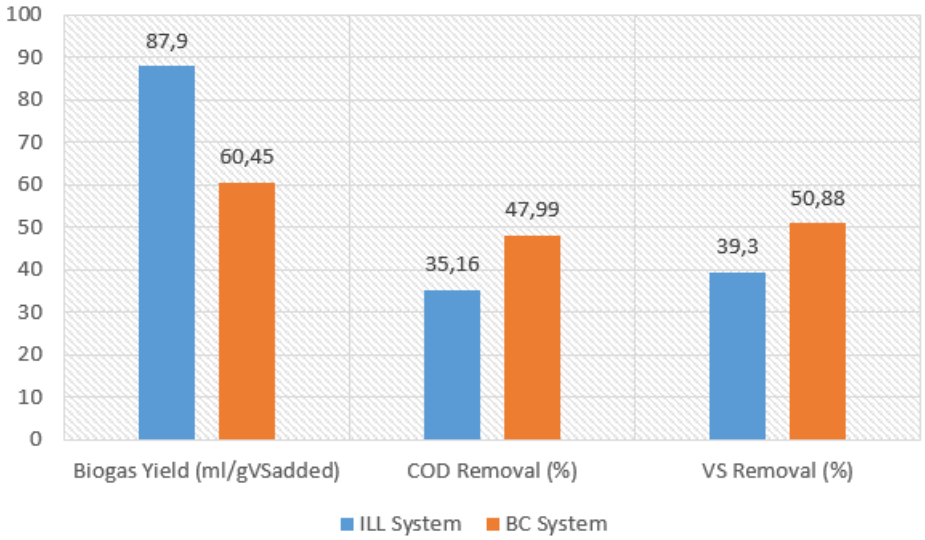


Figure 4-33: Optimized ILL VS BC BMP system.

Figure 4-33 presents the biogas yields, COD and VS removals for the optimized ILL and BC BMP systems, respectively. ILL was observed to have the highest biogas yields of 87.9 (mL/gVS) compared to 60.45 (mL/gVS) for the optimized BC system. While the BC system was observed to increase COD and VS removal by 26.73 % and 22.76 % respectively. The increased in COD and VS removal is attributed to BC ability to enhance the rate of complex organic decomposition and increase in soluble chemical oxygen demand (COD) in anaerobic digestion systems for sludge (Zhai et al., 2020; Khalid et al., 2021). Biochar enhances microorganisms' density, facilitating their interaction with substrates effectively addressing the inherent AD process issue (Khalid et al., 2021). The decrease in biogas yield for the BC system is attributed to BC loading impeding mass transfer and organic matter decomposition at the later stages of AD, resulting in premature halting of biogas production; this is attributed to the BC's absorption of dissolved organic matter, restricting the availability of substrates for methanogenesis.

### 4.8.1. Biomethane composition.

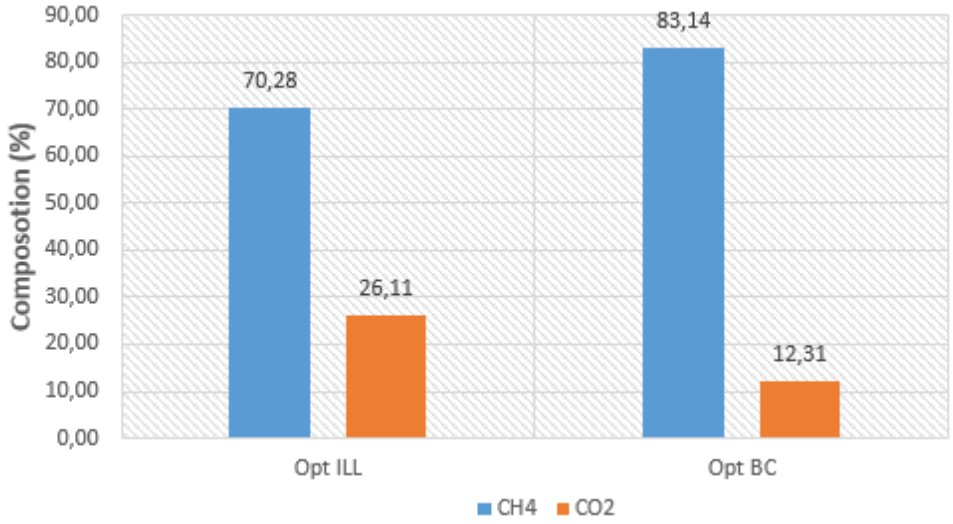


Figure 4-34: Optimized ILL VS BC BMP system biomethane yield.

The optimized BC system was found to have the highest biomethane yield. This was attributed to BC's ability to enhance the rate of complex organic decomposition, increasing the production of $CH_4$ by improving the activity of glucanase, protease, and lipase enzymes, potentially leading to an increase in soluble chemical oxygen demand (COD) in anaerobic digestion systems for sludge (Zhai et al., 2020; Khalid et al., 2021). Biochar enhances microorganisms' density, facilitating their interaction with substrates effectively addressing the inherent issue (Khalid et al., 2021).

### 4.9.Effect of ultrasonic pre-treatment of ILL on the anaerobic digestion process.

This study was conducted to evaluate the effect of USP of ILL on the anaerobic co-digestion of ILL with Municipal primary sludge. The raw leachate is ultrasonically pretreated prior to undergoing aerobic treatment in the landfill site aerobic treatment plant. A sample of the pretreated leachate sample was retrieved, analysed, and compared with the raw untreated sample of intermediate landfill leachate (ILL). The results are presented in Table 4-21: The BMP tests were conducted under the optimum condition determined in the BC BMP optimization runs and are as follows: temperature of 54.99 $^0$C, co-substrate loading ratio of 1:20 and a BC loading rate of 6.7 g/L.

Table 4-21: Characterisation of UP ILL vs Raw ILL

| Methods | Determinands | Units | LOVU: RAW LEACHATE | LOVU: TREATED LEACHATE |
|---|---|---|---|---|
| 10G | Total Alkalinity | mg $CaCO_3$/L | 3312 | 303 |
| Calc. | Free Ammonia | mg N/L | 50 | <1.5 |
| Calc. | Saline Ammonia | mg N/L | 867 | 58 |
| 93 | Dissolved Calcium | mg Ca/L | 153 | 157 |
| 16G | Chloride | mg Cl/L | 2799 | 2958 |
| 68G | Hexavalent Chromium | mg Cr/L | <0.0031 | 0.0073 |
| 83A | Total Chromium | µg Cr/L | 1056 | 1873 |
| 2B | Electrical Conductivity at 25°C | mS/m | 1665 | 1408 |
| 83A | Dissolved Aluminium | µg Al/L | 1495 | 2774 |
| 83A | Dissolved Lead | µg Pb/L | 34 | 42 |
| 41 | Total Dissolved Solids at 180°C | mg/L | 10452 | 11914 |
| 93 | Dissolved Magnesium | mg Mg/L | 130 | 97 |
| 1 | pH at 25°C | pH units | 8.0 | 6.0 |
| 93 | Dissolved Potassium | mg K/L | 1527 | 1334 |
| 93 | Sodium | mg Na/L | 2996 | 2889 |
| 67G | Sulphate | mg $SO_4$/L | 18.0 | 99.7 |
| 83A | Dissolved Mercury | µg Hg/L | 608 | 5.8 |
| 83A | Dissolved Iron | µg Fe/L | 3287 | 5480 |
| 3 | Chemical Oxygen Demand (Total) | mg $O_2$/L | 5346 | 3824 |
| 83A | Dissolved Barium | µg Ba/L | 409 | 468 |
| 83A | Dissolved Cadmium | µg Cd/L | 3.0 | 18.9 |
| 104 | Soluble Organic Carbon | mg C/L | 1776 | 1056 |
| 18G | Fluoride | mg F/L | <0.06 | <0.06 |
| 83A | Dissolved Manganese | µg Mn/L | 752 | 2799 |
| 83A | Dissolved Nickel | µg Ni/L | 385 | 307 |
| 104 | Total Organic Carbon | mg C/L | 1776 | 1056 |
| 133 | Total Phenols* | µg/L | 1080 | 160 |
| 83A | Dissolved Selenium | µg Se/L | 17.3 | 18.4 |
| 83A | Dissolved Zinc | µg Zn/L | 516 | 1054 |

Surprisingly, the COD of the treated ILL was found to be lower than that of the untreated sample, 3824 mg/L and 5346 mg/L, respectively. This is potentially the result of excessive pretreatment; when a high amount of power is applied (causing brief cavitation in the solution), organic matter is degraded by oxidising radicals produced by the cavitation bubbles. This degradation leads to a reduction in the sCOD value, resulting in a low output of biogas during anaerobic digestion (Nazimudheen et al., 2018) the UP ILL also displayed a lower pH this is attributed to the lysis of the macromolecules and decease in the total alkalinity (mg $CaCO_3$/L).

Table 4-22: UP ILL BMP runs.

| Run | Biogas Yield ($mL/gVS_{added}$) | COD Removal (%) | VS Removal (%) |
|---|---|---|---|
| 1 | 68.46 | 50.10 | 51.67 |
| 2 | 53.88 | 42.56 | 47.81 |
| 3 | 52.59 | 45.88 | 48.15 |
| Average | 58.31 | 46.18 | 49.21 |

| Bioreactor | Inoculum Substrate ratio | Co-substrate loading rate | Inoculum (mL) | Primary Sludge (mL) | Landfill Leachate (mL) | Biochar Loading (g/L) |
|---|---|---|---|---|---|---|
| **R1** | 1.5:1 | 1:20 | 485 | 277 | 38 | 6.7 |
| **R2** | 1.5:1 | 1:20 | 485 | 277 | 38 | 6.7 |
| **R3** | 1.5:1 | 1:20 | 485 | 277 | 38 | 6.7 |

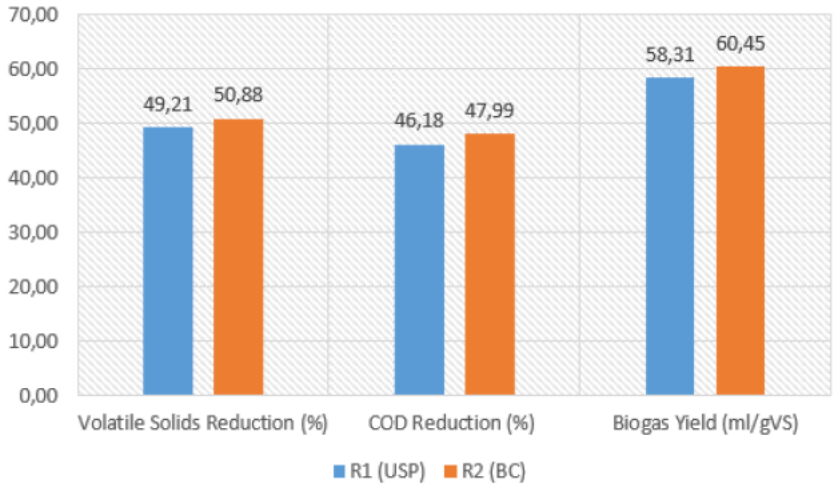


Figure 4-35: UP ILL vs Untreated ILL

The UP of ILL was observed to have a negligible effect on the performance of the AD system in terms of biogas yield and COD and VS removal, producing a biogas yield and COD and VS removal of 58.31 mL/gVS, 46.18 % and 49.1 %, respectively compared to 60.45 mL/gVS, 47.99 % and 50.88 % for the optimized BC system. According to Nazimudheen et al. (2018), when excessive UP of power is applied (causing brief cavitation in the solution), organic matter is degraded by oxidising radicals produced by the cavitation bubbles. This degradation leads

to a reduction in the COD value, resulting in lower biogas yield and biomethane yield during anaerobic digestion.

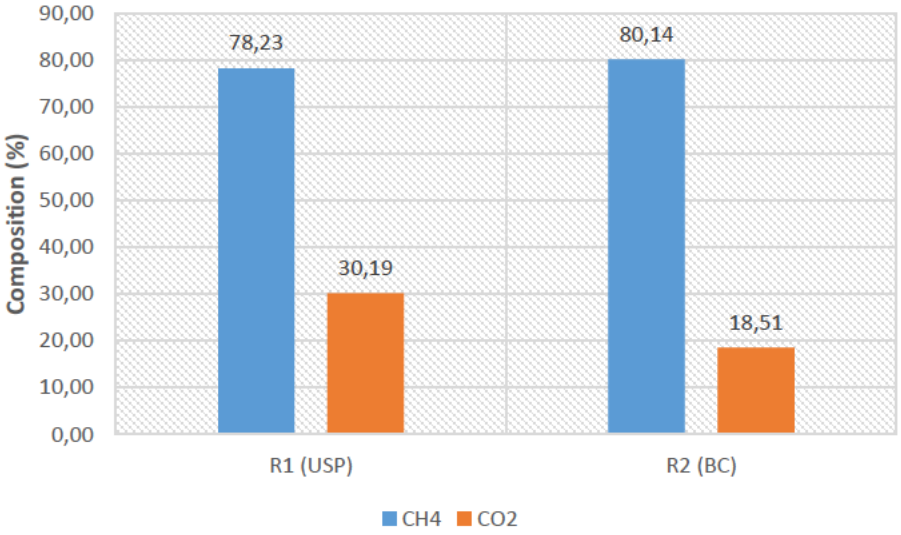


Figure 4-36: Effect of UP ILL on biomethane yield.

Figure 4-36 shows the impact of UP on biomethane yield. UP results in a decrease in biomethane yield (78.23% $CH_4$) compared to (80.14% $CH_4$). This was largely due to the decreased COD of the UP ILL, resulting in decreased availability of degradable matter. This observed effect was attributed to the effect of excessive UP resulting degradation of organic matter by oxidising radicals (Nazimudheen et al., 2018)

### 4.9.1. Summary

The application of UP of ILL was found to have a negligible impact on the performance of the AD process, which was attributed to the decrease in COD recorded for the UP ILL. According to Nazimudheen et al. (2018), when excessive UP of power is applied (causing brief cavitation in the solution), organic matter is degraded by oxidising radicals produced by the cavitation bubbles. This degradation leads to a reduction in the sCOD value, resulting in lower biogas yield and biomethane yield during anaerobic digestion.

# Chapter 5: Conclusion and Recommendations

This study considered the use of two industrial wastewaters, namely, sugar industry effluent and Intermediate landfill leachate, as co-substrates for anaerobic digestion of primary sewage sludge. The characteristics of these industrial wastewaters indicate their suitability for the AD process in that they supply the necessary nutrients needed for the consortia of anaerobes. Initial BMP tests were conducted as a discriminative approach to pick the most optimal industrial wastewater among the two based on their performance during the digesting process with respect to biogas yield (mL/gVS), COD and VS removal. The effect of biochar addition and ultrasonic pre-treatment as potential AD enhancement methods on the anaerobic co-digestion were evaluated.

The specific objectives of the study were as follows:

i. Characterization of primary sewage sludge, inoculum, and industrial wastewater.
ii. Synthesis and characterisation of Biochar derived from sugarcane bagasse.
iii. Investigate the effect of Municipal Landfill Leachate and Sugar Industry wastewater as co-substrates and optimisation of process parameters with RSM.
iv. Investigate the effect of the addition of Biochar as an additive on the anaerobic digestion process with respect to biogas yield and quality optimisation of process parameters with RSM.
v. Investigate the effect of ultrasonic pre-treatment of industrial wastewater on the anaerobic digestion process with respect to biogas yield and quality.

## 5.1.Conclusion

- The TS for PS was 39.02 (gTS/l), and VS was 29.72 (gVS/l), falling within the expected range. The results also suggest that the sludge exhibits excellent biodegradability, as seen by a VS/TS ratio over 50%. Furthermore, the SIWW sample exhibited a VS/TS ratio of 0.68, indicating a greater presence of organic substances compared to insoluble substances. The inoculum had the lowest VS/TS value, measuring 0.52, indicating a higher concentration of microorganisms compared to the organic materials. Therefore, it demonstrates its potential use as an inoculum rather than as a substrate.

- Biochar was successfully synthesised fom sugarcane bagasse the effect of pyrolysis temperature of the poperties of the synthesised BCs was evaluated . Increase in pyrolysis temperature resulted in BC pH, carbon content and electrical coductivity. BC 450 was found to have the greatest degree of micropore formation evidenced by the SEM analysis.

- The effects of each IWW were evaluated with respect to their impact of four key performance indicators (biogas yield, biomethane yield and COD and VS removal). ILL was found increase the biogas yield by 29 % when compared to the control, ILL was also found to increase the COD removal by 5.36% compared to the control but, IIL exhibited a 14.36 % decrease in VS removal. The ILL also exhibited a 11.39 % increase in biomethane yield compared to the CNTRL. Hence ILL was identified at the best performing IWW and was selected for further evaluation in terms of process optimization.

- The optimal operating parameters for the ILL system were determined using RSM. A numerical optimisation technique was employed to optimise the desired goals, including maximum Biogas yield (ml/gVSadded), COD, and VS removal (%). It was discovered that with a temperature of 39 $^{0}$C, a ISR 1.5:1, co-substrate loading ration of 1:20, at a desirability performance of 90.10%, biogas yield of 90.76 mL/gVS, COD removal of 33.62 % and a VS removal of 43.25 % achieved.

- The effects of each BC were evaluated with respect to their impact of four key performance indicators (biogas yield, biomethane yield and COD and VS removal). BC 450 was found increase the biogas yield by 15 % when compared to the control these results correlate well with previous studies conducted and are attributed to the reduction of lags phase as a result of BC addition, BC 450 was also found to increase the COD removal by 8 % compared to the control. The addition of BC 450 exhibited a 27.11 % increase in VS removal. BC 450 also exhibited a 14.84 % increase in biomethane yield compared to the CNTRL. Hence BC 450 was identified as the best performing IWW and was selected for further evaluation in terms of process optimization.

- The optimal operating parameters for the BC system were determined using RSM. A numerical optimisation technique was employed to optimise the desired goals, including maximum Biogas yield (ml/gVSadded), COD, and VS removal (%). It was discovered that with a temperature of 54.99 $^{0}$C, co-substrate loading ratio of 1:20 and a BC loading rate of

6.7 g/L at a desirability performance of 94.00%, biogas yield of 59.75 mL/gVS, COD removal of 48.47 % and a VS removal of 44.11 % achieved.

- The application of UP of ILL was found to have a negligible impact on the performance of the AD process, the was attributed to the decrease in COD recorded for the UP ILL caused excessive UP of power is applied (causing brief cavitation in the solution) organic matter is degraded by oxidising radicals produced by the cavitation bubbles. This degradation leads to a reduction in the sCOD value, resulting in lower biogas yield and biomethane yield during anaerobic digestion.

**5.2.Recommendations.**

- Although the acquired results show promise and are applicable, it is recommended that the study be scaled up to more accurately mimic actual conditions research, which would aid in identifying full-scale applicability.
- An in-depth study of the impact of various biochar activation methods should be investigated to further enhance the properties of the synthesized biochars.
- An in-depth study on the impacts of biochar addition on the anaerobe consortia should be undertaken to better explain the impacts of the AD system with special attention to methanogenic anaerobes.
- An in-depth study on the impacts of the parameters related to the ultrasonic pretreatment of IWW should be conducted to better understand the impacts of this mechanism.
- A techno-economic analysis of the feasibility of biochar synthesis from sugarcane bagasse should be conducted.

# References

Abdallah, M.S., Hassaneen, F.Y., Faisal, Y., Mansour, M.S., Ibrahim, A.M., Abo-Elfadl, S., Salem, H.G., Allam, N.K., 2019. Effect of ni-ferrite and ni-co-ferrite nanostructures on biogas production from anaerobic digestion. Fuel, 254: 115673.

Abdel-Shafy, H.I., Ibrahim, A.M., Al-Sulaiman, A.M., and Okasha, R.A., 2024. Landfill leachate: Sources, nature, organic composition, and treatment: An environmental overview. Ain Shams Engineering Journal, 15(1): 102293.

Afifah, U., and Priadi, C.R., 2017. Biogas potential from anaerobic co-digestion of faecal sludge with food waste and garden waste. AIP Conference Proceedings.

Ahmad, M., Rajapaksha, A.U., Lim, J.E., Zhang, M., Bolan, N., Mohan, D., Vithanage, M., Lee, S.S., and Ok, Y.S., 2014. Biochar as a sorbent for contaminant management in soil and water: A Review. Chemosphere, 99: 19–33.

Ahmadi-Pirlou, M., and Mesri Gundoshmian, T., 2021. The effect of substrate ratio and total solids on biogas production from anaerobic co-digestion of municipal solid waste and sewage sludge. Journal of Material Cycles and Waste Management, 23(5): 1938–1946.

Akinbami, O.M, Oke, S.R and Bodunrin, M.O. 2021. The state of renewable energy development in South Africa: An overview. Alexandria Engineering Journal. 60(6): 5077–5093, https://doi.org/10.1016/j.aej.2021.03.065.

Akpor, O.B., 2014. Heavy metal pollutants in wastewater effluents: Sources, effects and remediation. Advances in Bioscience and Bioengineering, 2(4): 37.

Al-Sulaimi, I.N., Nayak, J.K., Alhimali, H., Sana, A., and Al-Mamun, A., 2022. Effect of volatile fatty acids accumulation on biogas production by sludge-feeding thermophilic anaerobic digester and predicting process parameters. Fermentation, 8(4): 184.

Al-Wabel, M.I., Al-Omran, A., El-Naggar, A.H., Nadeem, M., and Usman, A.R.A., 2013. Pyrolysis temperature induced changes in characteristics and chemical composition of biochar produced from Conocarpus Wastes. Bioresource Technology, 131: 374–379.

Amonette, J.E., and Joseph, S.D., 2015. Characteristics of biochar: Macro-molecular properties. Biochar for Environmental Management.:143–170.

Anukam, A., Mohammadi, A., Naqvi, M., and Granström, K., 2019a. A review of the chemistry of anaerobic digestion: Methods of accelerating and Optimizing Process Efficiency. Processes, 7(8): 504.

Appels, L., Baeyens, J., Degrève, J., and Dewil, R., 2008. Principles and potential of the anaerobic digestion of waste-activated sludge. Progress in Energy and Combustion Science, 34(6): 755–781.

Arif, S., Liaquat, R. and Adil, M., 2018. Applications of materials as additives in anaerobic digestion technology. Renewable and Sustainable Energy Reviews, 97: 354-366.

Ariunbaatar, J., Panico, A., Esposito, G., Pirozzi, F., and Lens, P.N.L., 2014. Pretreatment methods to enhance anaerobic digestion of organic solid waste. Applied Energy, 123: 143–156.

Azizi, A., Hosseini Koupaie, E., Hafez, H., and Elbeshbishy, E., 2019. Improving single- and two-stage anaerobic digestion of source separated organics by hydrothermal pretreatment. Biochemical Engineering Journal, 148: 77–86.

Bachman N. (2015) Sustainable biogas production in municipal wastewater treatment plants. IEA Bioenergy. ISBN 978-1-910154-22-9.

Baek, G., Kim, J., and Lee, C., 2016. A long-term study on the effect of magnetite supplementation in continuous anaerobic digestion of dairy effluent – enhancement in process performance and stability. Bioresource Technology, 222: 344–354.

Bajpai, P., 2017. Anaerobic treatment of pulp and paper industry effluents. Anaerobic Technology in Pulp and Paper Industry: 69–85.

Bhajani, S.S., 2022. Review: Factors affecting biogas production. International Journal for Research in Applied Science and Engineering Technology, 10(2): .79–88.

Bhattarai, K.P., and Mandal, T.N., 2018. Variation in carbon stock in Litterfall, fine root and soil in Sal (Shorea robusta Gaertn.) forests of eastern Nepal. Our Nature, 16(1), pp.68–73.

Blake, L.I., Tveit, A., Øvreås, L., Head, I.M., and Gray, N.D., 2015. Response of methanogens in Arctic sediments to temperature and methanogenic substrate availability. PLOS ONE, 10(6).

Bonelli, P.R., Buonomo, E.L., and Cukierman, A.L., 2007. Pyrolysis of sugarcane bagasse and co-pyrolysis with an Argentinean sub bituminous coal. Energy Sources, Part A: Recovery, Utilization, and Environmental Effects, 29(8): 731–740.

Cantrell, K.B., Hunt, P.G., Uchimiya, M., Novak, J.M., and Ro, K.S., 2012. Impact of pyrolysis temperature and manure source on physicochemical characteristics of biochar. Bioresource Technology, 107: 419–428.

Cárdenas- Aguiar, E., Gascó, G., Paz-Ferreiro, J., and Méndez, A., 2017. The effect of biochar and compost from urban organic waste on plant biomass and properties of an artificially copper polluted soil. International Biodeterioration & Biodegradation, 124: 223–232.

Carrere H, Antonopoulou G, Affes R, Passos F, Battimelli A, Lyberatos G, et al. 2016. Review of feedstock pre-treatment strategies for improved anaerobic digestion: from lab-scale research to full-scale application. Bioresource Technology (199): 386–97.

Cayetano, R.D, Oliwit, A.T., Kumar, G., Kim, J.S., and Kim, S.-H., 2019. Optimization of soaking in aqueous ammonia pretreatment for anaerobic digestion of African maize bran. Fuel, 253: 552–560.

Chan, Y., Chong, M. and Law, C., 2016. Performance and kinetic evaluation of an integrated anaerobic–aerobic bioreactor in the treatment of palm oil mill effluent. Environmental Technology, 38(8): 1005-1021.

Chauhan, C., Shah, D., and Sutaria, F., 2018. Various bio-mechanical factors affecting heat generation during osteotomy preparation: A systematic review. Indian Journal of Dental Research, 29(1): 81.

Chen, H., Gao, Y., Li, J., Fang, Z., Bolan, N., Bhatnagar, A., Gao, B., Hou, D., Wang, S., Song, H., Yang, X., Shaheen, S.M., Meng, J., Chen, W., Rinklebe, J., and Wang, H., 2022. Engineered biochar for environmental decontamination in aquatic and Soil Systems: A Review. Carbon Research, 1(1).

Chiappero, M., Norouzi, O., Hu, M., Demichelis, F., Berruti, F., Di Maria, F., Mašek, O., Fiore, S., 2020. Review of biochar role as additive in anaerobic digestion processes. Renewable and Sustainable Energy Reviews 131, 110037.

Chopra, A.K., Srivastava, S., Kumar, V., and Pathak, C., 2012. Agro potentiality of distillery effluent on soil and agronomical characteristics of Abelmoschus esculentus L. (OKRA). Environmental Monitoring and Assessment, 185(8): 6635–6644.

Chrispim, M.C., Scholz, M., and Nolasco, M.A., 2021. Biogas recovery for Sustainable Cities: A Critical Review of enhancement techniques and key local conditions for implementation. Sustainable Cities and Society, 72: 103033.

Christofoletti, C.A., Escher, J.P., Correia, J.E., Marinho, J.F., and Fontanetti, C.S., 2013. Sugarcane vinasse: Environmental implications of its use. Waste Management, 33(12): 2752–2761.

Chynoweth, D.P., and Pullammanappallil, P., 2020. Anaerobic digestion of municipal solid wastes. Microbiology of Solid Waste,: 71–113

Claoston, N., Samsuri, A., Ahmad Husni, M., and Mohd Amran, M., 2014. Effects of pyrolysis temperature on the physicochemical properties of empty fruit bunch and rice husk biochars. Waste Management & Research: The Journal for a Sustainable Circular Economy, 32(4): 331–339.

Cornelissen, S., Koper, M. and Deng, Y., 2012. The role of bioenergy in a fully sustainable global energy system. Biomass and Bioenergy, 41: 21-33.

Costa, A.M., Alfaia, R.G. and Campos, J.C. 2019 ‘Landfill leachate treatment in Brazil – an overview’, Journal of Environmental Management, 232: 110–116. doi: 10.1016/j.jenvman.2018.11.006.

Cruz-Salomón, A., Ríos-Valdovinos, E., Pola-Albores, F., Meza-Gordillo, R., Lagunas-Rivera, S., and Ruíz-Valdiviezo, V.M., 2017. Anaerobic treatment of agro-industrial wastewaters for cod removal in expanded granular sludge bed bioreactor. Biofuel Research Journal, 4(4): 715–720.

Davidsson Åsa (2007) Increase of biogas production at wastewater treatment plants: Addition of urban organic waste and pre-treatment of sludge. dissertation. Lund University.

Demirbas, A., and Arin, G., 2002. An overview of biomass pyrolysis. Energy Sources, 24(5): 471–482.

Dereli, R.K., Clifford, E. and Casey, E. 2020. 'Co-treatment of leachate in municipal wastewater treatment plants: Critical issues and emerging technologies', Critical Reviews in Environmental Science and Technology, 51(11): 1079–1128. doi:10.1080/10643389.2020.1745014.

Dewil, R., Baeyens, J., and Goutvrind, R., 2006. Ultrasonic treatment of waste activated sludge. Environmental Progress, 25(2): 121–128.

Ding, W., Dong, X., Ime, I.M., Gao, B., and Ma, L.Q., 2014. Pyrolytic temperatures impact lead sorption mechanisms by Bagasse Biochars. Chemosphere, 105: 68–74.

Dixon, P.J., Ergas, S.J., Mihelcic, J.R., and Hobbs, S.R., 2019. Effect of substrate to inoculum ratio on bioenergy recovery from food waste, yard waste, and biosolids by High Solids Anaerobic Digestion. Environmental Engineering Science, 36(12): 1459–1465.

Doğruel, S., and Özgen, A.S., 2016. Effect of ultrasonic and microwave disintegration on physico-chemical and biodegradation characteristics of waste-activated sludge. Environmental Technology, 38(7): 844–859.

Du, J. et al. (2019) "Hydrothermal and alkaline thermal pretreatment at mild temperature in solid state for physicochemical properties and biogas production from anaerobic digestion of Rice Straw," Renewable Energy, 139: 261–267. Available at: https://doi.org/10.1016/j.renene.2019.01.097.

Effenberger, J., Jahn, L., and Kuehn, V., 2016. Co-digestion of press liquids of source-sorted municipal organic waste in anaerobic sludge treatment of municipal wastewater treatment plants. Water Science and Technology, 73(12): 3080–3086.

Fabbri, D. and Torri, C., 2016. Linking pyrolysis and anaerobic digestion (Py-AD) for the conversion of lignocellulosic biomass. Current Opinion in Biotechnology, 38: 167-173.

Fang, W. et al. (2020) "Overview of key operation factors and strategies for improving fermentative volatile fatty acid production and product regulation from Sewage Sludge," Journal of Environmental Sciences, 87: 93–111. Available at: https://doi.org/10.1016/j.jes.2019.05.027.

Fito, J., Tefera, N., and Van Hulle, S.W., 2019. Sugarcane biorefineries wastewater: Bioremediation Technologies for Environmental Sustainability. Chemical and Biological Technologies in Agriculture, 6(1).

Fito, J., Tefera, N., and Van Hulle, S.W., 2019a. Sugarcane biorefineries wastewater: Bioremediation Technologies for Environmental Sustainability. Chemical and Biological Technologies in Agriculture, 6(1).

Gayathri, T., Kavitha, S., Adish Kumar, S., Kaliappan, S., Yeom, I.T., and Rajesh Banu, J., 2015. Effect of citric acid induced deflocculation on the ultrasonic pretreatment efficiency of dairy waste activated sludge. Ultrasonics Sonochemistry, 22: 333–340.

Ghani, W.A., Mohd, A., da Silva, G., Bachmann, R.T., Taufiq-Yap, Y.H., Rashid, U., and Al-Muhtaseb, A.H., 2013. Biochar production from waste rubber-wood-sawdust and its potential use in C sequestration: Chemical and physical characterisation. Industrial Crops and Products, 44: 18–24.

Gil, A. et al. (2018) 'Effect of microwave pretreatment on semi-continuous anaerobic digestion of sewage sludge', Renewable Energy, 115: 917–925. doi:10.1016/j.renene.2017.07.112.

González, J., Sánchez, M. and Gómez, X., 2018. Enhancing Anaerobic Digestion: The Effect of Carbon Conductive Materials. C, 4(4):59.

Goswami, R., Chattopadhyay, P., Shome, A., Banerjee, S.N., Chakraborty, A.K., Mathew, A.K., and Chaudhury, S., 2016. An overview of physico-chemical mechanisms of biogas production by microbial communities: A step towards sustainable waste management. 3 Biotech, 6(1).

Guo, W.-Q., Yang, S.-S., Pang, J.-W., Ding, J., Zhou, X.-J., Feng, X.-C., Zheng, H.-S., and Ren, N.-Q., 2013. Application of low frequency ultrasound to stimulate the bio-activity of activated sludge for use as an inoculum in enhanced hydrogen production. RSC Advances, 3(44): 21848.

Hamoda, M.F., and Al-Sharekh, H.A., 1999. Sugar wastewater treatment with aerated fixed-film biological systems. Water Science and Technology, 40(1): 313–321.

Hossain, M.K., Strezov, V., Chan, K.Y., Ziolkowski, A., and Nelson, P.F., 2011. Influence of pyrolysis temperature on production and nutrient properties of wastewater sludge biochar. Journal of Environmental Management, 92(1): .223–228.

Hübner, T and Mumme J. 2015. Integration of pyrolysis and anaerobic digestion - use of aqueous liquor from digestate pyrolysis for biogas production. Bioresource Technology (183): 86–92.

Ibro, M.K., Ancha, V.R., and Lemma, D.B., 2022. Impacts of anaerobic co-digestion on different influencing parameters: A critical review. Sustainability, 14(15): 9387.

Indren, M., Birzer, C.H., Kidd, S.P., and Medwell, P.R., 2020. Effect of total solids content on anaerobic digestion of poultry litter with biochar. Journal of Environmental Management, 255, p.109744.

Ippolito, J.A., Laird, D.A., and Busscher, W.J., 2012. Environmental benefits of biochar. Journal of Environmental Quality, 41(4): 967–972.

Iwuozor, K.O., Emenike, E.C., Omonayin, E.O., Bamigbola, J.O., Ojo, H.T., Awoyale, A.A., Eletta, O.A.A., and Adeniyi, A.G., 2023. Unlocking the hidden value of pods: A review of thermochemical conversion processes for biochar production. Bioresource Technology Reports, 22: 101488.

Kamaruddin, M.A., Abdullah, M.M., Yusoff, M.S., Alrozi, R., and Neculai, O., 2017. Coagulation-flocculation process in landfill leachate treatment: Focus on coagulants and Coagulants aid. IOP Conference Series: Materials Science and Engineering, 209, p.012083.

Kardam, A., Raj, K.R., Arora, J.K., and Srivastava, S., 2012. Artificial neural network modeling for Biosorption of pb (ii) ions on nanocellulose fibers. BioNanoScience, 2(3): 153–160.

Karrabi, M., Ranjbar, F.M., Shahnavaz, B., and Seyedi, S., 2023. A comprehensive review on biogas production from lignocellulosic wastes through Anaerobic Digestion: An insight into performance improvement strategies. Fuel, 340: 127239.

Khalid, Z.B., Siddique, Md.N., Nayeem, A., Adyel, T.M., Ismail, S.B., and Ibrahim, M.Z., 2021. Biochar application as sustainable precursors for enhanced ANAEROBIC DIGESTION: A systematic review. Journal of Environmental Chemical Engineering, 9(4): 105489.

Khan, M., Ngo, H. H., Guo, W., Liu, Y., Nghiem, L. D., Hai, F. I., Deng, L., Wang, J. And Wu, Y. 2016. Optimization of process parameters for production of volatile fatty acid, biohydrogen and methane from anaerobic digestion. Bioresource Technology, 219**:** 738-748.

Khanh Nguyen, V., Kumar Chaudhary, D., Hari Dahal, R., Hoang Trinh, N., Kim, J., Chang, S.W., Hong, Y., Duc La, D., Nguyen, X.C., Hao Ngo, H., Chung, W.J., and Nguyen, D.D., 2021. Review on pretreatment techniques to improve anaerobic digestion of sewage sludge. Fuel, 285: 119105.

Khanh Nguyen, V., Kumar Chaudhary, D., Hari Dahal, R., Hoang Trinh, N., Kim, J., Chang, S.W., Hong, Y., Duc La, D., Nguyen, X.C., Hao Ngo, H., Chung, W.J., and Nguyen, D.D., 2021. Review on pretreatment techniques to improve anaerobic digestion of sewage sludge. Fuel, 285: 119105.

Kim, M., Ahn, Y.-H., and Speece, R.E., 2002. Comparative process stability and efficiency of anaerobic digestion.

Koul, B., Yadav, D., Singh, S., Kumar, M., and Song, M., 2022. Insights into the domestic wastewater treatment (DWWT) regimes: A Review. Water, 14(21): 3542.

Kwietniewska, E. and Tys, J., 2014. Process characteristics, inhibition factors and methane yield of anaerobic digestion process, with particular focus on microalgal biomass fermentation. Renewable and Sustainable Energy Reviews, 34: 491-500.

Latif, M.A., Ghufran, R., Wahid, Z.A., and Ahmad, A., 2011. Integrated application of upflow anaerobic sludge blanket reactor for the treatment of Wastewaters. Water Research, 45(16): 4683–4699.

Lee, X.J., Lee, L.Y., Gan, S., Thangalazhy-Gopakumar, S., and Ng, H.K., 2017. Biochar potential evaluation of palm oil wastes through slow pyrolysis: Thermochemical Characterization and pyrolytic kinetic studies. Bioresource Technology, 236: 155–163.

Levesque, M. and Martin, J., 2002. Stade de France, Paris, France. Structural Engineering International, 12(4): 242-244.

Linville JL, Shen Y, Ignacio-de Leon PA, Schoene RP, Urgun-Demirtas M. In-situ biogas upgrading during anaerobic digestion of food waste amended with walnut shell biochar at bench scale. Waste Manag Res 2017;35: 669–79. https://doi.org/ 10.1177/0734242X17704716.

Lü, F., Hua, Z., Shao, L., and He, P., 2018. Loop bioenergy production and carbon sequestration of polymeric waste by integrating biochemical and Thermochemical Conversion Processes: A conceptual framework and recent advances. Renewable Energy, 124: 202–211.

Lü, F., Hua, Z., Shao, L., and He, P., 2018. Loop bioenergy production and carbon sequestration of polymeric waste by integrating biochemical and Thermochemical Conversion Processes: A conceptual framework and recent advances. Renewable Energy, 124: 202–211.

Luo, K., Yang, Q., Li, X., Yang, G., Liu, Y., Wang, D., Zheng, W., and Zeng, G., 2012. Hydrolysis kinetics in anaerobic digestion of waste activated sludge enhanced by α-amylase. Biochemical Engineering Journal, 62:17–21.

Luste, S., and Luostarinen, S., 2010. Anaerobic co-digestion of meat-processing by-products and sewage sludge – effect of hygienization and organic loading rate. Bioresource Technology, 101(8): 2657–2664.

Mata-Alvarez J, Dosta J, Romero-Güiza MS, Fonoll X, Peces M, Astals S. 2014. A critical review on anaerobic co-digestion achievements between 2010 and 2013. Renew Sustain Energy Rev; 36: 412–27.

Mata-Alvarez, J., Dosta, J., Romero-Güiza, M.S., Fonoll, X., Peces, M., and Astals, S., 2014. A critical review on anaerobic co-digestion achievements between 2010 and 2013. Renewable and Sustainable Energy Reviews, 36: 412–427.

Metje, M., and Frenzel, P., 2007. Methanogenesis and methanogenic pathways in a peat from subarctic permafrost. Environmental Microbiology, 9(4): 954–964.

Mia, S., Singh, B., and Dijkstra, F.A., 2017. Aged biochar affects gross nitrogen mineralization and recovery: A 15N study in two contrasting soils. GCB Bioenergy, 9(7): 1196–1206.

Mitraka, G.-C., Kontogiannopoulos, K.N., Tsivintzelis, I., Zouboulis, A.I., and Kougias, P.G., 2022. Optimization of supercritical carbon dioxide explosion for sewage sludge pre-treatment using response surface methodology. Chemosphere, 297: 133989.

Mojiri, A. et al. (2020) 'Treatment of landfill leachate with different techniques: An overview', Journal of Water Reuse and Desalination, 11(1): 66–96. doi:10.2166/wrd.2020.079.

Montwedi, M., Munyaradzi, M., Pinoy, L., Dutta, A., Ikumi, DS., Motoasca, E and Van Der Bruggen, B. 2021. Resource recovery from and management of wastewater in rural South Africa: Possibilities and practices. Journal of Water Process Engineering, 40101978, https://doi.org/10.1016/j.jwpe.2021.101978.

Müller, N. et al. (2010) "Syntrophic butyrate and propionate oxidation processes: From genomes to reaction mechanisms," Environmental Microbiology Reports, 2(4): 489–499. Available at: https://doi.org/10.1111/j.1758-2229.2010.00147.x.

Musvoto, E., Mgwenya, N., Mangashena, H., and Mackintosh, A. (2018) Energy Recovery from Wastewater Sludge – A Review of Appropriate Emerging and Established Technologies for the South African Industry. Water Research Commission, Report no TT 752/18 Pretoria, South Africa.

Nabi, M. et al. (2019) 'Contribution of solid and liquid fractions of sewage sludge pretreated by high pressure homogenization to biogas production', Bioresource Technology, 286: 121378. doi:10.1016/j.biortech.2019.121378.

Nacheva, P.M., Chávez, G.M., Chacón, J.M., and Chuil, A.C., 2009. Treatment of cane sugar mill wastewater in an upflow anaerobic sludge bed reactor. Water Science and Technology, 60(5): 1347–1352.

Nanda S, Dalai AK, Berruti F, Kozinski JA., 2016. Biochar as an exceptional bioresource for energy, agronomy, carbon sequestration, activated carbon and specialty materials. Waste and Biomass Valorization (7): 201–35.

Niju, S., Ajieth Kanna, S.K., Ramalingam, V., Satheesh Kumar, M., and Balajii, M., 2019. Sugarcane bagasse derived biochar – a potential heterogeneous catalyst for transesterification process. Energy Sources, Part A: Recovery, Utilization, and Environmental Effects, 45(4): 9815–9826.

Palatsi, J., Illa, J., Prenafeta-Boldú, F.X., Laureni, M., Fernandez, B., Angelidaki, I., and Flotats, X., 2010. Long-chain fatty acids inhibition and adaptation process in anaerobic thermophilic digestion: Batch tests, microbial community structure and Mathematical Modelling. Bioresource Technology, 101(7): 2243–2251.

Pan, J. et al. (2019) 'Achievements of biochar application for enhanced Anaerobic Digestion: A Review', Bioresource Technology, 292: 122058. doi:10.1016/j.biortech.2019.122058.

Pecchi, M. and Baratieri, M., 2019. Coupling anaerobic digestion with gasification, pyrolysis or hydrothermal carbonization: A review. Renewable and Sustainable Energy Reviews, 105 :462-475.

Polestya, A., Sharma, S., and Khanna, D.R., 2008. Study of physico-chemical characteristics of treated effluent  of sugar industry. Environment Conservation Journal, 9(1 & 2): 69–71.

Pradeep, N.V., Anupama, S., Arun Kumar, J.M., Vidyashree, K.G., Lakshmi, P., Ankitha, K., and Pooja, J., 2013. Treatment of sugar industry wastewater in anaerobic downflow stationary fixed film (DSFF) reactor. Sugar Tech, 16(1): 9–14.

Qasim, S.R., 2017. Wastewater characteristics. Wastewater Treatment Plants,: 29–63.

Rafiq, M.K., Bachmann, R.T., Rafiq, M.T., Shang, Z., Joseph, S., and Long, R., 2016. Influence of pyrolysis temperature on physicochemical properties of corn stover (Zea mays L.) biochar and feasibility for carbon capture and Energy Balance. PLOS ONE, 11(6).

Rajeshwari, K.V. et al. (2000) "State-of-the-art of anaerobic digestion technology for industrial wastewater treatment," Renewable and Sustainable Energy Reviews, 4(2): 135–156. Available at: https://doi.org/10.1016/s1364-0321(99)00014-3.

Ramakrishnan, A. et al. (2014) 'Emerging contaminants in landfill leachate and their sustainable management', Environmental Earth Sciences, 73(3): 1357–1368. doi:10.1007/s12665-014-3489-x.

Ramjeawon, T., and Baguant, J., 1995. Evaluation of critical BOD loadings from Mauritian sugar factories to streams and standards setting. Journal of Environmental Management, 45(2), pp.163–176.

Rasapoor, M., Young, B., Brar, R., Sarmah, A., Zhuang, W.-Q., and Baroutian, S., 2020. Recognizing the challenges of anaerobic digestion: Critical steps toward improving biogas generation. Fuel, 261: 116497.

Rasi, S., Veijanen, A. and Rintala, J., 2007. Trace compounds of biogas from different biogas production plants. Energy, 32(8): 1375-1380.

Ren, W., Xiong, L., Nie, G., Zhang, H., Duan, X., and Wang, S., 2019. Insights into the electron-transfer regime of peroxydisulfate activation on carbon nanotubes: The role of oxygen functional groups. Environmental Science & Technology, 54(2): 1267–1275.

Romero-Güiza MS, Vila J, Mata-Alvarez J, Chimenos JM, Astals S. The role of additives on anaerobic digestion: a review. Renew Sustain Energy Rev 2016;58: 1486–99.

Ronsse, F., van Hecke, S., Dickinson, D., and Prins, W., 2012. Production and characterization of slow pyrolysis biochar: Influence of feedstock type and pyrolysis conditions. GCB Bioenergy, 5(2): 104–115.

Rowan, M., Umenweke, GC., Epelle, E.I., Afolabi, I.C., Okoye, P.U., Gunes, B and Okolie, J.A. 2022. Anaerobic co-digestion of food waste and agricultural residues: An overview of feedstock properties and the impact of biochar addition. Digital Chemical Engineering, 4100046, https://doi.org/10.1016/j.dche.2022.100046.

Ruthiraan, M., Mubarak, N.M., Thines, R.K, Abdullah, E.C., Sahu, J.N., Jayakumar, N.S., and Ganesan, P., 2015. Comparative kinetic study of functionalized carbon nanotubes and magnetic biochar for removal of CD2+ ions from wastewater. Korean Journal of Chemical Engineering, 32(3): 446–457.

Salman CA, Schwede S, Thorin E, Yan J. 2017. Enhancing biomethane production by integrating pyrolysis and anaerobic digestion processes. Applied Energy 204: 1074–83.

Schink, B., 1997. Energetics of syntrophic cooperation in methanogenic degradation. Microbiology and molecular biology reviews: MMBR, 61(2): 262–280.

Senés-Guerrero, C., Colón-Contreras, F.A., Reynoso-Lobo, J.F., Tinoco-Pérez, B., Siller-Cepeda, J.H., and Pacheco, A., 2019. Biogas-producing microbial composition of an anaerobic digester and associated bovine residues. MicrobiologyOpen, 8(9).

Shen, Y., Forrester, S., Koval, J., and Urgun-Demirtas, M., 2017. Yearlong semi-continuous operation of thermophilic two-stage anaerobic digesters amended with biochar for enhanced biomethane production. Journal of Cleaner Production, 167, pp.863–874.

Shi, Y., Liu, M., Li, J., Yao, Y., Tang, J., and Niu, Q., 2022. The dosage-effect of biochar on anaerobic digestion under the suppression of oily sludge: Performance variation, Microbial Community Succession and potential detoxification mechanisms. Journal of Hazardous Materials, 421:126819.

Sihlangu, E., Luseba, D., Regnier, T., Magama, P., Chiyanzu, I. and Nephawe, K.A. 2024. Investigating Methane, Carbon Dioxide, Ammonia, and Hydrogen Sulphide Content in Agricultural Waste during Biogas Production. Sustainability, 16(12): 5145, https://doi.org/10.3390/su16125145.

Silvestre, G., Illa, J., Fernández, B., and Bonmatí, A., 2014. Thermophilic anaerobic co-digestion of sewage sludge with grease waste: Effect of long chain fatty acids in the methane yield and its dewatering properties. Applied Energy, 117: 87–94.)

Sinervo, R., 2017. Effects of biochar addition on anaerobic digestion and comparison of different biochar qualities. thesis.

Somani, M. et al. (2019) ‘Comprehensive assessment of the leachate quality and its pollution potential from six municipal waste dumpsites of India’, Bioresource Technology Reports, 6, pp. 198–206. doi: 10.1016/j.biteb.2019.03.003.

Song, W., and Guo, M., 2012. Quality variations of poultry litter biochar generated at different pyrolysis temperatures. Journal of Analytical and Applied Pyrolysis, 94: 138–145.

Steiniger, B., Hupfauf, S., Insam, H. and Schaum, C. 2023. .Exploring Anaerobic Digestion from Mesophilic to Thermophilic Temperatures—Operational and Microbial Aspects, Fermentation, 9(9): 798, https://doi.org/10.3390/fermentation9090798.

Storck, T., Virdis, B., and Batstone, D.J., 2015. Modelling extracellular limitations for mediated versus direct interspecies electron transfer. The ISME Journal, 10(3): 621–631.

Sugiarto, Y., Sunyoto, N.M., Zhu, M., Jones, I., and Zhang, D., 2021. Effect of biochar addition on microbial community and methane production during anaerobic digestion of food wastes: The role of minerals in biochar. Bioresource Technology, 323: 124585.

Summers, Z.M., Fogarty, H.E., Leang, C., Franks, A.E., Malvankar, N.S., and Lovley, D.R., 2010. Direct exchange of electrons within aggregates of an evolved syntrophic Coculture of anaerobic bacteria. Science, 330(6009): 1413–1415.

Sun, X., Atiyeh, H.K., Adesanya, Y., Okonkwo, C., Zhang, H., Huhnke, R.L., and Ezeji, T., 2020. Feasibility of using biochar as buffer and mineral nutrients replacement for acetone-butanol-ethanol production from non-detoxified switchgrass hydrolysate. Bioresource Technology, 298: 122569.

Sunyoto, N.M.S., Zhu, M., Zhang, Z., and Zhang, D., 2016. Effect of biochar addition on hydrogen and methane production in two-phase anaerobic digestion of aqueous carbohydrates food waste. Bioresource Technology, 219: 29–36.

Taherzadeh M, Karimi K, Taherzadeh MJ, Karimi K. 2008. Pre-treatment of lignocellulosic wastes to improve ethanol and biogas production: a review. International Journal of Molecular Science: 1621–51.

Templeton, M. R. And Butler, D. 2011. Introduction to wastewater treatment, UK, Bookboon.

Teng, C. et al. (2021) 'Characterization and treatment of Landfill Leachate: A Review', Water Research, 203: 117525. doi:10.1016/j.watres.2021.117525.

Thanarasu, A., Periyasamy, K. and Subramanian, S. 2021. An integrated anaerobic digestion and microbial electrolysis system for the enhancement of methane production from organic waste: Fundamentals, innovative design and scale-up deliberation. Chemosphere, 287131886, https://doi.org/10.1016/j.chemosphere.2021.131886.

Tomczyk, A., Sokołowska, Z. and Boguta., P. 2020. Biochar physicochemical properties: pyrolysis temperature and feedstock kind effects. Reviews in Environmental Science and Bio/Technology, 19(1): 191–215, https://doi.org/10.1007/s11157-020-09523-3.

Tomczyk, A., Sokołowska, Z., and Boguta, P., 2020. Biochar physicochemical properties: Pyrolysis temperature and feedstock kind effects. Reviews in Environmental Science and Bio/Technology, 19(1): 191–215.

Torretta, V., Ferronato, N., Katsoyiannis, I., Tolkou, A., and Airoldi, M., 2016. Novel and conventional technologies for landfill leachates treatment: A Review. Sustainability, 9(1): 9.

Valderrama, L.T., Del Campo, C.M., Rodriguez, C.M., de-Bashan, L.E., and Bashan, Y., 2002. Treatment of recalcitrant wastewater from ethanol and citric acid production using the microalga chlorella vulgaris and the macrophyte Lemna minuscula. Water Research, 36(17): 4185–4192.

Vamvuka, D., and Sfakiotakis, S., 2011. Combustion behaviour of biomass fuels and their blends with lignite. Thermochimica Acta, 526(1–2): 192–199.

Velásquez, F., Espitia, J., Mendieta, O., Escobar, S., and Rodríguez, J., 2019. Non-centrifugal cane sugar processing: A review on recent advances and the influence of process variables on qualities attributes of final products. Journal of Food Engineering, 255: 32–40.

Verlicchi, P. and Grillini, V. 2020. Surface Water and Groundwater Quality in South Africa and Mozambique—Analysis of the Most Critical Pollutants for Drinking Purposes and Challenges in Water Treatment Selection. Water, 12(1): 305, https://doi.org/10.3390/w12010305.

Vieira Novais, S., Oliveira Zenero, M.D., Frade Junior, E.F., Paiva de Lima, R., and Pelegrino Cerri, C.E., 2017. Mitigation of greenhouse gas emissions from tropical soils amended with poultry manure and sugar cane straw Biochars. Agricultural Sciences, 08(09): 887–903.

Volschan Junior, I., de Almeida, R. and Cammarota, M., 2021. A review of sludge pre-treatment methods and co-digestion to boost biogas production and energy self-sufficiency in wastewater treatment plants. Journal of Water Process Engineering, 40: 101857.

Vorobyova, O., 2022. Anaerobic filters, anaerobic fluidized bed reactors, upflow anaerobic sludge blanket reactors - anaerobic reactor for industrial wastewater treatment. grundlagen der modernen wissenschaftlichen forschung.

Walter, A., Probst, M., Franke-Whittle, I.H., Ebner, C., Podmirseg, S.M., Etemadi-Shalamzari, M., Hupfauf, S., and Insam, H., 2018. Microbiota in anaerobic digestion of sewage sludge with and without co-substrates. Water and Environment Journal, 33(2): 214–222.

Wang, S., Yu, S., Lu, Q., Liao, Y., Li, H., Sun, L., Wang, H., and Zhang, Y., 2020. Development of an alkaline/acid pre-treatment and Anaerobic Digestion (APAD) process for methane generation from waste activated sludge. Science of The Total Environment, 708: 134564.

Wang, Z., Jiang, Y., Wang, S., Zhang, Y., Hu, Y., Hu, Z-H., Wu, G. and Zhan, X. 2020. Impact of total solids content on anaerobic co-digestion of pig manure and food waste: Insights into shifting of the methanogenic pathway. Waste Management, 11496–106, https://doi.org/10.1016/j.wasman.2020.06.048.

Ward, A.J., Hobbs, P.J., Holliman, P.J., and Jones, D.L., 2008. Optimisation of the anaerobic digestion of agricultural resources. Bioresource Technology, 99(17): 7928–7940.

Wei, W., Zhang, S., Wu, L., Cui, D., and Ding, X., 2020. Biochar and phosphorus fertilization improved soil quality and inorganic phosphorus fractions in saline-alkaline soils. Archives of Agronomy and Soil Science, 67(9): 1177–1190.

Weiland, P., 2009. Biogas production: Current State and Perspectives. Applied Microbiology and Biotechnology, 85(4): 849–860.

White, J.K., Beaven, R.P., Powrie, W., and Knox, K., 2011. Leachate recirculation in a landfill: Some insights obtained from the development of a simple 1-D model. Waste Management, 31(6): 1210–1221.

Wright, M.M., and Uddin, M.M., 2022. 3 anaerobic digestion fundamentals, challenges, and technological advances. Green Chemistry: 19–38.

Yang, Y., Zhang, Y., Li, Z., Zhao, Z., Quan, X., and Zhao, Z., 2017. Adding granular activated carbon into anaerobic sludge digestion to promote methane production and sludge decomposition. Journal of Cleaner Production, 149: 1101–1108.

Yao, Y., Gao, B., Inyang, M., Zimmerman, A.R., Cao, X., Pullammanappallil, P., and Yang, L., 2011. Biochar derived from anaerobically digested sugar beet tailings: Characterization and phosphate removal potential. Bioresource Technology, 102(10): 6273–6278.

Ye, M., Liu, J., Ma, C., Li, Y., Zou, L., Qian, G. and Xu, Z., 2018. Improving the stability and efficiency of anaerobic digestion of food waste using additives: A critical review. Journal of Cleaner Production, 192: 316-326.

Yongabi, K. 2010. Bio coagulants for water and wastewater purification: a review. International Review of Chemical Engineering, 2, 444-458.

Youcai, Z. (2018) 'Leachate irrigation for plants', Pollution Control Technology for Leachate from Municipal Solid Waste, pp. 325–359. doi:10.1016/b978-0-12-815813-5.00004-8.

Yu, T. et al. (2017) "Effect of alkaline microwaving pretreatment on anaerobic digestion and biogas production of swine manure," Scientific Reports, 7(1). Available at: https://doi.org/10.1038/s41598-017-01706-3.

Yuan, J.-H., Xu, R.-K., and Zhang, H., 2011. The forms of alkalis in the biochar produced from crop residues at different temperatures. Bioresource Technology, 102(3): 3488–3497.

Yukesh Kannah, R., Kavitha, S., Rajesh Banu, J., Parthiba Karthikeyan, O., and Sivashanmugham, P., 2017. Dispersion induced ozone pretreatment of waste activated biosolids: Arriving biomethanation modelling parameters, energetic and cost assessment. Bioresource Technology, 244: 679–687.

Yusaf, T. and Al-Juboori, R.A. (2014) 'Alternative methods of microorganism disruption for agricultural applications', Applied Energy, 114, pp. 909–923. doi: 10.1016/j.apenergy.2013.08.085.

Zábranská, J., Štěpová, J., Wachtl, R., Jeníček, P., and Dohányos, M., 2000. The activity of anaerobic biomass in thermophilic and mesophilic digesters at different loading rates. Water Science and Technology, 42(9): 49–56.

Zhang J, Zhao W, Zhang H, Wang Z, Fan C, Zang L. 2018. Recent achievements in enhancing anaerobic digestion with carbon-based functional materials. Bioresource Technology 266: 555–67.

Zhang, Y., Wang, J., Wang, G., Gao, C., Yan, Y., and Wen, B., 2015. Optimization of derivatization procedure and gas chromatography–mass spectrometry method for determination of bensulfuron-methyl herbicide residues in water. Journal of Chromatography B, 995–996: 31–37.

Zhao, S.-X., Ta, N., and Wang, X.-D., 2017. Effect of temperature on the structural and physicochemical properties of biochar with apple tree branches as feedstock material. Energies, 10(9): 1293.

# Appendix A1

**A1.1 Municipal and Industrial Wastewater Characterisation**

- **Total solids**.

  Equipment:

  - Drying oven
  - Analytical Balance
  - 20 mL porcelain Crucibles
  - Desiccator

  Procedure:

  The TS was analysed by measuring 20 ml of each sample into a crucible and drying it for 24 hours is a drying oven set to 105°C according to APHA (2005) section 2540B.

  $$Total\ Solids\ \left(\frac{mg}{L}\right) = \frac{B-A}{Vs} \times 1000$$

  Where:

  A = weight of crucible (mg)

  B = weight of crucible + residue (mg)

  Vs = sample volume in mL

  $$TS\ (Inoculum)\left(\frac{mg}{L}\right) = \frac{24.5290-23.4616}{20} \times 1000 = 53.37\frac{g}{L} \times 1000\frac{mg}{g} = 53\ 370\frac{mg}{l}$$

- **Standard Deviation**

  $$Standard\ Deviation = \sqrt{\frac{\sum(x-\bar{X})^2}{n-1}}$$

  Where:

  $\bar{X}$ is the mean value.

  $$Standard\ Deviation = \sqrt{\frac{(50.3-53.4)^2 + (59.11-53.4)^2}{2-1}}$$

  $$Standard\ Deviation = 6.5$$

- **Volatile Solids**

  Equipment:

  - Muffle furnace.

- Analytical Balance
- 20 mL porcelain Crucibles
- Desiccator

Procedure:

VS content refers to the reduction in weight that occurs when a sample is heated in a furnace at a temperature of 550°C for a duration of 1 hour and when liquids (slurry or wastewaters) are heated for a duration of 30 minutes and is conducted according to the APHA 2005 standard methodology.

$$Volatile\ Solids\ \left(\frac{mg}{L}\right) = \frac{B-C}{Vs} \times 1000$$

C = weight of crucible + residue after combustion (mg)

$$Volatile\ Solids\ \left(\frac{mg}{L}\right) = \frac{24.5290-23.9696}{20} \times 1000 = 27.9714\frac{g}{L} \times 1000\frac{mg}{g} = 27\,971.4\frac{mg}{L}$$

Table A1. 1: Feedstock characterisation raw data

| Parameter | Units | Sugar Industry Wastewater | Intermediate Landfill Leachate | Primary Sludge | Inoculum |
|---|---|---|---|---|---|
| pH | n/a | 5.5 | 7.85 | 5.05 | 7.83 |
| COD | mg/L | 202 650 ± 27.5 | 5 346 ± 46 | 59 040 ± 31,5 | 42 080 ± 24,5 |
| TS | gTS/L | 168.46 ± 8.8 | 2.56 ± 7.5 | 39.02 ± 7.1 | 53.4 ± 6.5 |
| VS | gVS/L | 115.36 ± 10.7 | 4.385 ± 9.8 | 29.72 ± 6.6 | 27.96 ± 5.8 |
| VS/TS | n/a | 0.68 | - | 0.76 | 0.52 |

### A1.2 Industrial Wastewater Selection BMP tests

Table A1. 2: Reactor loading raw data.

| Bioreactor | Inoculum Substrate ratio | Co-substrate loading rate | Inoculum (mL) | Primary Sludge (mL) | Landfill Leachate (mL) | Sugar Industry Wastewater (mL) | Total Volatile Solid loaded (g) |
|---|---|---|---|---|---|---|---|
| R1 | 1:1 | N/A | 800 | 0 | 0 | 0 | 22.13 |
| R2 | 1:1 | N/A | 270 | 530 | 0 | 0 | 20.84 |
| R3 (SIWW) | 1:1 | 1:5 | 230 | 440 | 0 | 130 | 35.04 |
| R4 (ILL) | 1:1 | 1:5 | 495 | 175 | 130 | 0 | 17.48 |

Table A1. 3: Bioreactor Characterization (IWW selection)

| Bioreactor | TS (g) | VS (g) | COD (mg/l) | pH (before digestion) | pH (after digestion) | Biogas Yield (ml) | Biogas Yield (ml/gVS$_a$) |
|---|---|---|---|---|---|---|---|
| **R1** | 42,80 | 22.13 | 38 800,00 | 7.5 | 8.0 | 270 | 12,20 |
| **R2 (CNTRL)** | 31,93 | 20.84 | 48 050,00 | 5.93 | 7,23 | 800 | 38.39 |
| **R3** (SIWW) | 51,66 | 35.04 | 71 950,00 | 4.93 | 6.5 | 440 | 12.55 |
| **R4** (ILL) | 27,70 | 17.48 | 35 500,00 | 5.63 | 7.23 | 950 | 54,35 |

- **Inoculum Substrate Ratio Calculation (R2)**

$$ISR = \frac{VS_{inoc}}{VS_{sub}}$$

Where:

$VS_{inc}$ is the volatile solids content of the inoculum in g/l.

$VS_{sub}$ is the sum of the volatile solids content of the substrate and co-substrate in g/l.

$$ISR = \frac{VS_{inoc}}{VS_{sub}} = \frac{VS_{inoc} \times V_{inoc}}{VS_{sub} \times V_{sub}}$$

Let:

$$V_{total} = V_{sub} + V_{inoc}$$

$$0.8 = V_{sub} + V_{inoc}$$

$$0.8 - V_{sub} = V_{inoc}$$

Therefore:

$$ISR = \frac{VS_{inoc} \times (0.8 - V_{sub})}{VS_{sub} \times V_{\text{sub}}}$$

$$1 = \frac{37.71 \times (0.8 - V_{sub})}{18.99 \times V_{\text{sub}}}$$

$$V_{sub} = 0.53\ L$$

Therefore:

$$V_{inoc} = 0.8 - V_{sub} = 0.8 - 0.53 = 0.27\ L$$

- **COD Removal (R2)**

$$Removal\ Effiency\ (\%) = \frac{Initial\ Concentation\ \ (Ic) - Final\ Concetration\ (Fc)}{Initial\ Concentation\ \ (Ic)}$$

$$Removal\ Effiency\ (\%) = \frac{48\,050\frac{mg}{L} - 26\,750\ mg/L}{48\,050\frac{mg}{L}} \times 100 = 44.33\%$$

- **VS Removal (R2)**

$$Removal\ Effiency\ (\%) = \frac{Initial\ Concentation\ \ (Ic) - Final\ Concetration\ (Fc)}{Initial\ Concentation\ \ (Ic)}$$

$$Removal\ Effiency\ (\%) = \frac{20.84\frac{g}{L} - 14.26\ g/L}{20.84\ \frac{g}{L}} \times 100 = 29.88\%$$

- **Biogas Yield Trend Data**

Table A1. 4: Average Accumulative Biogas Yield raw data.

| Daily Biogas Log (ml/gVSfed) | | | | |
|---|---|---|---|---|
| **Day** | **R 1** | **R 2** | **R 3** | **R 4** |
| Day 1 | 0 | 0 | 0 | 0 |
| Day 2 | 6,778741866 | 11,99385914 | 14,87414188 | 9,133462724 |
| Day 3 | 11,29790311 | 16,7914028 | 19,45080092 | 11,41682841 |
| Day 4 | 11,29790311 | 18,71042026 | 21,73913043 | 11,41682841 |
| Day 5 | 11,29790311 | 19,669929 | 24,02745995 | 11,41682841 |
| Day 6 | 11,29790311 | 21,58894646 | 26,31578947 | 11,41682841 |
| Day 7 | 11,29790311 | 23,02820956 | 28,60411899 | 11,41682841 |
| Day 8 | 11,29790311 | 24,94722702 | 31,46453089 | 11,41682841 |
| Day 9 | 11,29790311 | 26,86624448 | 33,18077803 | 11,41682841 |
| Day 10 | 11,29790311 | 28,78526195 | 35,46910755 | 11,41682841 |
| Day 11 | 11,29790311 | 33,10305124 | 38,90160183 | 11,41682841 |
| Day 12 | 11,29790311 | 36,4613318 | 44,05034325 | 11,41682841 |
| Day 13 | 11,74981923 | 38,38034926 | 48,62700229 | 11,41682841 |
| Day 14 | 11,74981923 | 38,38034926 | 51,48741419 | 11,41682841 |

| | | | | |
|---|---|---|---|---|
| Day 15 | 12,20173536 | 38,38034926 | 52,05949657 | 11,41682841 |
| Day 16 | 12,20173536 | 38,38034926 | 53,77574371 | 11,41682841 |
| Day 17 | 12,20173536 | 38,38034926 | 54,34782609 | 11,98766983 |
| Day 18 | 12,20173536 | 38,38034926 | 54,34782609 | 11,98766983 |
| Day 19 | 12,20173536 | 38,38034926 | 54,34782609 | 11,98766983 |
| Day 20 | 12,20173536 | 38,38034926 | 54,34782609 | 12,55851125 |
| Day 21 | 12,20173536 | 38,38034926 | 54,34782609 | 12,84393196 |

- **Gas Chromatography reports.**

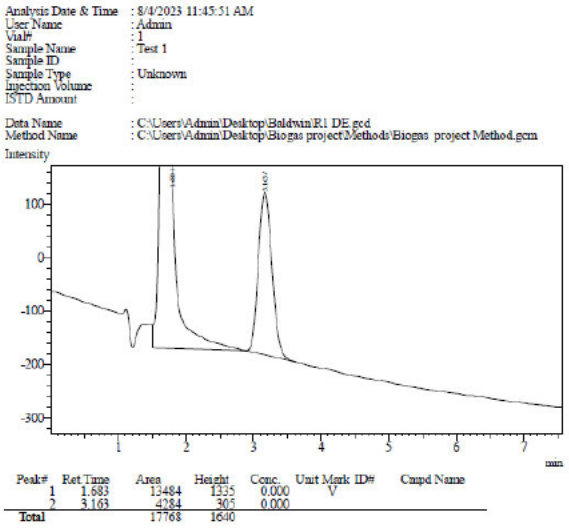

Analysis Date & Time : 8/4/2023 11:45:51 AM
User Name : Admin
Vial# : 1
Sample Name : Test 1
Sample ID :
Sample Type : Unknown
Injection Volume :
ISTD Amount :

Data Name : C:\Users\Admin\Desktop\Baldwin\R1 DE.gcd
Method Name : C:\Users\Admin\Desktop\Biogas project\Methods\Biogas project Method.gcm

Intensity




| Peak# | Ret.Time | Area | Height | Conc. | Unit | Mark | ID# | Cmpd Name |
|---|---|---|---|---|---|---|---|---|
| 1 | 1.683 | 13484 | 1335 | 0.000 | | V | | |
| 2 | 3.163 | 4284 | 305 | 0.000 | | | | |
| Total | | 17768 | 1640 | | | | | |

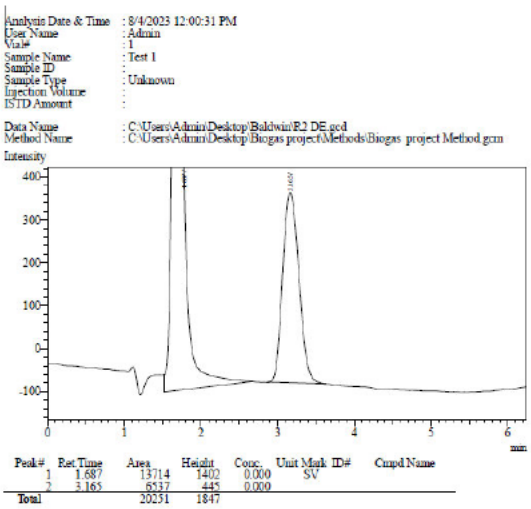

Analysis Date & Time : 8/4/2023 12:00:31 PM
User Name : Admin
Vial# : 1
Sample Name : Test 1
Sample ID :
Sample Type : Unknown
Injection Volume :
ISTD Amount :

Data Name : C:\Users\Admin\Desktop\Baldwin\R2 DE.gcd
Method Name : C:\Users\Admin\Desktop\Biogas project\Methods\Biogas project Method.gcm

Intensity




| Peak# | Ret.Time | Area | Height | Conc. | Unit | Mark | ID# | Cmpd Name |
|---|---|---|---|---|---|---|---|---|
| 1 | 1.687 | 13714 | 1402 | 0.000 | | SV | | |
| 2 | 3.165 | 6537 | 445 | 0.000 | | | | |
| Total | | 20251 | 1847 | | | | | |

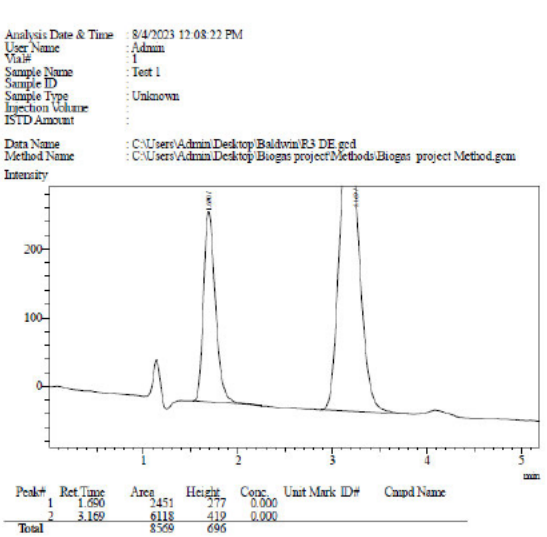

Analysis Date & Time : 8/4/2023 12:08:22 PM
User Name : Admin
Vial# : 1
Sample Name : Test 1
Sample ID :
Sample Type : Unknown
Injection Volume :
ISTD Amount :

Data Name : C:\Users\Admin\Desktop\Baldwin\R3 DE.gcd
Method Name : C:\Users\Admin\Desktop\Biogas project\Methods\Biogas project Method.gcm

Intensity




| Peak# | Ret.Time | Area | Height | Conc. | Unit | Mark | ID# | Cmpd Name |
|---|---|---|---|---|---|---|---|---|
| 1 | 1.690 | 2451 | 277 | 0.000 | | | | |
| 2 | 3.169 | 6118 | 419 | 0.000 | | | | |
| Total | | 8569 | 696 | | | | | |

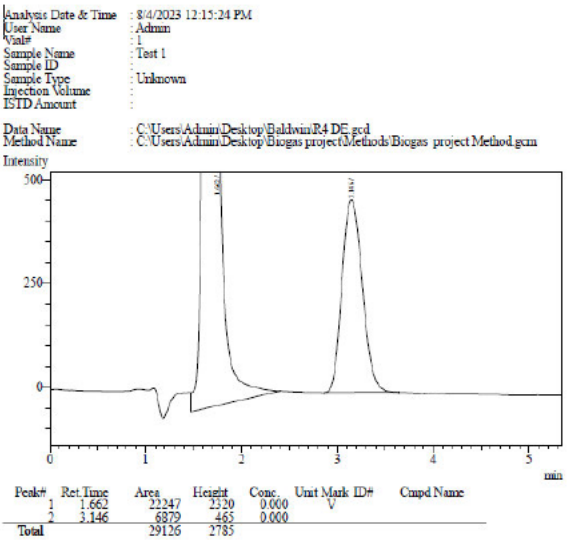

Analysis Date & Time : 8/4/2023 12:15:24 PM
User Name : Admin
Vial# : 1
Sample Name : Test 1
Sample ID :
Sample Type : Unknown
Injection Volume :
ISTD Amount :

Data Name : C:\Users\Admin\Desktop\Baldwin\R4 DE.gcd
Method Name : C:\Users\Admin\Desktop\Biogas project\Methods\Biogas project Method.gcm

Intensity




| Peak# | Ret.Time | Area | Height | Conc. | Unit | Mark | ID# | Cmpd Name |
|---|---|---|---|---|---|---|---|---|
| 1 | 1.662 | 22247 | 2320 | 0.000 | | V | | |
| 2 | 3.146 | 6879 | 465 | 0.000 | | | | |
| Total | | 29126 | 2785 | | | | | |

# Appendix A2

RSM data Optimisation of IWW BMP System

Table A2 1: IWW optimization DOE and results

| | | | | | Experimental Results | | | Predicted Values | | |
|---|---|---|---|---|---|---|---|---|---|---|
| Std | Run | Factor 1 A: Temperature | Factor 2 B: ISR | Factor 3 C: Co-substrate Ratio | Response 1 Biogas Yield | Response 2 COD Removal | Response 3 VS Removal | Response 1 Biogas Yield | Response 2 COD Removal | Response 3 VS Removal |
| | | Degrees Celsius | | | (ml/gVS) | % | % | % | % | % |
| 2 | 1 | 1 | -1 | 0 | 42.0463 | 22.1229 | 34.7057 | 40.78 | 22.87 | 34.81 |
| 13 | 2 | 0 | 0 | 0 | 61.5787 | 31 | 27.18 | 59.97 | 31.81 | 26.34 |
| 3 | 3 | -1 | 1 | 0 | 46 | 13.9191 | 21.9813 | 47.26 | 13.18 | 21.87 |
| 14 | 4 | 0 | 0 | 0 | 58.3301 | 30.9 | 26.3401 | 59.97 | 31.81 | 26.34 |
| 10 | 5 | 0 | 1 | -1 | 91.3679 | 33.3013 | 41.15 | 91.65 | 33.11 | 41.71 |
| 9 | 6 | 0 | -1 | -1 | 27.4424 | 33.046 | 35 | 28.34 | 33.32 | 35.56 |
| 1 | 7 | -1 | -1 | 0 | 13.5 | 35.9799 | 29.2744 | 14.15 | 34.77 | 29.17 |
| 4 | 8 | 1 | 1 | 0 | 34.63 | 34.6801 | 36.5871 | 33.98 | 35.89 | 36.69 |
| 15 | 9 | 0 | 0 | 0 | 60 | 33.5429 | 25.4899 | 59.97 | 31.81 | 26.34 |
| 5 | 10 | -1 | 0 | -1 | 32 | 27.3 | 22.1 | 30.45 | 28.23 | 21.64 |
| 12 | 11 | 0 | 1 | 1 | 42 | 32.7414 | 39.5514 | 41.11 | 22.87 | 38.99 |
| 7 | 12 | -1 | 0 | 1 | 38.6751 | 17 | 28.3 | 38.31 | 31.81 | 28.97 |
| 6 | 13 | 1 | 0 | -1 | 45 | 21 | 40.1 | 45.37 | 13.18 | 39.43 |
| 8 | 14 | 1 | 0 | 1 | 35.1983 | 38 | 31.1949 | 36.74 | 31.81 | 31.65 |
| 11 | 15 | 0 | -1 | 1 | 78.4006 | 40.6436 | 38.4116 | 78.12 | 33.11 | 37.85 |

- **Bioreactor characterisation**

Table A2 2: Bioreactor Characterisation Raw Data Total Solids (IWW optimization)

| Reactor | pH | B-Weight of crucible (g) | A-Weight of crucible + residue (g) | C-Volume of Sample (ml) | Total Solids (TS) in g/l |
|---|---|---|---|---|---|
| R 1 | 7,81 | 23,4539 | 24,1555 | 20 | 35,08 |
| R 2 | 7,78 | 21,9920 | 22,6961 | 20 | 35,205 |
| R 3 | 7,47 | 21,0018 | 21,8341 | 20 | 41,615 |
| R 4 | 7,84 | 28,4329 | 29,1891 | 20 | 37,81 |

| | | | | | |
|---|---|---|---|---|---|
| R 5 | 7,81 | 22,9034 | 23,6075 | 20 | 35,205 |
| R 6 | 7,52 | 26,8853 | 27,5509 | 20 | 33,28 |
| R 7 | 7,39 | 28,2773 | 28,9562 | 20 | 33,945 |
| R 8 | 7,81 | 21,4168 | 22,2784 | 20 | 43,08 |
| R 9 | 7,78 | 45,5111 | 46,3187 | 20 | 40,38 |
| R 10 | 7,67 | 28,9279 | 29,7442 | 20 | 40,815 |
| R 11 | 7,82 | 28,4254 | 29,0574 | 20 | 31,6 |
| R 12 | 7,60 | 30,1866 | 30,9104 | 20 | 36,19 |
| R 13 | 7,89 | 43,1276 | 43,6962 | 20 | 28,43 |
| R 14 | 7,90 | 41,0959 | 41,6388 | 20 | 27,145 |
| R 15 | 7,95 | 52,8218 | 53,2668 | 20 | 22,25 |

Table A2. 3: Bioreactor Characterisation Raw Data Total Solids (IWW optimization)

| Variable | Temperature © | B-Weight of crucible + residue after TS test (g) | D-Weight of crucible + residue atfter ignition (g) | C-Volume of sample (mL) | Volatile Solids (VS) in g/l |
|---|---|---|---|---|---|
| R 1 | 550 | 24,1555 | 23,7828 | 20 | 18,635 |
| R 2 | 550 | 22,6961 | 22,3337 | 20 | 18,12 |
| R 3 | 550 | 21,8341 | 21,4167 | 20 | 20,87 |
| R 4 | 550 | 29,1891 | 28,8071 | 20 | 19,1 |
| R 5 | 550 | 23,6075 | 23,2587 | 20 | 17,44 |
| R 6 | 550 | 27,5509 | 27,1824 | 20 | 18,425 |
| R 7 | 550 | 28,9562 | 28,5897 | 20 | 18,325 |
| R 8 | 550 | 22,2784 | 21,8416 | 20 | 21,84 |
| R 9 | 550 | 46,3187 | 45,8928 | 20 | 21,295 |
| R 10 | 550 | 29,7442 | 29,3218 | 20 | 21,12 |
| R 11 | 550 | 29,0574 | 28,7421 | 20 | 15,765 |
| R 12 | 550 | 30,9104 | 30,5398 | 20 | 18,53 |
| R 13 | 550 | 43,6962 | 43,3947 | 20 | 15,075 |

| | | | | | |
|---|---|---|---|---|---|
| R 14 | 550 | 41,6388 | 41,3578 | 20 | 14,05 |
| R 15 | 550 | 53,2668 | 53,0138 | 20 | 12,65 |

- **Biogas Yield Trend Data**

Table A2 4: Average Accumulative Biogas Yield Raw Data

| Daily Biogas Log (ml/gVSfed) | | | | | | | | | | | | | | | |
|---|---|---|---|---|---|---|---|---|---|---|---|---|---|---|---|
| | | | | | | | | | | | | | | | |
| Date | R 1 | R 2 | R 3 | R 4 | R 5 | R 6 | R 7 | R 8 | R 9 | R 10 | R 11 | R 12 | R 13 | R 14 | R 15 |
| day 1 | 0 | 0 | 0 | 0 | 0 | 0 | 0 | 0 | 0 | 0 | 0 | 0 | 0 | 0 | 0 |
| day 2 | 9,197617 | 11,15206 | 6,542056 | 9,641342 | 10,87713 | 8,232711 | 4,824392 | 14,2315 | 12,24633 | 5,915544 | 10,54448 | 4,95835 | 11,74371 | 12,2429 | 10,29008 |
| day 3 | 17,51927 | 22,78898 | 12,61682 | 19,28268 | 19,57884 | 16,46542 | 9,648784 | 23,71917 | 21,86844 | 13,19621 | 21,56825 | 12,39587 | 22,07817 | 21,42507 | 17,15014 |
| day 4 | 18,39523 | 24,2436 | 16,35514 | 19,76475 | 21,75426 | 16,9228 | 9,648784 | 25,14231 | 22,30581 | 14,78886 | 23,00613 | 12,39587 | 23,48741 | 22,03722 | 19,60016 |
| day 5 | 20,14716 | 25,69822 | 17,75701 | 23,13922 | 23,92969 | 16,9228 | 9,648784 | 28,463 | 22,74318 | 14,78886 | 26,84049 | 14,87505 | 28,18489 | 26,32223 | 19,60016 |
| day 6 | 21,89909 | 26,66796 | 19,15888 | 24,10336 | 26,97529 | 16,9228 | 10,13122 | 31,78368 | 23,18055 | 15,47142 | 29,71626 | 17,35422 | 31,00338 | 30,60725 | 20,09016 |
| day 7 | 22,33707 | 32,48642 | 21,02804 | 28,92403 | 30,45597 | 18,75229 | 10,13122 | 32,25806 | 27,55423 | 17,29159 | 34,02991 | 18,84173 | 35,23112 | 30,60725 | 21,07017 |
| day 8 | 22,55606 | 36,3654 | 22,42991 | 33,7447 | 34,37174 | 21,49652 | 10,13122 | 32,73245 | 32,36529 | 19,11176 | 37,38497 | 20,32923 | 38,9891 | 31,83154 | 22,05018 |
| day 9 | 23,21303 | 42,66874 | 24,76636 | 38,56537 | 36,98225 | 22,86864 | 10,13122 | 32,96964 | 37,17635 | 19,11176 | 40,26074 | 22,31257 | 42,74709 | 32,44368 | 23,03018 |
| day 10 | 23,65102 | 46,06284 | 26,16822 | 43,38604 | 40,02785 | 25,15551 | 10,13122 | 33,20683 | 39,36319 | 19,5668 | 43,6158 | 23,30424 | 46,97482 | 32,44368 | 23,03018 |
| day 11 | 24,089 | 50,91156 | 28,03738 | 48,20671 | 43,50853 | 25,15551 | 10,13122 | 33,44402 | 44,17425 | 20,93193 | 47,92945 | 23,80008 | 51,6723 | 33,66797 | 24,5002 |
| day 12 | 24,089 | 53,33592 | 33,17757 | 49,17084 | 43,94361 | 25,38419 | 10,13122 | 33,91841 | 45,48635 | 23,66218 | 47,92945 | 26,27925 | 52,14205 | 33,66797 | 30,87025 |
| day 13 | 24,089 | 54,79054 | 36,4486 | 49,65291 | 44,3787 | 25,38419 | 10,13122 | 34,1556 | 45,92372 | 27,30251 | 47,92945 | 27,76676 | 52,14205 | 33,66797 | 34,30027 |
| day 14 | 24,089 | 56,24515 | 37,38318 | 50,61705 | 44,59624 | 25,61288 | 10,13122 | 34,62998 | 46,79846 | 29,57772 | 48,40874 | 29,7501 | 52,6118 | 34,28012 | 36,75029 |
| day 15 | 25,84093 | 56,73002 | 37,85047 | 51,58118 | 53,0804 | 26,52763 | 10,13122 | 34,62998 | 47,6732 | 31,85293 | 48,40874 | 30,74177 | 52,6118 | 34,28012 | 42,63034 |
| day 16 | 27,59285 | 57,2149 | 37,85047 | 52,06325 | 58,73651 | 26,985 | 10,13122 | 34,62998 | 48,54794 | 31,85293 | 48,40874 | 33,71678 | 52,6118 | 34,28012 | 46,55037 |
| day 17 | 28,46882 | 57,69977 | 37,85047 | 52,54531 | 65,26279 | 27,44237 | 10,13122 | 34,62998 | 48,54794 | 34,12814 | 48,40874 | 34,70845 | 52,6118 | 34,28012 | 53,90043 |
| day 18 | 30,65872 | 58,66951 | 37,85047 | 54,47358 | 65,69788 | 27,44237 | 10,13122 | 34,62998 | 49,86004 | 36,40335 | 51,7638 | 34,70845 | 52,6118 | 34,28012 | 61,25049 |
| day 19 | 32,84863 | 59,15438 | 37,85047 | 57,36599 | 66,3505 | 27,44237 | 10,13122 | 34,62998 | 51,17215 | 39,1336 | 53,20169 | 37,18762 | 53,08155 | 34,89226 | 68,60055 |
| day 20 | 35,47652 | 59,88169 | 37,85047 | 57,84805 | 71,35399 | 27,44237 | 10,13122 | 34,62998 | 51,60952 | 40,95377 | 53,20169 | 37,68346 | 53,08155 | 34,89226 | 72,52058 |
| day 21 | 38,5424 | 60,36656 | 37,85047 | 58,33012 | 77,88026 | 27,44237 | 10,13122 | 34,62998 | 52,04689 | 42,31889 | 53,20169 | 38,17929 | 53,08155 | 34,89226 | 73,99059 |
| day 22 | 39,41836 | 60,85144 | 37,85047 | 58,33012 | 82,23112 | 27,44237 | 10,13122 | 34,62998 | 52,04689 | 43,68402 | 53,20169 | 38,17929 | 53,08155 | 34,89226 | 75,95061 |
| day 23 | 40,73231 | 61,33631 | 37,85047 | 58,33012 | 87,01706 | 27,44237 | 10,13122 | 34,62998 | 52,04689 | 44,5941 | 53,20169 | 39,17096 | 53,08155 | 34,89226 | 77,42062 |
| day 24 | 42,04625 | 61,57874 | 37,85047 | 58,33012 | 91,36791 | 27,44237 | 10,13122 | 34,62998 | 52,04689 | 45,50419 | 53,20169 | 39,6668 | 53,08155 | 35,19833 | 78,40063 |
| day 25 | 42,04625 | 61,57874 | 37,85047 | 58,33012 | 91,36791 | 27,44237 | 10,13122 | 34,62998 | 52,04689 | 45,50419 | 53,20169 | 39,6668 | 53,08155 | 35,19833 | 78,40063 |
| day 26 | 42,04625 | 61,57874 | 37,85047 | 58,33012 | 91,36791 | 27,44237 | 10,13122 | 34,62998 | 52,04689 | 45,50419 | 53,20169 | 39,6668 | 53,08155 | 35,19833 | 78,40063 |
| day 27 | 42,04625 | 61,57874 | 37,85047 | 58,33012 | 91,36791 | 27,44237 | 10,13122 | 34,62998 | 52,04689 | 45,50419 | 53,20169 | 39,6668 | 53,08155 | 35,19833 | 78,40063 |

- **Gas Chromatography reports.**

Analysis Date & Time : 5/5/2023 2:45:34 PM
User Name : Admin
Vial# : 1
Sample Name :
Sample ID :
Sample Type : Unknown
Injection Volume :
ISTD Amount :

Data Name : C:\Users\Admin\Desktop\Biogas project\Gas Standard.gcd
Method Name : C:\Users\Admin\Desktop\Biogas project\Biogas project.gcm

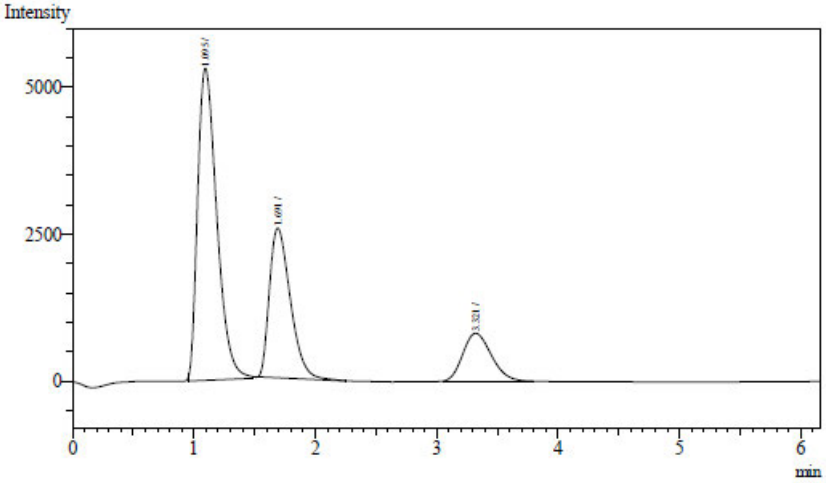


| Peak# | Ret.Time | Area | Height | Conc. | Unit | Mark | ID# | Cmpd Name |
|---|---|---|---|---|---|---|---|---|
| 1 | 1.095 | 58147 | 5308 | 57.054 | | | | |
| 2 | 1.691 | 30535 | 2545 | 29.961 | | | | |
| 3 | 3.321 | 13234 | 812 | 12.986 | | | | |
| Total | | 101916 | 8665 | | | | | |

Figure A2. 1: Chromatograph for IWW Optimization Gas standard

Analysis Date & Time : 5/5/2023 4:34:15 PM
User Name : Admin
Vial# : 1
Sample Name :
Sample ID :
Sample Type : Unknown
Injection Volume :
ISTD Amount :

Data Name : C:\Users\Admin\Desktop\Biogas project\R1.gcd
Method Name : C:\Users\Admin\Desktop\Biogas project\Biogas project.gcm

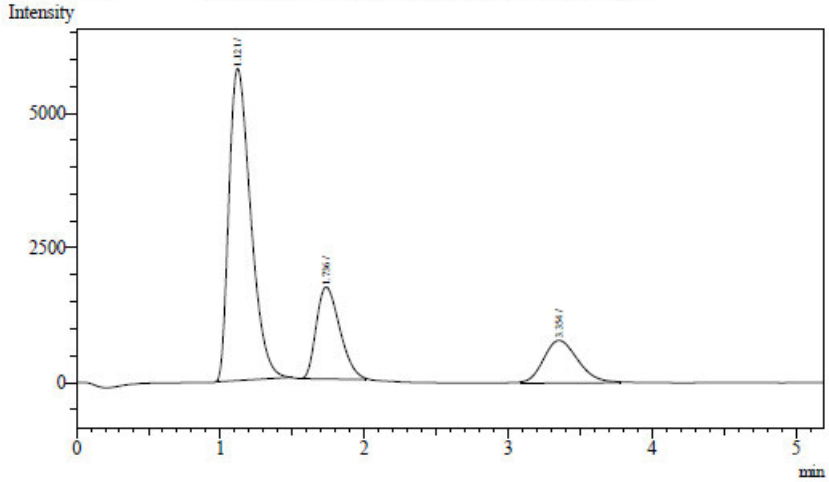


| Peak# | Ret.Time | Area | Height | Conc. | Unit | Mark | ID# | Cmpd Name |
|---|---|---|---|---|---|---|---|---|
| 1 | 1.121 | 60772 | 5790 | 65.123 | | | | |
| 2 | 1.736 | 19409 | 1706 | 20.799 | | | | |
| 3 | 3.354 | 13138 | 790 | 14.078 | | | | |
| Total | | 93319 | 8286 | | | | | |

Figure A2. 2: Chromatograph for IWW Optimization R1

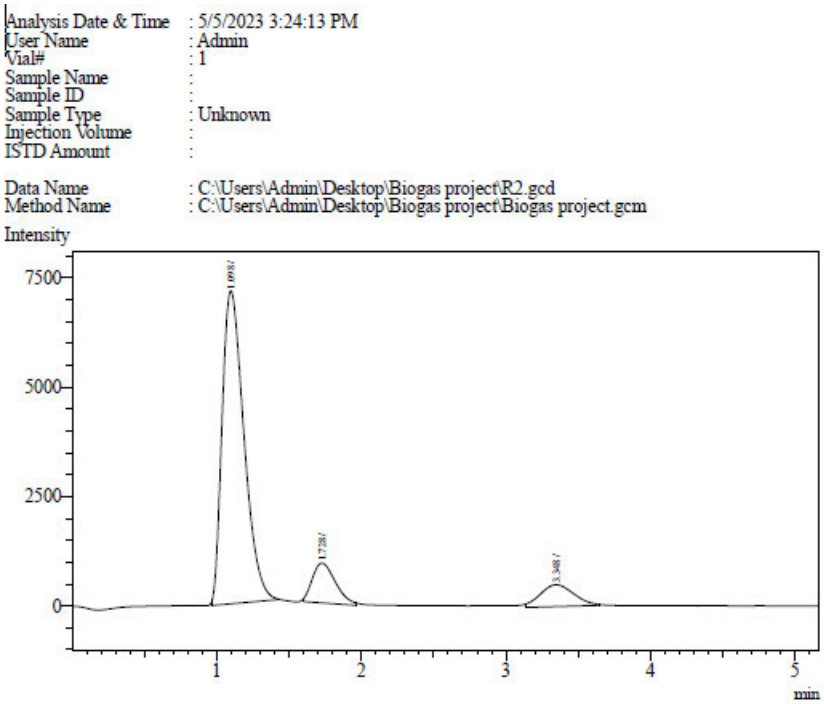


| Peak# | Ret.Time | Area | Height | Conc. | Unit Mark | ID# | Cmpd Name |
|---|---|---|---|---|---|---|---|
| 1 | 1.098 | 74960 | 7151 | 80.448 | | | |
| 2 | 1.728 | 10109 | 910 | 10.850 | | | |
| 3 | 3.348 | 8109 | 500 | 8.702 | | | |
| Total | | 93178 | 8561 | | | | |

Figure A2. 3: Chromatograph for IWW Optimization R2

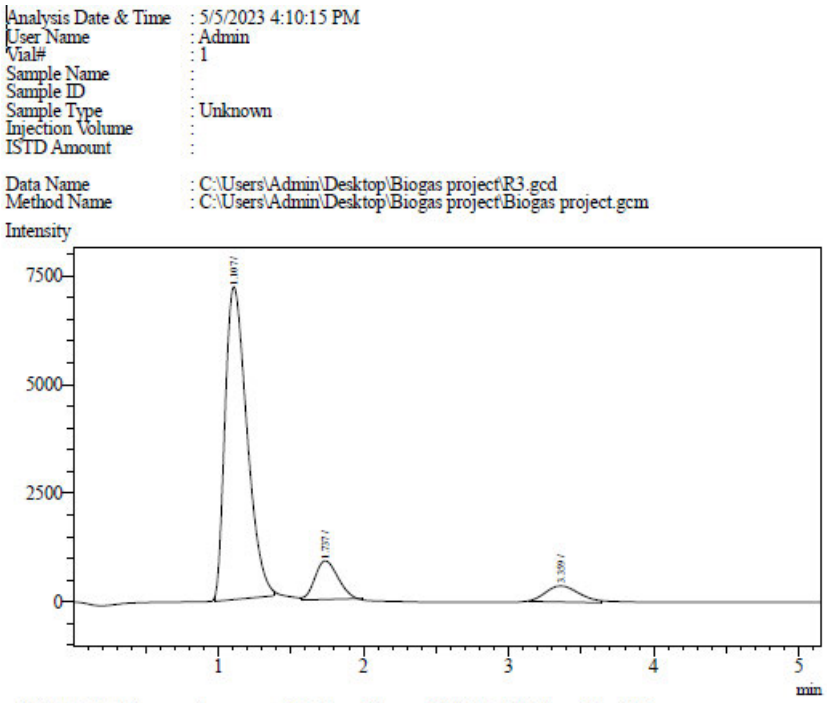


| Peak# | Ret.Time | Area | Height | Conc. | Unit Mark | ID# | Cmpd Name |
|---|---|---|---|---|---|---|---|
| 1 | 1.107 | 75532 | 7187 | 82.869 | | | |
| 2 | 1.737 | 9723 | 887 | 10.668 | | | |
| 3 | 3.359 | 5891 | 368 | 6.464 | | | |
| Total | | 91146 | 8442 | | | | |

Figure A2. 4:Chromatograph for IWW Optimization R3

Analysis Date & Time : 5/5/2023 2:38:10 PM
User Name : Admin
Vial# : 1
Sample Name :
Sample ID :
Sample Type : Unknown
Injection Volume :
ISTD Amount :

Data Name : C:\Users\Admin\Desktop\Biogas project\R4.gcd
Method Name : C:\Users\Admin\Desktop\Biogas project\Biogas project.gcm

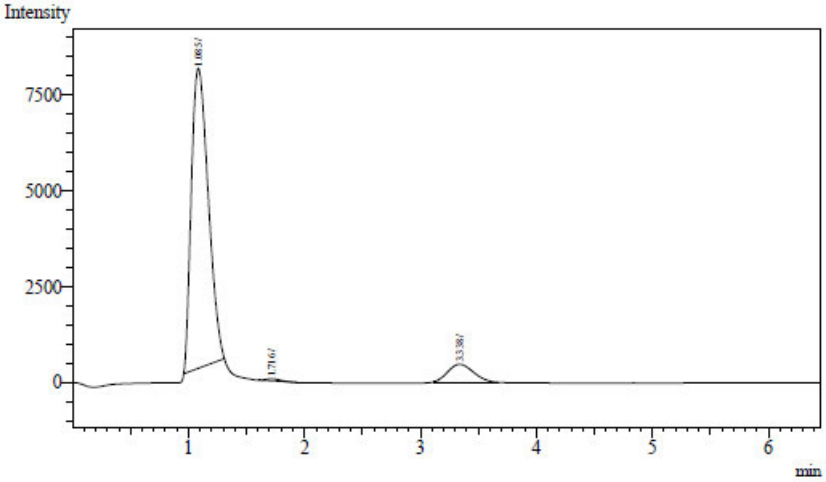


| Peak# | Ret.Time | Area | Height | Conc. | Unit | Mark | ID# | Cmpd Name |
|---|---|---|---|---|---|---|---|---|
| 1 | 1.085 | 79053 | 7820 | 91.005 | | | | |
| 2 | 1.716 | 349 | 49 | 0.402 | | | | |
| 3 | 3.338 | 7464 | 477 | 8.593 | | | | |
| Total | | 86866 | 8346 | | | | | |

Figure A2. 5: Chromatograph for IWW Optimization R4

Analysis Date & Time : 5/5/2023 4:42:42 PM
User Name : Admin
Vial# : 1
Sample Name :
Sample ID :
Sample Type : Unknown
Injection Volume :
ISTD Amount :

Data Name : C:\Users\Admin\Desktop\Biogas project\R5 Duplicate.gcd
Method Name : C:\Users\Admin\Desktop\Biogas project\Biogas project.gcm

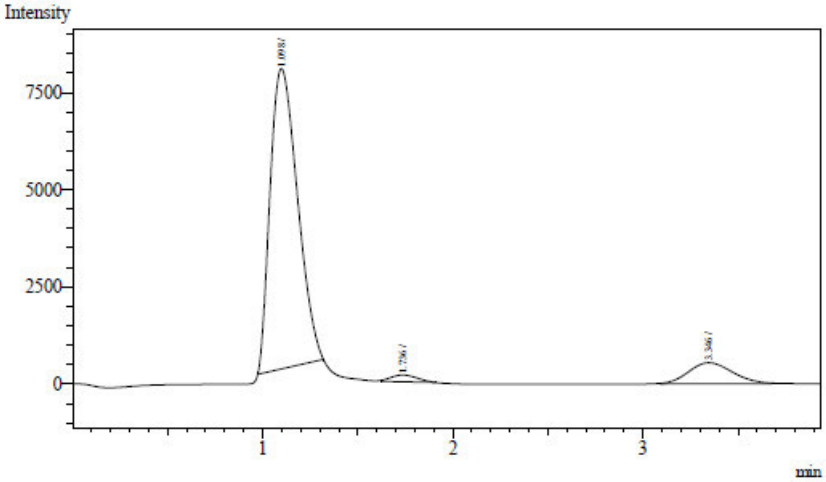


| Peak# | Ret.Time | Area | Height | Conc. | Unit | Mark | ID# | Cmpd Name |
|---|---|---|---|---|---|---|---|---|
| 1 | 1.098 | 77181 | 7727 | 88.194 | | | | |
| 2 | 1.736 | 1623 | 171 | 1.855 | | | | |
| 3 | 3.346 | 8708 | 541 | 9.951 | | | | |
| Total | | 87512 | 8439 | | | | | |

Figure A2. 6: Chromatograph for IWW Optimization R5

Analysis Date & Time : 5/5/2023 2:23:06 PM
User Name : Admin
Vial# : 1
Sample Name :
Sample ID :
Sample Type : Unknown
Injection Volume :
ISTD Amount :

Data Name : C:\Users\Admin\Desktop\Biogas project\R6.gcd
Method Name : C:\Users\Admin\Desktop\Biogas project\Biogas project.gcm

Intensity

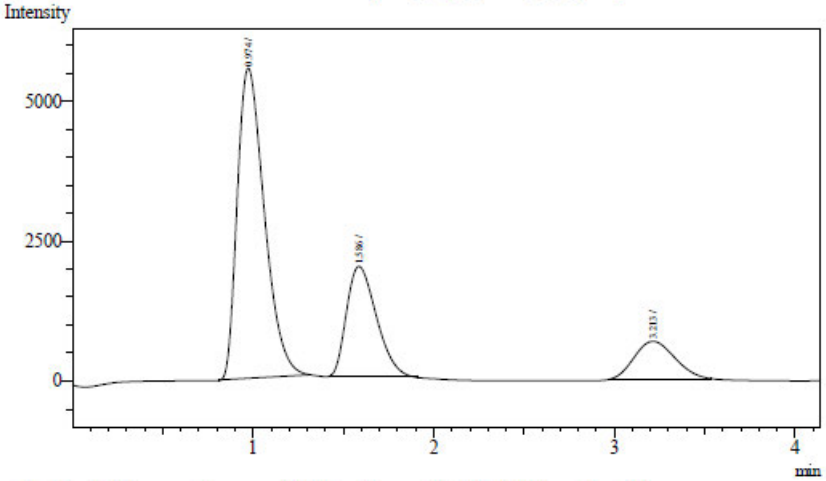


| Peak# | Ret.Time | Area | Height | Conc. | Unit | Mark | ID# | Cmpd Name |
|---|---|---|---|---|---|---|---|---|
| 1 | 0.974 | 57781 | 5542 | 63.089 | | | | |
| 2 | 1.586 | 22745 | 1972 | 24.834 | | | | |
| 3 | 3.213 | 11061 | 691 | 12.077 | | | | |
| Total | | 91587 | 8205 | | | | | |

Figure A2. 7: Chromatograph for IWW Optimization R6

Analysis Date & Time : 8/4/2023 12:35:46 PM
User Name : Admin
Vial# : 1
Sample Name : Test 1
Sample ID :
Sample Type : Unknown
Injection Volume :
ISTD Amount :

Data Name : C:\Users\Admin\Desktop\Baldwin\R7 DE.gcd
Method Name : C:\Users\Admin\Desktop\Biogas project\Methods\Biogas project Method.gcm

Intensity

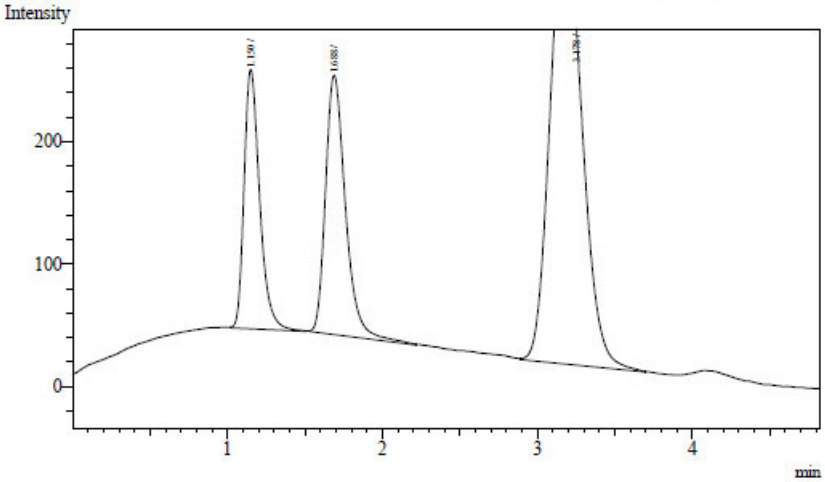


| Peak# | Ret.Time | Area | Height | Conc. | Unit | Mark | ID# | Cmpd Name |
|---|---|---|---|---|---|---|---|---|
| 1 | 1.150 | 1461 | 211 | 0.000 | | | | |
| 2 | 1.688 | 1870 | 211 | 0.000 | | | | |
| 3 | 3.178 | 5142 | 361 | 0.000 | | | | |
| Total | | 8473 | 783 | | | | | |

Figure A2. 8: Chromatograph for IWW Optimization R7

Analysis Date & Time : 5/5/2023 3:31:00 PM
User Name : Admin
Vial# : 1
Sample Name :
Sample ID :
Sample Type : Unknown
Injection Volume :
ISTD Amount :

Data Name : C:\Users\Admin\Desktop\Biogas project\R8.gcd
Method Name : C:\Users\Admin\Desktop\Biogas project\Biogas project.gcm

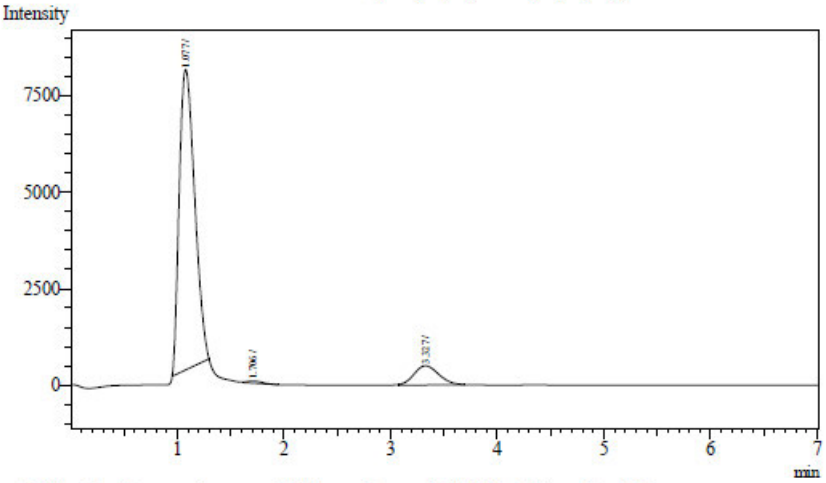


| Peak# | Ret.Time | Area | Height | Conc. | Unit | Mark | ID# | Cmpd Name |
|---|---|---|---|---|---|---|---|---|
| 1 | 1.077 | 77976 | 7780 | 90.189 | | | | |
| 2 | 1.706 | 482 | 53 | 0.558 | | | | |
| 3 | 3.327 | 8001 | 498 | 9.254 | | | | |
| Total | | 86459 | 8331 | | | | | |

Figure A2. 9: Chromatograph for IWW Optimization R8

Analysis Date & Time : 5/5/2023 3:09:04 PM
User Name : Admin
Vial# : 1
Sample Name :
Sample ID :
Sample Type : Unknown
Injection Volume :
ISTD Amount :

Data Name : C:\Users\Admin\Desktop\Biogas project\R9.gcd
Method Name : C:\Users\Admin\Desktop\Biogas project\Biogas project.gcm

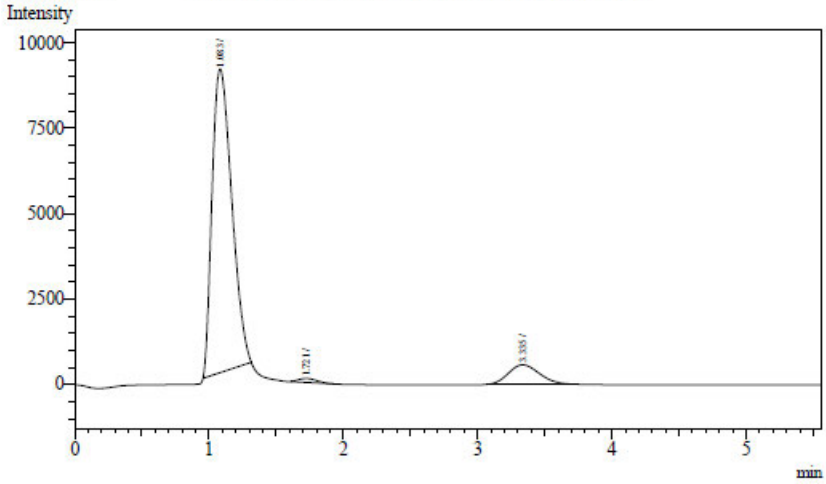


| Peak# | Ret.Time | Area | Height | Conc. | Unit | Mark | ID# | Cmpd Name |
|---|---|---|---|---|---|---|---|---|
| 1 | 1.083 | 90349 | 8882 | 89.672 | | | | |
| 2 | 1.721 | 1036 | 113 | 1.028 | | | | |
| 3 | 3.335 | 9370 | 576 | 9.300 | | | | |
| Total | | 100755 | 9571 | | | | | |

Figure A2. 10: Chromatograph for IWW Optimization R9

Analysis Date & Time : 5/5/2023 4:23:23 PM
User Name : Admin
Vial# : 1
Sample Name :
Sample ID :
Sample Type : Unknown
Injection Volume :
ISTD Amount :

Data Name : C:\Users\Admin\Desktop\Biogas project\R10.gcd
Method Name : C:\Users\Admin\Desktop\Biogas project\Biogas project.gcm

Intensity

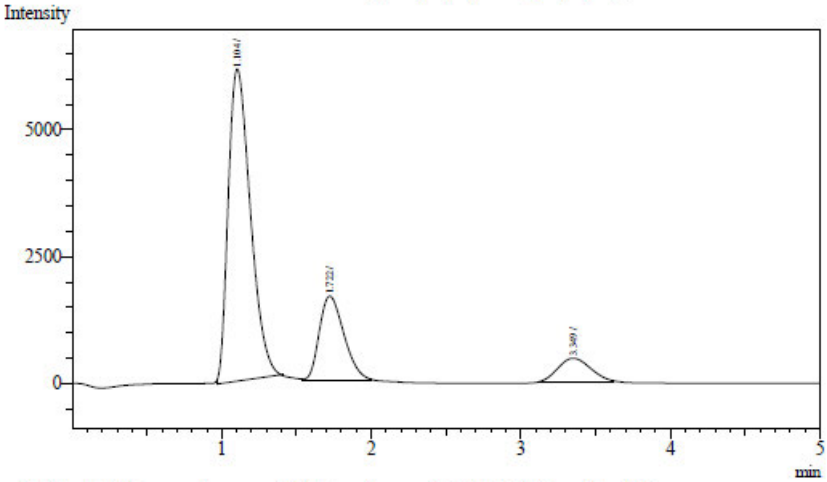


| Peak# | Ret.Time | Area | Height | Conc. | Unit Mark | ID# | Cmpd Name |
|---|---|---|---|---|---|---|---|
| 1 | 1.104 | 63297 | 6147 | 70.300 | | | |
| 2 | 1.722 | 19325 | 1668 | 21.463 | | | |
| 3 | 3.349 | 7416 | 477 | 8.237 | | | |
| **Total** | | 90038 | 8292 | | | | |

Figure A2. 11: Chromatograph for IWW Optimization R10

Analysis Date & Time : 5/5/2023 3:16:48 PM
User Name : Admin
Vial# : 1
Sample Name :
Sample ID :
Sample Type : Unknown
Injection Volume :
ISTD Amount :

Data Name : C:\Users\Admin\Desktop\Biogas project\R11.gcd
Method Name : C:\Users\Admin\Desktop\Biogas project\Biogas project.gcm

Intensity

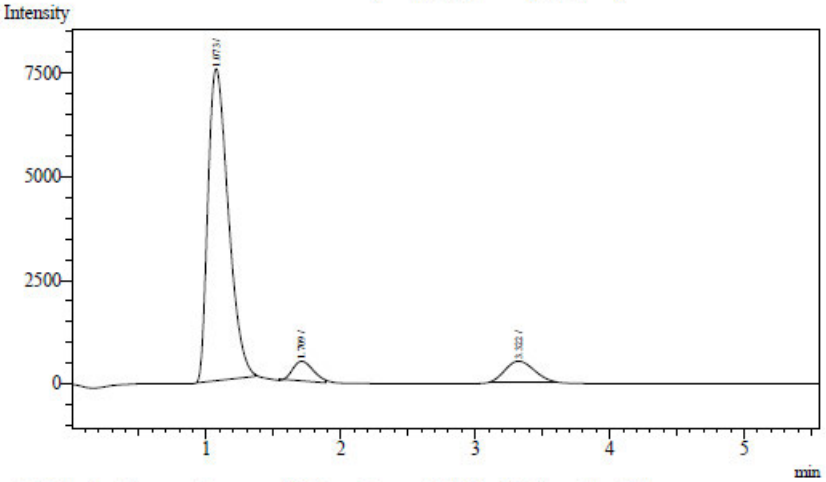


| Peak# | Ret.Time | Area | Height | Conc. | Unit Mark | ID# | Cmpd Name |
|---|---|---|---|---|---|---|---|
| 1 | 1.073 | 79166 | 7517 | 86.942 | | | |
| 2 | 1.709 | 4870 | 470 | 5.348 | | | |
| 3 | 3.322 | 7020 | 490 | 7.710 | | | |
| **Total** | | 91056 | 8477 | | | | |

Figure A2. 12: Chromatograph for IWW Optimization R11

Analysis Date & Time : 5/5/2023 4:17:11 PM
User Name : Admin
Vial# : 1
Sample Name :
Sample ID :
Sample Type : Unknown
Injection Volume :
ISTD Amount :

Data Name : C:\Users\Admin\Desktop\Biogas project\R12.gcd
Method Name : C:\Users\Admin\Desktop\Biogas project\Biogas project.gcm

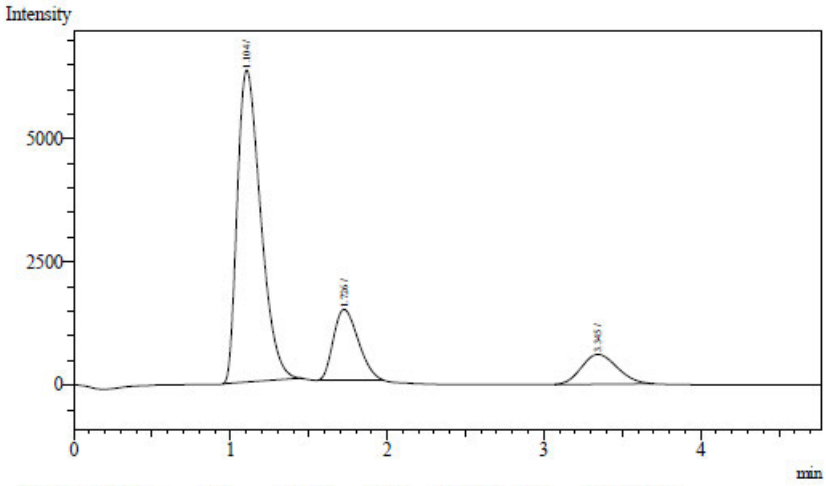


| Peak# | Ret.Time | Area | Height | Conc. | Unit | Mark | ID# | Cmpd Name |
|---|---|---|---|---|---|---|---|---|
| 1 | 1.104 | 65580 | 6327 | 72.026 | | | | |
| 2 | 1.726 | 15850 | 1433 | 17.408 | | | | |
| 3 | 3.345 | 9620 | 605 | 10.565 | | | | |
| Total | | 91050 | 8365 | | | | | |

Figure A2. 13: Chromatograph for IWW Optimization R12

Analysis Date & Time : 5/5/2023 3:39:36 PM
User Name : Admin
Vial# : 1
Sample Name :
Sample ID :
Sample Type : Unknown
Injection Volume :
ISTD Amount :

Data Name : C:\Users\Admin\Desktop\Biogas project\R13.gcd
Method Name : C:\Users\Admin\Desktop\Biogas project\Biogas project.gcm

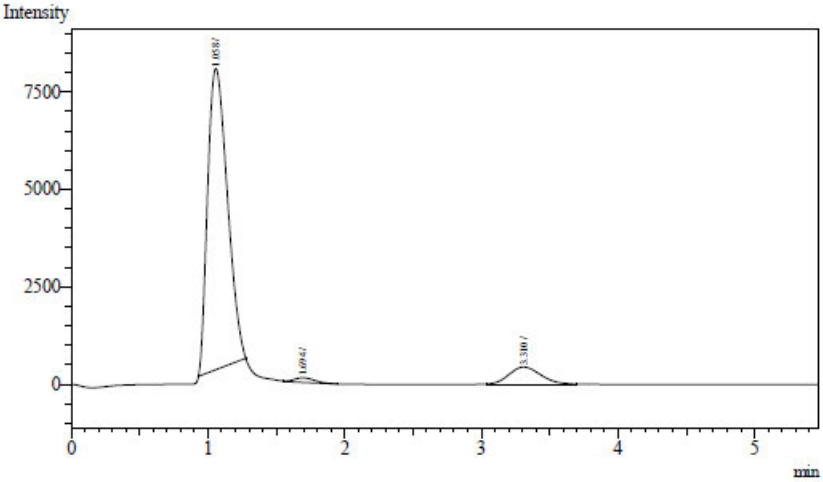


| Peak# | Ret.Time | Area | Height | Conc. | Unit | Mark | ID# | Cmpd Name |
|---|---|---|---|---|---|---|---|---|
| 1 | 1.058 | 77373 | 7730 | 90.126 | | | | |
| 2 | 1.694 | 1266 | 121 | 1.475 | | | | |
| 3 | 3.310 | 7211 | 443 | 8.399 | | | | |
| Total | | 85850 | 8294 | | | | | |

Figure A2. 14: Chromatograph for IWW Optimization R13

Analysis Date & Time : 5/5/2023 3:47:03 PM
User Name : Admin
Vial# : 1
Sample Name :
Sample ID :
Sample Type : Unknown
Injection Volume :
ISTD Amount :

Data Name : C:\Users\Admin\Desktop\Biogas project\R14.gcd
Method Name : C:\Users\Admin\Desktop\Biogas project\Biogas project.gcm

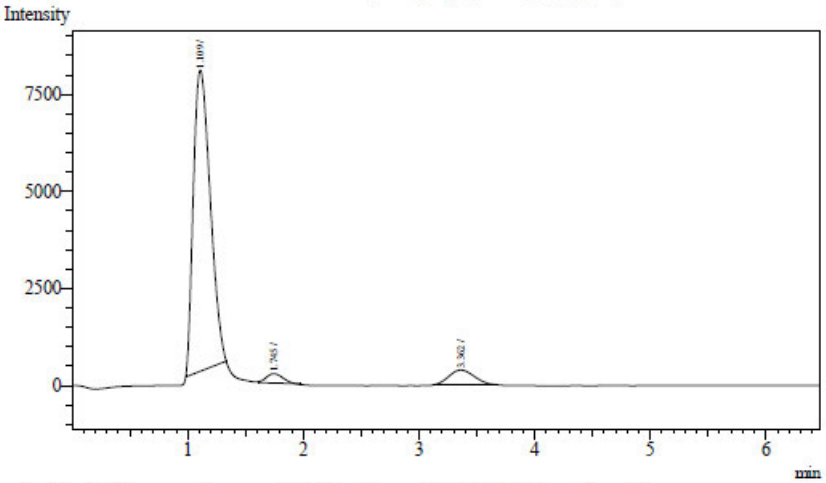


| Peak# | Ret.Time | Area | Height | Conc. | Unit | Mark | ID# | Cmpd Name |
|---|---|---|---|---|---|---|---|---|
| 1 | 1.109 | 78359 | 7754 | 90.444 | | | | |
| 2 | 1.745 | 2296 | 237 | 2.650 | | | | |
| 3 | 3.362 | 5984 | 387 | 6.906 | | | | |
| Total | | 86639 | 8378 | | | | | |

Figure A2. 15: Chromatograph for IWW Optimization R14

Analysis Date & Time : 5/5/2023 3:56:42 PM
User Name : Admin
Vial# : 1
Sample Name :
Sample ID :
Sample Type : Unknown
Injection Volume :
ISTD Amount :

Data Name : C:\Users\Admin\Desktop\Biogas project\R15.gcd
Method Name : C:\Users\Admin\Desktop\Biogas project\Biogas project.gcm

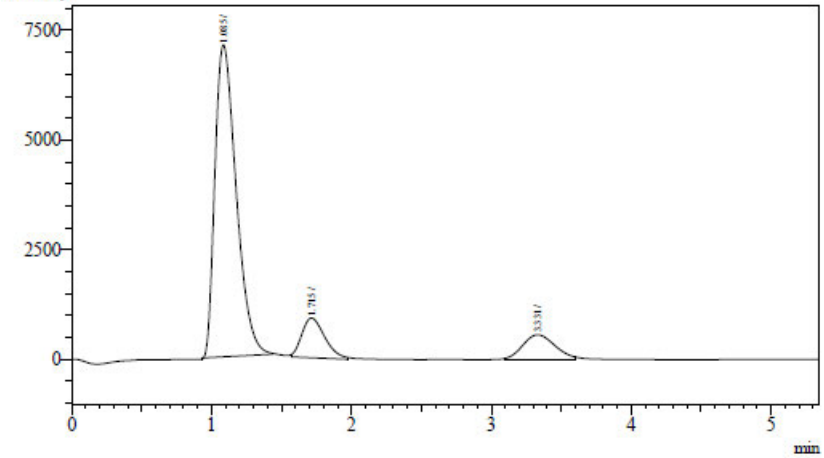


| Peak# | Ret.Time | Area | Height | Conc. | Unit | Mark | ID# | Cmpd Name |
|---|---|---|---|---|---|---|---|---|
| 1 | 1.085 | 75135 | 7111 | 78.972 | | | | |
| 2 | 1.715 | 10287 | 902 | 10.812 | | | | |
| 3 | 3.331 | 9720 | 585 | 10.216 | | | | |
| Total | | 95142 | 8598 | | | | | |

Figure A2. 16: Chromatograph for IWW Optimization R15